

การสังเคราะห์โคพอลิเมอร์ของเอทีลีนกับ แอลฟา-โอเลฟิน ด้วยตัวเร่งปฏิกิริยาเซอร์โคเนียมชนิดแบบมีตัวรองรับ



นางสาว ภาณี แก้วกระจ่าง

สถาบันวิทยบริการ

จุฬาลงกรณ์มหาวิทยาลัย

วิทยานิพนธ์นี้เป็นส่วนหนึ่งของการศึกษาตามหลักสูตรปริญญาวิศวกรรมศาสตรมหาบัณฑิต

สาขาวิชาวิศวกรรมเคมี ภาควิชาวิศวกรรมเคมี


คณะวิศวกรรมศาสตร์ จุฬาลงกรณ์มหาวิทยาลัย

ปีการศึกษา 2545

ISBN 974-17-2538-8

ลิขสิทธิ์ของจุฬาลงกรณ์มหาวิทยาลัย

COPOLYMERIZATION OF ETHYLENE/ALPHA-OLEFINS ON THE SUPPORTED ZIRCONOCENE
CATALYST



Miss Paninee Kaewkrajang

สถาบันวิทยบริการ
จุฬาลงกรณ์มหาวิทยาลัย

A Thesis Submitted in Partial Fulfillment of the Requirements
for the Degree of Master of Engineering in Chemical Engineering

Department of Chemical Engineering

Faculty of Engineering

Chulalongkorn University

Academic Year 2002

ISBN 974-17-2538-8

Thesis Title COPOLYMERIZATION OF ETHYLENE/ALPHA-OLEFINS
ON THE SUPPORTED ZIRCONOCENE CATALYST
By Miss Paninee Kaewkrajang
Field of Study Chemical Engineering
Thesis Advisor Professor Piyasan Prasertthdam, Dr.Ing.

Accepted by the Faculty of Engineering, Chulalongkorn University in Partial
Fulfillment of the Requirements for the Master's Degree

.....Dean of Faculty of Engineering
(Professor Somsak Panyakeow, D.Eng.)

THESIS COMMITTEE

.....Chairman
(Montree Wongsri, D.Sc.)

.....Thesis Advisor
(Professor Piyasan Prasertthdam, Dr.Ing.)

.....Member
(Assistant Professor ML. Supakanok Thongyai, Ph.D.)

.....Member
(Assistant Professor Siriporn Damrongsakkul, Ph.D.)

นางสาวภาณี แก้วกระจ่าง: การสังเคราะห์โคพอลิเมอร์ของเอทิลีนกับ แอลฟา-โอเลฟิน ด้วย
ตัวเร่งปฏิกิริยาเซอร์โคโนซีนแบบมีตัวรองรับ (COPOLYMERIZATION OF
ETHYLENE/ALPHA-OLEFINS ON THE SUPPORTED ZIRCONOCENE
CATALYST) อ.ที่ปรึกษา : ศาสตราจารย์ ดร. ปิยะสาร ประเสริฐธรรม, 109 หน้า ISBN 974-
17-2538-8

งานวิจัยนี้ได้ศึกษาผลของความเข้มข้นของตัวเร่งปฏิกิริยาและอุณหภูมิในการสังเคราะห์พอลิเมอร์ต่อการเตรียมพอลิเมอร์แบบผสมของเอทิลีน/1-ออกทีนด้วยระบบตัวเร่งปฏิกิริยาเอทิลีนบิสอินดีนิลเซอร์โคเนียมไดคลอไรด์-ไตรเมทิลอะลูมิเนียม (TMA) บนตัวรองรับซิลิกาซึ่งมีการปรับปรุงด้วยเมทิลอะลูมิเนียมออกเซน (MAO) จากการทดลองพบว่าความว่องไวของตัวเร่งปฏิกิริยาปฏิกิริยาก่อนการเกิดปฏิกิริยา ($\text{SiO}_2/\text{MAO}/\text{Et}(\text{Ind})_2\text{ZrCl}_2$) ในปฏิกิริยาการเตรียมโคพอลิเมอร์ของเอ-ทิลีน/แอลฟา-โอเลฟิน (1-เฮกซีน 1-ออกทีน และ 1-เดกซีน) พบว่าการใช้ตัวรองรับซิลิกาที่ถูกรับปรุงด้วยเมทิลอะลูมิเนียมออกเซนเพียงอย่างเดียว มีค่าสูงสุดของความเข้มข้นของตัวเร่งปฏิกิริยา คือ 5.00×10^{-5} โมลต่อลิตร และอุณหภูมิที่ใช้ในการสังเคราะห์พอลิเมอร์คือ 70 องศาเซลเซียส จากนั้นได้ศึกษาผลของอัตราส่วนเชิงโมลของอะลูมิเนียมในMAOต่อเซอร์โคเนียมในตัวเร่งปฏิกิริยา ($\text{Al}_{(\text{MAO})}/\text{Zr}$) และศึกษาผลของอัตราส่วนเชิงโมลของอะลูมิเนียมในTMAต่อเซอร์โคเนียมในตัวเร่งปฏิกิริยา ($\text{Al}_{(\text{TMA})}/\text{Zr}$) โดยใช้ตัวรองรับที่ผ่านการปรับปรุงที่แตกต่างกัน 2 แบบ คือ ซิลิกาที่ถูกรับปรุงด้วยเมทิลอะลูมิเนียมออกเซนเพียงอย่างเดียว (SiO_2/MAO) และซิลิกาที่ถูกรับปรุงด้วยเมทิลอะลูมิเนียมออกเซนแล้วนำมารองรับตัวเร่ง (SiO_2/MAO) จะมีความว่องไวในการเกิดพอลิเมอร์แบบผสมสูงกว่าการใช้ตัวรองรับซิลิกาที่ถูกรับปรุงด้วยเมทิลอะลูมิเนียมออกเซนแล้วนำมารองรับตัวเร่งปฏิกิริยาก่อนการเกิดปฏิกิริยา ($\text{SiO}_2/\text{MAO}/\text{Et}(\text{Ind})_2\text{ZrCl}_2$) นอกจากนี้ผลของอัตราส่วนเชิงโมลของอะลูมิเนียมในMAO ต่อเซอร์โคเนียมในตัวเร่งปฏิกิริยา ($\text{Al}_{(\text{MAO})}/\text{Zr}$) จะให้รูปแบบของความสัมพันธ์ระหว่างความว่องไวในการเกิดปฏิกิริยากับอัตราส่วน $\text{Al}_{(\text{MAO})}/\text{Zr}$ ที่เหมือนกันทั้งในระบบ SiO_2/MAO และ ระบบ $\text{SiO}_2/\text{MAO}/\text{Et}(\text{Ind})_2\text{ZrCl}_2$ คือความว่องไวในการเกิดปฏิกิริยามีค่าสูงขึ้นเมื่อเพิ่มอัตราส่วน $\text{Al}_{(\text{MAO})}/\text{Zr}$ และเมื่อพิจารณาผลของอัตราส่วนเชิงโมลของอะลูมิเนียมใน TMA ต่อเซอร์โคเนียมในตัวเร่งปฏิกิริยา ($\text{Al}_{(\text{TMA})}/\text{Zr}$) จะพบว่ารูปแบบของความสัมพันธ์ระหว่างความว่องไวในการเกิดปฏิกิริยากับอัตราส่วน ($\text{Al}_{(\text{TMA})}/\text{Zr}$) ของระบบ SiO_2/MAO ที่ใช้ในเอทิลีน/1-ออกทีน โคพอลิเมอร์ไรเซชันจะให้รูปแบบที่แตกต่างจาก เอทิลีน/1-เฮกซีน และ เอ-ทิลีน/1-เดกซีน โคพอลิเมอร์ไรเซชัน ซึ่งในระบบ $\text{SiO}_2/\text{MAO}/\text{Et}(\text{Ind})_2\text{ZrCl}_2$ จะพบว่าเอทิลีน/แอลฟา-โอเลฟินทั้ง 3 ชนิด (1-เฮกซีน 1-ออกทีน และ 1-เดกซีน) ให้รูปแบบที่เหมือนกัน

ภาควิชา.....วิศวกรรมเคมี.....

ลายมือชื่อนิสิต.....

สาขาวิชา.....วิศวกรรมเคมี.....

ลายมือชื่ออาจารย์ที่ปรึกษา.....

ปีการศึกษา.....2545.....

##4370442621 : MAJOR CHEMICAL ENGINEERING

KEY WORD : SUPPORTED METALLOCENE CATALYST / COPOLYMERIZATION OF ETHYLENE/ALPHA-OLEFINS / ZIRCONOCENE

PANINEE KAEWKRAJANG : COPOLYMERIZATION OF ETHYLENE/ALPHA-OLEFINS ON THE SUPPORTED ZIRCONOCENE CATALYST. THESIS ADVISOR : PROF. PIYASAN PRASERTHDAM, Dr.Ing. 109 pp. ISBN 974-17-2538-8

In this research, effect of catalyst concentration and polymerization temperature on catalyst activity of the ethylene/1-octene copolymerization with ethylenebis(indenyl) zirconium dichloride ($\text{Et}(\text{Ind})_2\text{ZrCl}_2$) catalyst system–trimethylaluminum (TMA) using silica modified with methylaluminoxane (MAO) as support was studied. It was found that the highest catalytic activity was obtained at the catalyst concentration of 5.0×10^{-5} mole/litre and polymerization temperature of 70°C . Subsequently, effect of $\text{Al}_{(\text{MAO})}/\text{Zr}$ molar ratio and $\text{Al}_{(\text{TMA})}/\text{Zr}$ molar ratio on catalyst activity of the ethylene/ α -olefin (1-hexene, 1-octene and 1-decene) copolymerizations with ethylenebis(indenyl)zirconium dichloride ($\text{Et}(\text{Ind})_2\text{ZrCl}_2$) catalyst was investigated by using in-situ supported system (SiO_2/MAO) and preformed supported system ($\text{SiO}_2/\text{MAO}/\text{Et}(\text{Ind})_2\text{ZrCl}_2$). It was found that the catalytic activity of the in-situ supported system was higher than that of the preformed supported system in ethylene/ α -olefin (1-hexene, 1-octene and 1-decene) copolymerizations. Moreover, the results from effect of $\text{Al}_{(\text{MAO})}/\text{Zr}$ molar ratio on the catalytic activity in both of SiO_2/MAO and $\text{SiO}_2/\text{MAO}/\text{Et}(\text{Ind})_2\text{ZrCl}_2$ catalyst system showed the same pattern of an increase of the catalytic activity with increasing of $\text{Al}_{(\text{MAO})}/\text{Zr}$ mole ratio. On the other hand, the results from effect of $\text{Al}_{(\text{TMA})}/\text{Zr}$ molar ratio on the catalytic activity exhibited that the pattern of ethylene/1-octene copolymerization in in-situ supported system was different from that of ethylene/1-hexene and ethylene/1-decene copolymerization. While the preformed supported catalyst system indicated the similarity of the pattern of relationship between the catalytic activity and $\text{Al}_{(\text{TMA})}/\text{Zr}$ molar ratio for all ethylene/alpha-olefin copolymerizations.

Department....Chemical Engineering..... Student's signature.....

Field of study...Chemical Engineering.... Advisor's signature.....

Academic year.....2002.....

ACKNOWLEDGEMENT

I would like to express my gratitude to Professor Dr. Piyasan Prasertthdam, my advisor. His advice is always worthwhile and without him this work could not be possible.

I cannot miss to thanks Dr. Takeshi Shiono for his kindness in a part of experiment and valuable guidance of this study.

I wish to thank Dr. Montree Wongsri, Assistant Professor Dr. ML. Supakanok Thongyai and Assistant Professor Dr. Siriporn Damrongsakkul as a chairman and members of this thesis committee for their valuable guidance and revision throughout my thesis, respectively.

Sincere thanks are given to Bangkok Polyethylene Co., Ltd., Tosho Akzo, Japan, BASF and Caprolactam Thai Co., Ltd. for chemical supply. And many thanks to Thai Polyethylene Co., Ltd., for GPC measurement, National Metal and Material Technology Center (M-TEC) for NMR analysis, Scientific and Technological Research Equipment Center (STREC) for SEM, DSC and ICP measurements.

Finally, I would like to express my highest gratitude to my parent and brothers who are always beside me and support throughout this study.

สถาบันวิทยบริการ
จุฬาลงกรณ์มหาวิทยาลัย

CONTENTS

	Page
ABSTRACT (IN THAI)	iv
ABSTRACT (IN ENGLISH)	v
ACKNOWLEDGMENT	vi
CONTENTS	vii
LIST OF TABLES	xi
LIST OF FIGURES	xii
CHAPTER I INTRODUCTION	1
1.1 Objective of the Thesis.....	3
1.2 Scope of the Thesis.....	3
CHAPTER II LITERATURE REVIEWS	5
2.1 Background on Polyolefin Catalysts.....	5
2.1.1 Catalyst Structure.....	5
2.1.2 Polymerization mechanism.....	8
2.1.3 Cocatalysts.....	11
2.1.4 Catalyst Activity.....	14
2.1.5 Copolymerization.....	15
2.2 Heterogenous Systems.....	18
2.2.1 Catalyst Chemistry.....	19
2.2.2 Supporting Methods.....	20
2.2.2.1 Direct Supporting of Inert Material.....	20
2.2.2.2 Supporting Catalyst on Material Treated with Alkylaluminum.....	23
2.2.2.3 Chhemically Anchoring catalyst on Support.....	25
2.2.2.4 Supporting on other Supports.....	27
2.3 Polymer Characterization.....	29
2.3.1 Size Exclusion Chromatography.....	29
2.3.2 Fraction Methods Based on Polymer Crystallinity.....	29
2.3.2.1 Temperature Rising Elution Fraction.....	29
2.3.2.2 Crystallization Analysis Fractionation.....	30
2.3.3 Other Characterization Methods.....	30

CONTENTS (CONT.)

	Page
2.3.3.1 Nuclear Magnetic Resonance (NMR).....	30
2.3.3.2 Differential Scanning Calorimetry (DSC).....	31
CHAPTER III EXPERIMENTAL	32
3.1 Chemicals.....	32
3.2 Equipments.....	33
3.2.1 Cooling System.....	33
3.2.2 Inert Gas Supply.....	33
3.2.3 Magnetic Stirrer and Heater.....	34
3.2.4 Reactor.....	34
3.2.5 Schlenk Line.....	34
3.2.6 Schlenk Tube.....	35
3.2.7 Vacuum Pump.....	35
3.3 Characterizing Instruments.....	36
3.3.1 Differential Scanning Calorimetry (DSC).....	36
3.3.2 Gel Permeation Chromatography (GPC).....	37
3.3.3 Nuclear Magnetic Resonance (NMR).....	37
3.3.4 Scanning Electron Microscope (SEM).....	37
3.3.5 Inductively Coupled Plasma (ICP).....	37
3.4 Supporting Procedure.....	38
3.4.1 Preparation of catalyst precursor SiO ₂ /MAO.....	38
3.4.2 Preparation of catalyst precursor SiO ₂ /MAO/Et(Ind) ₂ ZrCl ₂	38
3.5 Ethylene and α -olefins Copolymerization Procedure.....	38
3.5.1 The Effect of Catalyst concentration.....	39
3.5.2 The Effect of Polymerization Temperature.....	39
3.5.3 The Effect of Al _(MAO) /Zr mole ratios.....	39
3.5.4 The Effect of Al _(TMA) /Zr mole ratios.....	40
3.5.5 The effect of catalyst precursor.....	40
3.6 Characterizing of Catalyst Precursor.....	40
3.6.1 Morphology.....	40
3.6.2 The amount of Al and Zr on catalyst precursors.....	40

CONTENTS (CONT.)

	Page
3.7 Characterization of Ethylene/ α -olefins Copolymer products.....	41
3.7.1 Chemical Structure Determination.....	41
3.7.2 Morphology.....	41
3.7.3 Melting Temperature (T_m).....	41
3.7.4 Average Molecular Weight and Molecule Weight Distribution.....	41
CHAPTER IV RESULTS AND DISCUSSION.....	43
4.1 Ethylene and 1-octene Copolymerization on the in-situ supported (SiO_2/MAO) Catalyst.....	43
4.1.1 The Effect of Catalyst Concentration on the Catalytic Activity.....	43
4.1.2 The Effect of Polymerization Temperature on the Catalytic Activity.....	45
4.2 Ethylene / α -olefins Copolymerization on the in-situ supported (SiO_2/MAO) Catalyst.....	48
4.2.1 The Effect of $\text{Al}_{(\text{MAO})}/\text{Zr}$ Mole Ratio on the Catalytic Activity.....	48
4.2.2 The Effect of $\text{Al}_{(\text{TMA})}/\text{Zr}$ Mole Ratio on the Catalytic Activity.....	51
4.3 Ethylene/ α -olefins copolymerization on supported ($\text{SiO}_2/\text{MAO}/\text{Et}(\text{Ind})_2\text{ZrCl}_2$) catalyst.....	54
4.3.1 The Effect of $\text{Al}_{(\text{MAO})}/\text{Zr}$ Mole Ratio on the Catalytic Activity.....	54
4.3.2 The Effect of $\text{Al}_{(\text{TMA})}/\text{Zr}$ Mole Ratio on the Catalytic Activity.....	56
4.4 Ethylene/ α -olefins copolymerization and ethylene polymerization in different catalyst precursors.....	58
4.4.1 The Effect of different Catalyst Precursor on the Catalytic Activity.....	58
4.5 Characterization of Catalyst Precursor.....	61
4.5.1 Morphology.....	61
4.5.2 The amount of aluminum and zirconium on catalyst precursor.....	63
4.5.2.1 Inductively coupled plasma (ICP).....	63
4.6 Characterization of Ethylene/ α -olefins Copolymer.....	65
4.6.1 Chemical Structure Determination.....	65
4.6.1.1 Nuclear Magnetic Resonance (NMR).....	65

CONTENTS (CONT.)

	Page
4.6.2 Morphology.....	71
4.6.3 Melting Temperature (T _m)	76
4.6.4 Average Molecular Weight and Molecular Weight Distribution.....	77
CHAPTER V CONCLUSION & SUGGESTION.....	85
5.1 Conclusion.....	85
5.2 Suggestion.....	86
REFERENCES.....	87
APPENDICES.....	92
APPENDIX A.....	93
APPENDIX B.....	97
APPENDIX C.....	106
VITA.....	109



 สถาบันวิทยบริการ
 จุฬาลงกรณ์มหาวิทยาลัย

LIST OF TABLES

Table	Page
2.1	Representative examples of metallocenes.....6
4.1	Catalytic activity of different catalyst concentrations.....43
4.2	Catalytic activity of different polymerization temperatures.....46
4.3	Catalytic activity at different Al _(MAO) /Zr mole ratios on in-situ supported catalyst.....49
4.4	Catalytic activity at different Al _(TMA) /Zr mole ratios on in-situ supported catalyst.....51
4.5	Catalytic activity at different Al _(MAO) /Zr mole ratios on preformed supported catalyst.....54
4.6	Catalytic activity at different Al _(TMA) /Zr mole ratios on preformed supported catalyst.....56
4.7	Catalytic activity of different catalyst precursors.....59
4.8	The amount of aluminium on SiO ₂ supported MAO.....64
4.9	The amount of zirconium on SiO ₂ supported MAO and Et(Ind) ₂ ZrCl ₂64
4.10	The ¹³ C-NMR identification of ethylene/1-hexene copolymer.....66
4.11	The ¹³ C-NMR identification of ethylene/1-octene copolymer.....66
4.12	The ¹³ C-NMR identification of ethylene/1-decene copolymer.....67
4.13	Triad distribution of ethylene/ α -olefins copolymers produced with SiO ₂ /MAO-Et(Ind) ₂ ZrCl ₂ +TMA.....71
4.14	Melting temperature of ethylene/ α -olefin copolymers and polyethylene with various catalyst precursor.....76
4.15	Mw and MWD of the obtained ethylene/ α -olefin copolymer at various catalyst precursor.....77

LIST OF FIGURES

Figure	page
2.1	Molecular structure of metallocene.....5
2.2	Some of zirconocene catalyst structure.....6
2.3	Scheme of the different metallocene complex structure.....7
2.4	Cossee mechanism for Ziegler-Natta olefin polymerization.....8
2.5	The propagation step according to the trigger mechanism.....9
2.6	Propagation mechanism in polymerization.....9
2.7	Chain transfer via β -H elimination.....10
2.8	Chain transfer via β -CH ₃ elimination.....10
2.9	Chain transfer to aluminum.....11
2.10	Chain transfer to monomer.....11
2.11	Chain transfer to hydrogen.....11
2.12	Early structure models of MAO.....12
2.13	Representation of MAO showing the substitution of one bridging methyl group by X ligand extracted from $\text{racEt}(\text{Ind})_2\text{ZrCl}_2$ (X = Cl, NMe ₂ , CH ₂ Ph).....13
2.14	Structure of $\text{Et}[\text{Ind}]_2\text{ZrCl}_2$ supported on silica.....21
2.15	Structure of $\text{Et}[\text{Ind}]_2\text{ZrCl}_2$ supported on alumina.....21
2.16	Reaction of silica and metallocene during catalyst supporting.....22
2.17	Alkylation of supported metallocene MAO.....22
2.18	Effect of surface hydroxyl groups on ionic metallocene catalysts.....23
2.19	Structure of some silica supported metallocene catalysts.....25
2.20	Mechanism for supporting metallocene catalysts on silica using Spacer molecules.....26
2.21	Modification of silica with $\text{Cp}(\text{CH}_2)_3\text{Si}(\text{OCH}_2\text{CH}_3)_3$ and preparation of supported metallocene catalyst.....27
3.1	Inert gas supply system.....34
3.2	Schlenk. line.....35
3.3	Schlenk tube.....36
3.4	Basic instrumentation for gel permeation chromatography.....42
4.1	Catalytic activity of different catalyst concentrations.....44

LIST OF FIGURES (CONT.)

Figure	page
4.2 Catalytic activity of different polymerization temperatures.....	47
4.3 Catalytic activity of different Al _(MAO) /Zr mole ratios using in-situ supported catalyst.....	50
4.4 Polymerization time of different Al _(MAO) /Zr mole ratios using in-situ supported catalyst.....	50
4.5 Catalytic activity of different Al _(TMA) /Zr mole ratios using in-situ supported catalyst.....	52
4.6 Polymerization time of different Al _(TMA) /Zr mole ratios using in-situ supported catalyst.....	52
4.7 Catalytic activity of different Al _(MAO) /Zr mole ratios using supported catalyst.....	55
4.8 Polymerization time of different Al _(MAO) /Zr mole ratios on supported catalyst.....	55
4.9 Catalytic activity of different Al _(TMA) /Zr mole ratios using supported catalyst.....	57
4.10 Polymerization time of different Al _(TMA) /Zr mole ratios using supported catalyst.....	57
4.11 Catalytic activity of different catalyst precursors.....	60
4.12 SEM image of silica.....	62
4.13 SEM image of silica/MAO.....	62
4.14 SEM image of silica/ MAO/Et(Ind) ₂ ZrCl ₂	63
4.15 Amount of Al impregnated on the silica measured by ICP at various amount of MAO added.....	64
4.16 ¹³ C-NMR spectrum of ethylene/l-hexene copolymer from reference[67].....	68
4.17 ¹³ C-NMR spectrum of ethylene/l-hexene copolymer produced with SiO ₂ /MAO-Et(Ind) ₂ ZrCl ₂ +TMA.....	68
4.18 ¹³ C-NMR spectrum of ethylene/l-octene copolymer from reference[67].....	69

LIST OF FIGURES (CONT.)

Figure	page
4.19 ¹³ C-NMR spectrum of ethylene/l-octene copolymer produced with SiO ₂ /MAO-Et(Ind) ₂ ZrCl ₂ +TMA.....	69
4.20 ¹³ C-NMR spectrum of ethylene/l-decene copolymer from reference[67].....	70
4.21 ¹³ C-NMR spectrum of ethylene/l-decene copolymer produced with SiO ₂ /MAO-Et[Ind] ₂ ZrCl ₂ +TMA.....	70
4.22 SEM image of ethylene/l-hexene copolymer produced with SiO ₂ /MAO-Et(Ind) ₂ ZrCl ₂ +TMA.....	72
4.23 SEM image of ethylene/l-hexene copolymer produced with SiO ₂ /MAO/Et(Ind) ₂ ZrCl ₂ +TMA.....	72
4.24 SEM image of ethylene/l-octene copolymer produced with SiO ₂ /MAO-Et(Ind) ₂ ZrCl ₂ +TMA.....	73
4.25 SEM image of ethylene/l-octene copolymer produced with SiO ₂ /MAO/Et(Ind) ₂ ZrCl ₂ +TMA.....	73
4.26 SEM image of ethylene/l-decene copolymer produced with SiO ₂ /MAO-Et(Ind) ₂ ZrCl ₂ +TMA.....	74
4.27 SEM image of ethylene/l-decene copolymer produced with SiO ₂ /MAO/Et(Ind) ₂ ZrCl ₂ +TMA.....	74
4.28 SEM image of polyethylene produced with SiO ₂ /MAO-Et(Ind) ₂ ZrCl ₂ +TMA.....	75
4.29 SEM image of polyethylene produced with SiO ₂ /MAO/Et(Ind) ₂ ZrCl ₂ +TMA.....	75
A-1 ¹³ C-NMR spectrum of ethylene/l-hexene copolymer produced with SiO ₂ /MAO-Et[Ind] ₂ ZrCl ₂ +TMA.....	94
A-2 ¹³ C-NMR spectrum of ethylene/l-octene copolymer produced with SiO ₂ /MAO-Et[Ind] ₂ ZrCl ₂ +TMA.....	95
A-3 ¹³ C-NMR spectrum of ethylene/l-decene copolymer produced with SiO ₂ /MAO-Et[Ind] ₂ ZrCl ₂ +TMA.....	96
B-1 DSC curve of ethylene/l-hexene copolymer produced with SiO ₂ /MAO-Et(Ind) ₂ ZrCl ₂ +TMA.....	98

LIST OF FIGURES (CONT.)

Figure	page
B-2 DSC curve of ethylene/1-octene copolymer produced with SiO ₂ /MAO-Et(Ind) ₂ ZrCl ₂ +TMA.....	99
B-3 DSC curve of ethylene/1-decene copolymer produced with SiO ₂ /MAO-Et(Ind) ₂ ZrCl ₂ +TMA.....	100
B-4 DSC curve of polyethylene produced with SiO ₂ /MAO-Et(Ind) ₂ ZrCl ₂ +TMA.....	101
B-5 DSC curve of ethylene/1-hexene copolymer produced with SiO ₂ /MAO/Et(Ind) ₂ ZrCl ₂ +TMA.....	102
B-6 DSC curve of ethylene/1-octene copolymer produced with SiO ₂ /MAO/Et(Ind) ₂ ZrCl ₂ +TMA.....	103
B-7 DSC curve of ethylene/1-decene copolymer produced with SiO ₂ /MAO/Et(Ind) ₂ ZrCl ₂ +TMA.....	104
B-8 DSC curve of polyethylene produced with SiO ₂ /MAO/Et(Ind) ₂ ZrCl ₂ +TMA.....	105
C-1 GPC curve of ethylene/α-olefin copolymers produced with SiO ₂ /MAO-Et(Ind) ₂ ZrCl ₂ +TMA.....	107
C-2 GPC curve of ethylene/α-olefin copolymers produced with SiO ₂ /MAO/Et(Ind) ₂ ZrCl ₂ +TMA.....	108

CHAPTER I

INTRODUCTION

Fifty years ago, Karl Ziegler discovered a method to catalyze polymerization at low temperature and pressure through the use of transition metal catalysts. Shortly after his discovery, Giulio Natta visited Ziegler to learn more about his remarkable discovery. Building on Ziegler's earlier work, Natta efficiently polymerized stereoregular polypropylene and characterized its properties. Their combined efforts carried them a Nobel Prize in 1963 [1]. The era of transition metal polymerization catalysis began here.

The first homogeneous metallocene catalyst was discovered by Natta and Breslow in 1957. Natta reported the polymerization of ethylene with the titanocene catalyst Cp_2TiCl_2 and the cocatalyst triethylaluminum, a cocatalyst traditionally used in Ziegler-Natta olefin polymerization systems [1]. The activity of the metallocene with the Ziegler-Natta cocatalyst was very low and therefore showed little commercial promise. In the 1980's, Walter Kaminsky discovered new cocatalyst. While studying a homogeneous $\text{Cp}_2\text{ZrCl}_2/\text{Al}(\text{CH}_3)_3$ polymerization system, water was accidentally introduced into the reactor leading to an extremely active ethylene polymerization system. The high activity was due to the formation of the cocatalyst methylaluminoxane (MAO) as a result of the hydrolysis of the trimethylaluminum, $\text{Al}(\text{CH}_3)_3$ [2].

Since Kaminsky's discovery of the high activity $\text{Cp}_2\text{ZrCl}_2/\text{MAO}$ ethylene polymerization system, metallocene catalysts have slowly evolved as producers push to commercialize the technology. The most serious shortcoming being that, in order to achieve the high activities, extremely high molar Al to transition metal ratios (Al:M) of between 1000-15000:1 were required. Such ratios are commercially unacceptable in terms of the cost and the amount of residues left in the polymer (commercial Ziegler-Natta systems typically require Al to M ratios of between 50-200:1). A significant effort has been put into reducing the amount of MAO required and this has led to the development of many systems with non-aluminum cocatalysts, such as $[\text{B}(\text{C}_6\text{F}_5)_4]^-$ and $[\text{CH}_3\text{B}(\text{C}_6\text{F}_5)_3]^-$. Other developments include the mono-Cp constrained geometry catalysts which have been primarily developed by Dow and Exxon. Significant effort has also gone into heterogenizing the catalyst system by supporting the metallocene and

cocatalyst onto an inorganic support such as silica, alumina, magnesium chloride, starch, zeolites, cyclodextrin and polymers [3].

As results, heterogeneous catalysts offer several additional advantages important to industry, they improved product morphology and the ability to be used in gas and/or slurry phase synthesis methods more compatible with existing technology.

In general, supported metallocenes have a lower catalytic activity than their corresponding homogeneous metallocene systems. So some researchers have reported a new immobilization method by introducing a spacer group such as polysiloxane, between the support and metallocene. The new supported metallocene showed a better catalytic activity than previously reported, but the method introduced additional step to the supporting process. To overcome the preparation complexities of traditionally supported metallocene catalysts, metallocene can be supported in situ, which eliminates the need for a supporting step before polymerization. This system have a good catalytic activity, produce polymers with a good morphology and high bulk density and do not cause reactor fouling. Additionally, they can be activated with trimethylaluminum (TMA) alone in the absence of soluble methyl aluminoxane (MAO) in the polymerization reactor[3].

Copolymer of ethylene with 1-alkenes such as propene, 1-butene, 1-hexene, and 1-octene are very important commercial products classified as linear low density polyethylene (LLDPE) and/or very low density polyethylene (VLDPE) [4]. Rheological and mechanical properties of polymers do not depended only on their average molecular weight, but also on their molecular weight distribution (MWD) and short chain branching distribution (SCBD). Even though the control of MWD and SCBD is very important, conventional heterogeneous Ziegler-Natta catalysts have limitations in controlling MWD and SCBD because polymers produced by these catalysts show broad MWD and SCBD due to the presence of multiple types of active sites on the catalyst. Metallocene catalyst permit the synthesis of polymers with narrow and well controlling MWD and SCBD at high polymerization rates [5].

Metallocene-based polyethylene are entering a wide range of applications such as specialty foam (replacing PVC), selant, shipping bags and sensitivity packing, etc.

Copolymer based on ethylene with 1-butene, 1-hexene, and 1-octene are of great importance in the development of these new materials [6].

From the previous study, W. Pratchayawutthirat studied the ethylene/1-hexene copolymerization using Cp_2ZrCl_2 catalyst in in-situ supported system ($\text{SiO}_2/\text{SiCl}_4/\text{MAO}$) in toluene. The suitable conditions for good catalytic activity were Al/Zr mole ratio of 2500 at zirconium concentration of 5×10^{-5} M, and polymerization temperature of 70°C . Moreover, she found that the order of ethylene/1-hexene copolymerization ability of catalysts was $\text{Et}(\text{Ind})_2\text{ZrCl}_2 > \text{Cp}_2\text{ZrCl}_2 > (\text{nBuCp})_2\text{ZrCl}_2$ [7].

In this thesis, the attention is focused on effect of MAO and TMA in heterogeneous system in ethylene/ α -olefin (1-hexene, 1-octene and 1-decene) copolymerizations. Consideration was interested in these supported system: in-situ supported system (SiO_2/MAO) and preformed supported system ($\text{SiO}_2/\text{MAO}/\text{Et}(\text{Ind})_2\text{ZrCl}_2$).

1.1. Objective of the Thesis

To prepare silica supported zirconocene catalyst and to study its catalytic activity in the copolymerization of ethylene with various α -olefins and characterization.

1.2. Scope of the Thesis

1.2.1. Prepare and study the zirconocene catalyst on silica in in-situ supported system and preformed supported system.

1.2.2. Investigate the optimum conditions in the copolymerization of ethylene/1-octene with in-situ supported catalyst system.

1.2.2.1. Determine the effect of catalyst concentration on catalytic activity.

1.2.2.2. Examine the effect of polymerization temperature on catalytic activity.

1.2.3. Study the effect of MAO and TMA in in-situ supported catalyst and preformed supported catalyst on the ethylene/ α -olefins copolymerization.

1.2.4. Characterize copolymer obtained with conventional techniques: Scanning Electron Microscopy (SEM), Differential Scanning Calorimetry (DSC), Gel Permeation Chromatography (GPC) and Nuclear Magnetic Resonance (NMR).



สถาบันวิทยบริการ
จุฬาลงกรณ์มหาวิทยาลัย

CHAPTER II

LITERATURE REVIEWS

2.1. Background on Polyolefin Catalysts

Polyolefins can be produced with free radical initiators, Phillips type catalysts, Ziegler-Natta catalysts and metallocene catalysts. Ziegler-Natta catalysts have been most widely used because of their broad range of application. However, Ziegler-Natta catalyst provides polymers having broad molecular weight distribution (MWD) and composition distribution due to multiple active sites formed [8].

Metallocene catalysts have been used to polymerize ethylene and α -olefins commercially. The structural change of metallocene catalysts can control composition distribution, incorporation of various comonomers, MWD and stereoregularity [9].

2.1.1. Catalyst Structure

Metallocene is a class of compounds in which cyclopentadienyl or substituted cyclopentadienyl ligands are π -bonded to the metal atom. The stereochemistry of biscyclopentadienyl (or substituted cyclopentadienyl)-metal bis (unibidentate ligand) complexes can be most simply described as distorted tetrahedral, with each η^5 -L group (L = ligand) occupying a single co-ordination position, as in Figure 2.1 [10].

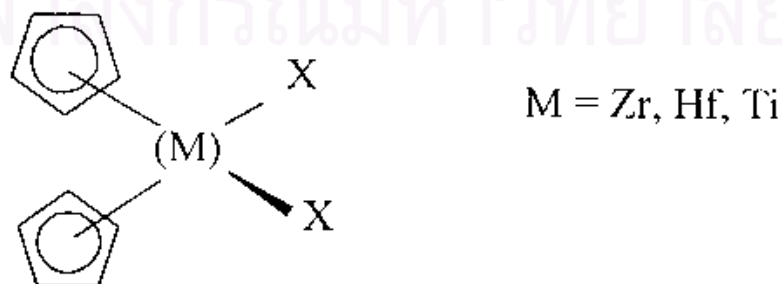


Figure 2.1 Molecular structure of metallocene

Representative examples of each category of metallocenes and some of zirconocene catalysts are shown in Table 2.1 and Figure 2.2, respectively.

Table 2.1 Representative Examples of Metallocenes [10]

Category of metallocenes	Metallocene Catalysts
[A] Nonstereorigid metallocenes	1) Cp_2MCl_2 (M = Ti, Zr, Hf) 2) Cp_2ZrR_2 (M = Me, Ph, CH_2Ph , CH_2SiMe_3) 3) $(\text{Ind})_2\text{ZrMe}_2$
[B] Nonstereorigid ring-substituted metallocenes	1) $(\text{Me}_5\text{C}_5)_2\text{MCl}_2$ (M = Ti, Zr, Hf) 2) $(\text{Me}_3\text{SiCp})_2\text{ZrCl}_2$
[C] Stereorigid metallocenes	1) $\text{Et}(\text{Ind})_2\text{ZrCl}_2$ 2) $\text{Et}(\text{Ind})_2\text{ZrMe}_2$ 3) $\text{Et}(\text{IndH}_4)_2\text{ZrCl}_2$
[D] Cationic metallocenes	1) $\text{Cp}_2\text{MR}(\text{L})^+[\text{BPh}_4]^-$ (M = Ti, Zr) 2) $[\text{Et}(\text{Ind})_2\text{ZrMe}]^+[\text{B}(\text{C}_6\text{F}_5)_4]^-$ 3) $[\text{Cp}_2\text{ZrMe}]^+[(\text{C}_2\text{B}_9\text{H}_{11})_2\text{M}]^-$ (M = Co)
[E] Supported metallocenes	1) $\text{Al}_2\text{O}_3\text{-Et}(\text{IndH}_4)_2\text{ZrCl}_2$ 2) $\text{MgCl}_2\text{.Cp}_2\text{ZrCl}_2$ 3) $\text{SiO}_2\text{.Et}(\text{Ind})_2\text{ZrCl}_2$

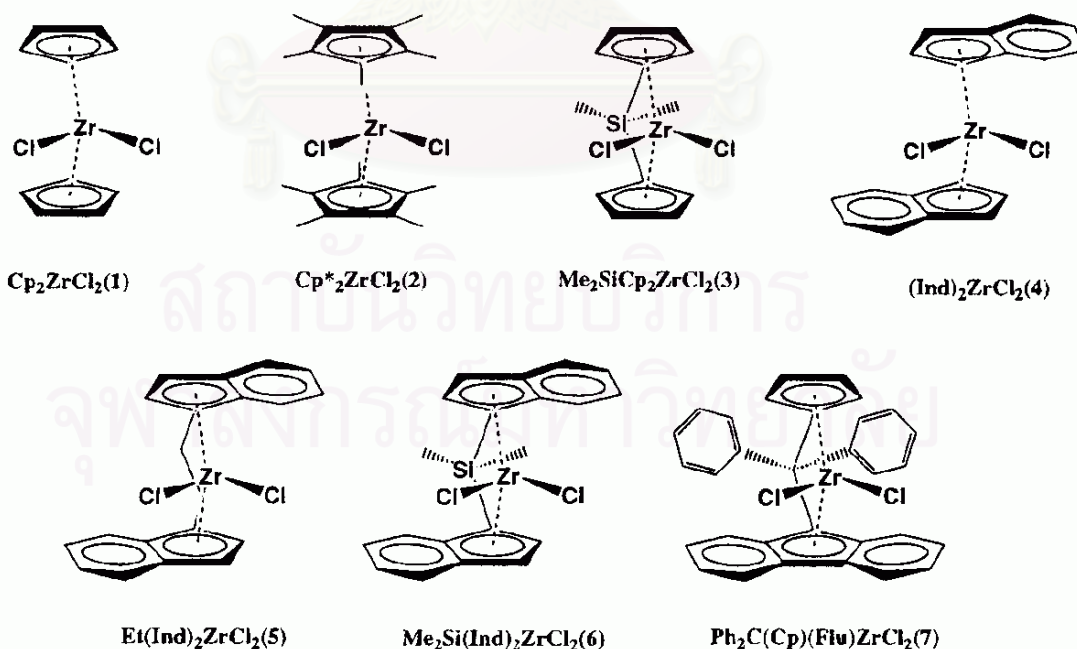


Figure 2.2 Some of zirconocene catalysts structure [11]

Composition and types of metallocene have several varieties. When the two cyclopentadienyl (Cp) rings on either side of the transition metal are unbridged, the metallocene is nonstereorigid and it is characterized by C_{2v} symmetry. The Cp_2M (M = metal) fragment is bent back with the centroid-metal-centroid angle θ about 140° due to an interaction with the other two σ bonding ligands [12]. When the Cp rings are bridged (two Cp rings arranged in a chiral array and connected together with chemical bonds by a bridging group), the stereorigid metallocene, so-called ansa-metallocene, could be characterized by either a C_1 , C_2 , or C_s symmetry depending upon the substituents on two Cp rings and the structure of the bridging unit as schematically illustrated in Figure 2.3[10].

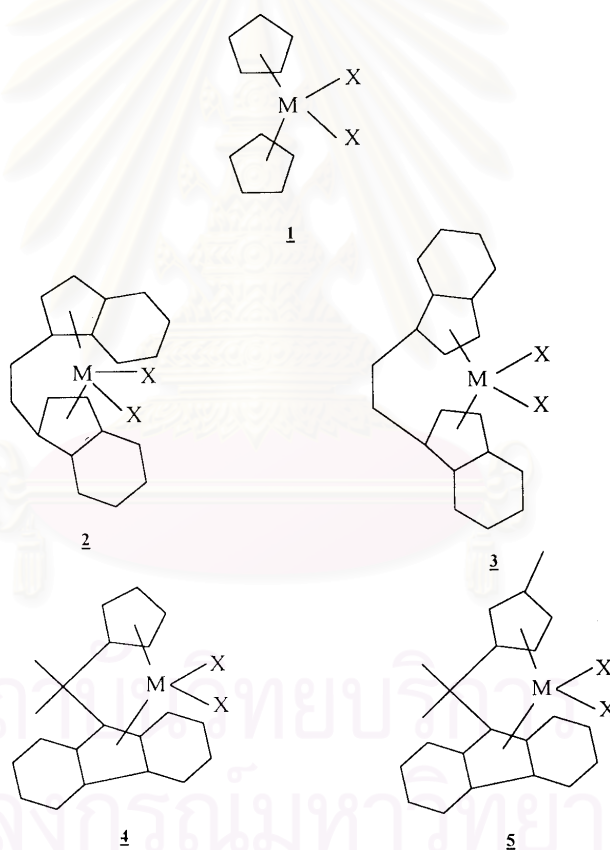


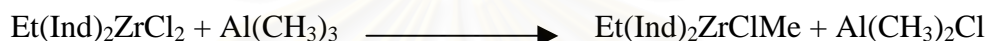
Figure 2.3 Scheme of the different metallocene complex structures [10]. Type 1 is C_{2v} -symmetric; Type 2 is C_2 -symmetric; Type 3 is C_s -symmetric; Type 4 is C_s -symmetric; Type 5 is C_1 -symmetric.

2.1.2. Polymerization Mechanism

The mechanism of catalyst activation is not clearly understood. However, alkylation and reduction of the metal site by a cocatalyst (generally alkyl aluminum or alkyl aluminoxane) is believed to generate the cationic active catalyst species.

First, in the polymerization, the initial mechanism started with formation of cationic species catalyst that is shown below.

Initiation



Propagation proceeds by coordination and insertion of new monomer unit in the metal carbon bond. Cossee mechanism is still one of the most generally accepted polymerization mechanism (Figure 2.4) [13]. In the first step, monomer forms a complex with the vacant coordination site at the active catalyst center. Then through a four-centered transition state, bond between monomer and metal center and between monomer and polymer chain are formed, increasing the length of the polymer chain by one monomer unit and generating another vacant site.

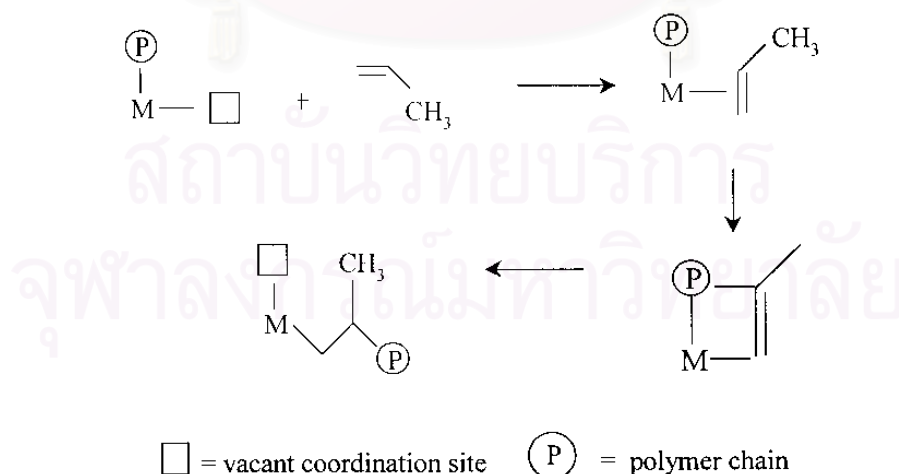


Figure 2.4 Cossee mechanism for Ziegler-Natta olefin polymerization [13].

The trigger mechanism has been proposed for the polymerization of α -olefin with Ziegler-Natta catalysts [1]. In this mechanism, two monomers interact with one active catalytic center in the transition state. A second monomer is required to form a new complex with the existing catalyst-monomer complex, thus trigger a chain propagation step. No vacant site is involved in this model. The trigger mechanism has been used to explain the rate enhancement effect observed when ethylene is copolymerized with α -olefins.

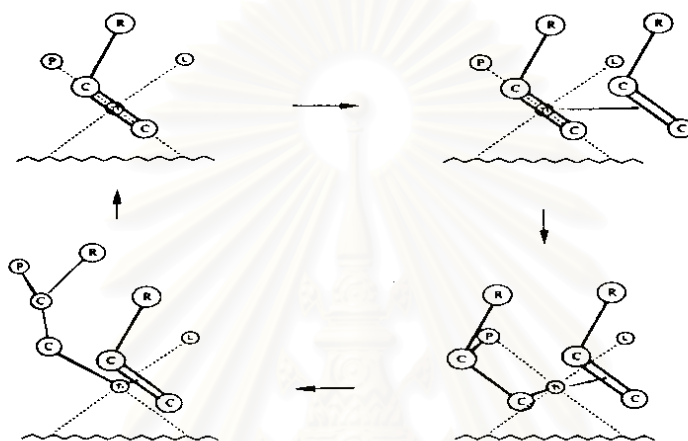


Figure 2.5 The propagation step according to the trigger mechanism [1].

After that, the propagation mechanism in polymerization shown in Figure 2.6.

Propagation

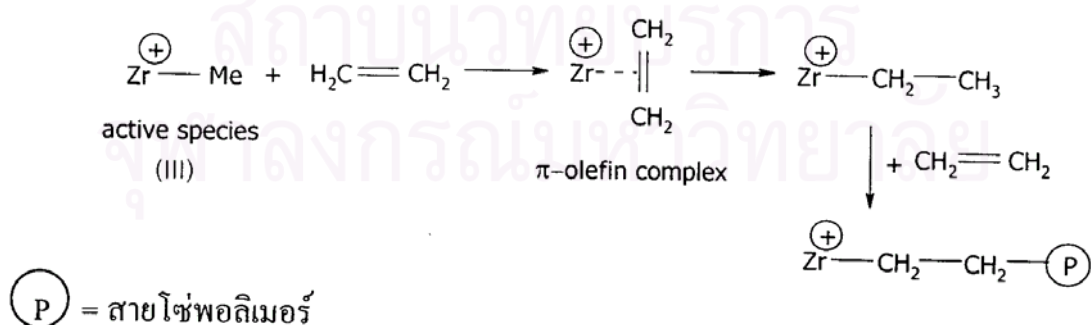


Figure 2.6 Propagation mechanism in polymerization

Finally, the termination of polymer chains can be formed by 1) chain transfer via β -H elimination, 2) chain transfer via β -Me elimination, 3) chain transfer to aluminum, 4) chain transfer to monomer, and 5) chain transfer to hydrogen (Figure 2.7-2.11)[10]. The first two transfer reactions form the polymer chains containing terminal double bonds.

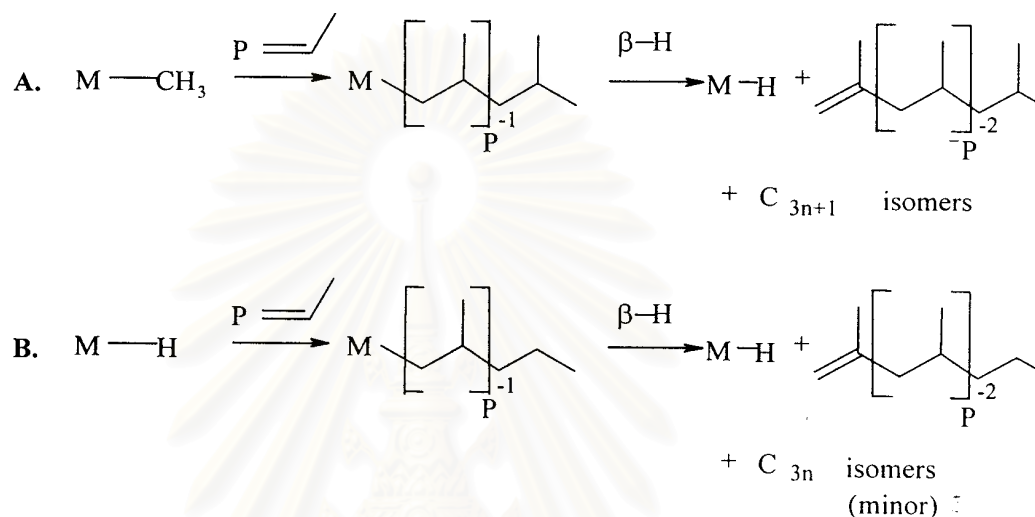


Figure 2.7 Chain transfer via β -H elimination [10]

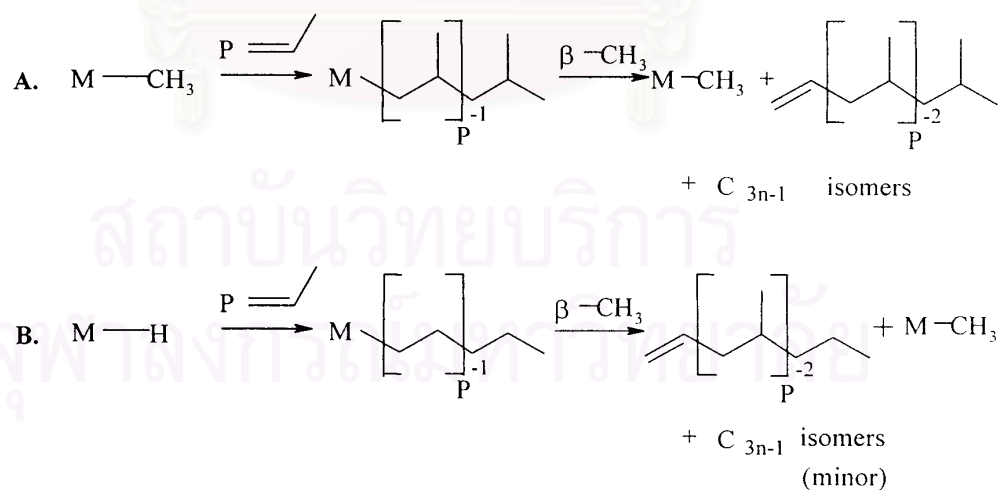


Figure 2.8 Chain transfer via β -CH₃ elimination [10]

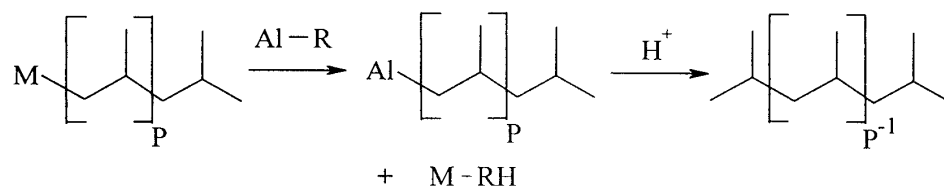


Figure 2.9 Chain transfer to aluminum [10]

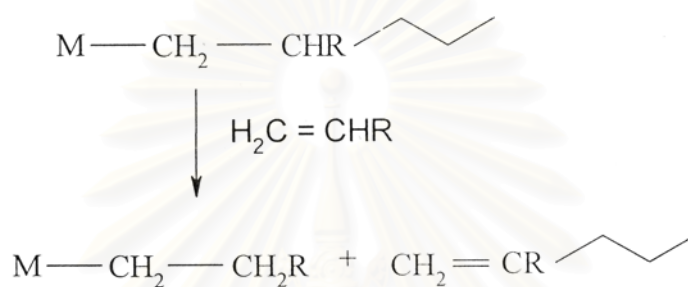


Figure 2.10 Chain transfer to monomer [10]

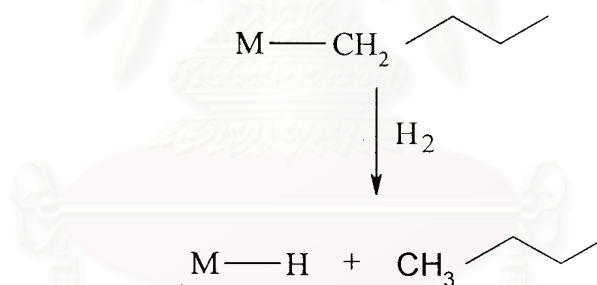


Figure 2.11 Chain transfer to hydrogen [10]

2.1.3. Cocatalysts

Metallocene catalysts have to be activated by a cocatalyst. The most common types of cocatalysts are alkylaluminums including methylaluminumoxane (MAO), trimethylaluminum (TMA), triethylaluminum (TEA), triisobutylaluminum (TIBA) and cation forming agents such as $(\text{C}_6\text{H}_5)_3\text{C}^+(\text{C}_6\text{F}_5)_4\text{B}^-$ and $\text{B}(\text{C}_6\text{F}_5)_3$ [14].

Among these, MAO is a very effective cocatalyst for metallocene. However, due to the difficulties and costs involved in the synthesis of MAO, there has been considerable effort done to reduce or elimination the use of MAO. Due to difficulties in separation, most commercially available MAO contains a significant fraction of TMA (about 10-30%) [15]. This TMA in MAO could be substantially eliminated by toluene-evaporation at 25°C.

Indeed, the difficulties encountered to better understand the important factors for an efficient activation are mainly due to the poor knowledge of the MAO composition and structure. Several types of macromolecular arrangements, involving linear chains, monocycles and/or various three-dimensional structures have been successively postulated. These are shown in Figure 2.12. In recent work, a more detailed image of MAO was proposed as a cage molecule, with a general formula $\text{Me}_{6m}\text{Al}_4\text{O}_{3m}$ (m equal to 3 or 4) [16].

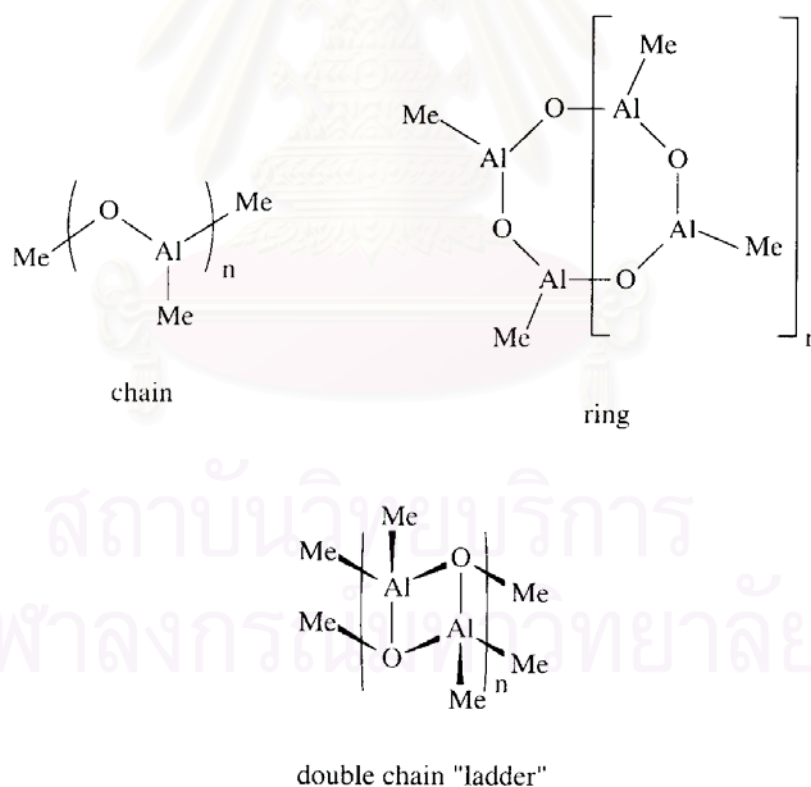


Figure 2.12 Early structure models for MAO [16]

In the case of $\text{rac-Et(Ind)}_2\text{ZrMe}_2$ as precursor, the extracted methyl ligands do not yield any modification in the structure and reactivity of the MAO counter-anion, thus allowing zirconium coordination site available for olefin that presented in Figure 2.13 [17].

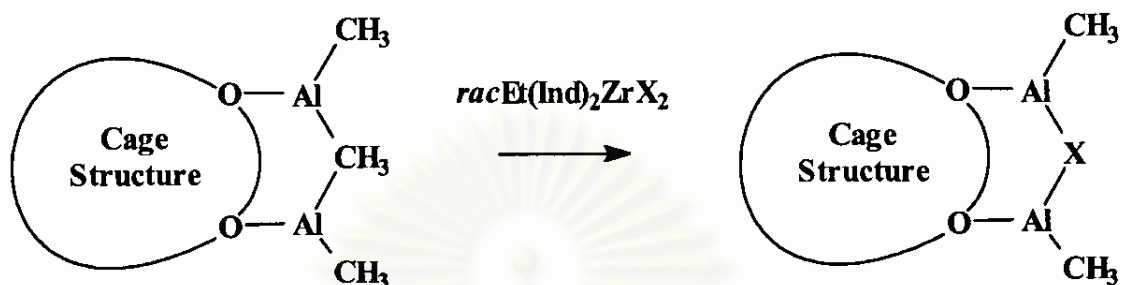


Figure 2.13 Representation of MAO showing the substitution of one bridging methyl group by X ligand extracted from $\text{racEt(Ind)}_2\text{ZrCl}_2$ ($X = \text{Cl}, \text{NMe}_2, \text{CH}_2\text{Ph}$) [17].

Cam and Giannini [18] investigated the role of TMA present in MAO by a direct analysis of $\text{Cp}_2\text{ZrCl}_2/\text{MAO}$ solution in toluene- d_8 using $^1\text{H-NMR}$. Their observation indicated that TMA might be the major alkylating agent and that MAO acted mainly as a polarization agent. However, in general it is believed that MAO is the key cocatalyst in polymerizations involving metallocene catalysts. The role of MAO included 1) alkylation of metallocene, thus forming catalyst active species, 2) scavenging impurities, 3) stabilizing the cationic center by ion-pair interaction and 4) preventing bimetallic deactivation of the active species.

The homogeneous metallocene catalyst cannot be activated by common trialkylaluminum only. However, Soga *et al.* [19] were able to produce polyethylene with modified homogeneous Cp_2ZrCl_2 activated by common trialkylaluminum in the presence of $\text{Si(CH}_3)_3\text{OH}$. Their results show that for an "optimum" yield aging of the catalyst and $\text{Si(CH}_3)_3\text{OH}$ mixture for four hours is required. However, MWD of the produced polymers is bimodal although the polymers obtained in the presence of MAO have narrow MWD.

Ethylene/ α -olefins copolymers with bimodal CCD were produced with homogeneous Cp_2ZrCl_2 with different cocatalysts such as MAO and mixture of

TEA/borate or TIBA/borate [20]. It seemed that the active species generated with different cocatalysts have different activities and produce polymers with different molecular weights.

2.1.4. Catalyst Activity

The ethylene polymerization rate of the copolymerization reaction with the catalyst system $\text{SiO}_2/\text{MAO}/\text{rac-Me}_2\text{Si [2-Me-4-Ph-Ind]}_2\text{ZrCl}_2$ was studied by Fink *et al.* [21]. The temperature was varied from 40 to 57°C. Small amount of hexene in the reaction solution increased the polymerization rate. The extent of the "comonomer effect" depended on the polymerization temperature. At 57°C the maximum activity of the ethylene/hexene copolymerization was 8 times higher than the homopolymerization under the same conditions. At 40°C the highest reaction rate for the copolymerization is only 5 times higher than that for the ethylene homopolymerization. For the polymer properties of the ethylene/ α -olefin copolymerization, the molecular weights of the polymers decreased with increasing comonomer incorporation. Ethylene/hexene copolymers produced by a metallocene catalyst also have the same melting point and glass transition temperature.

Series of ethylene copolymerization with 1-hexene or 1-hexadecene over four different siloxy-substituted ansa-metallocene/methylaluminoxane (MAO) catalyst systems were studied by Seppala *et al.* [22]. Metallocene catalysts $\text{rac-Et[2-(t-BuMe}_2\text{SiO)Ind]}_2\text{ZrCl}_2$ (1), $\text{rac-Et[1-(t-BuMe}_2\text{SiO)Ind]}_2\text{ZrCl}_2$ (2), $\text{rac-Et[2-(i-Pr}_3\text{SiO)Ind]}_2\text{ZrCl}_2$ (3) and $\text{rac-Et[1-(i-Pr}_3\text{SiO)Ind]}_2\text{ZrCl}_2$ (4) were used. The effects of minor changes in the catalyst structure, more precisely changes in the ligand substitution pattern were studied. They found that series of polymerization with siloxy-substituted bis(indenyl) ansa-metallocene are highly active catalyst precursors for ethylene- α -olefins copolymerizations. The comonomer response of all four catalyst precursors was good. Under the same conditions the order of copolymerization ability of the catalyst was $\text{rac-Et[2-(i-Pr}_3\text{SiO)Ind]}_2\text{ZrCl}_2 > \text{rac-Et[2-(t-BuMe}_2\text{SiO)Ind]}_2\text{ZrCl}_2$ and $\text{rac-Et[1-(i-Pr}_3\text{SiO)Ind]}_2\text{ZrCl}_2 > \text{rac-Et[1-(t-BuMe}_2\text{SiO)Ind]}_2\text{ZrCl}_2$. These catalysts are able to produce high molecular weight copolymers.

2.1.5. Copolymerization

By adding a small amount of comonomer to the polymerization reactor, the final polymer characteristics can be dramatically changed. For example, the Unipol process for linear low density polyethylene (LLDPE) uses hexene and the British Petroleum process (BP) uses 4-methylpentene to produce high-performance copolymers [23]. The comonomer can be affected the overall crystallinity, melting point, softening range, transparency and also structural, thermochemical, and rheological properties of the formed polymer. Copolymers can also be used to enhance mechanical properties by improving the miscibility in polymer blending [24].

Ethylene is copolymerized with α -olefin to produce polymers with lower densities. It is commonly observed that the addition of a comonomer generally increases the polymerization rate significantly. This comonomer effect is sometimes linked to the reduction of diffusion limitations by producing a lower crystallinity polymer or to the activation of catalytic sites by the comonomer. The polymer molecular weight often decreases with comonomer addition, possibly because of a transfer to comonomer reactions. Heterogeneous polymerization tends to be less sensitive to changes in the aluminum/transition metal ratio. Chain transfer to aluminum is also favored at high aluminum concentrations. This increase in chain transfer would presumably produce a lower molecular weight polymer. In addition, some researchers observed the decrease, and some observed no change in the molecular weight with increasing aluminum concentration [25].

The effect of polymerization conditions and molecular structure of the catalyst on ethylene/ α -olefin copolymerization have been investigated extensively. Pietikainen and Seppala [26] investigated the effect of polymerization temperature on catalyst activity and viscosity average molecular weights for low molecular weight ethylene/propylene copolymers produced with homogeneous Cp_2ZrCl_2 . Soga and Kaminaka [27] compared copolymerizations (ethylene/propylene, ethylene/1-hexene, and propylene/1-hexene) with $\text{Et}(\text{H}_4\text{Ind})_2\text{ZrCl}_2$ supported on SiO_2 , Al_2O_3 or MgCl_2 . Broadness of MWD was found to be related to the combination of support types and

types of monomers. The effect of silica and magnesium supports on copolymerization characteristics was also investigated by Nowlin *et al.* [28]. Their results indicated that comonomer incorporation was significantly affected by the way that support was treated based on the reactivity ratio estimation calculated with simplified Finemann Ross method. However, it should be noted that Finemann Ross method could be misleading due to linear estimation of nonlinear system.

Copolymer based on ethylene with different incorporation of 1-hexene, 1-octene, and 1-decene were investigated by Quijada [6]. The type and the concentration of the comonomer in the feed do not have a strong influence on the catalytic activity of the system, but the presence of the comonomer increases the activity compared with that in the absence of it. From ^{13}C -NMR it was found that the size of the lateral chain influences the percentage of comonomer incorporated, 1-hexene being the highest one incorporated. The molecular weight of the copolymers obtained was found to be dependent on the comonomer concentration in the feed, showing that there is a transfer reaction with the comonomer. The polydispersity (M_w/M_n) of the copolymers is rather narrow and dependent on the concentration of the comonomer incorporation.

Soga *et al.* [29] noted that some metallocene catalysts produce two-different types of copolymers in terms of crystallinity. They copolymerized ethylene and 1-alkenes using 6 different catalysts such as Cp_2ZrCl_2 , Cp_2TiCl_2 , Cp_2HfCl_2 , $\text{Cp}_2\text{Zr}(\text{CH}_3)_2$, $\text{Et}(\text{IndH}_4)_2\text{ZrCl}_2$ and $i\text{-Pr}(\text{Cp})(\text{Flu})\text{ZrCl}_2$. Polymers with bimodal crystallinity distribution (as measured by TREF-GPC analysis) were produced with some catalytic systems. Only $\text{Cp}_2\text{TiCl}_2\text{-MAO}$ and $\text{Et}(\text{H}_4\text{Ind})_2\text{ZrCl}_2\text{-MAO}$ produced polymers that have unimodal crystallinity distribution. The results seem to indicate that more than one active site type are present in some of these catalysts. However, it is also possible that unsteady-state polymerization conditions might have caused the broad distributions since the polymerization times were very short (5 minutes for most cases).

Marques *et al.* [30] investigated copolymerization of ethylene and 1-octene by using the homogeneous catalyst system based on $\text{Et}(\text{Flu})_2\text{ZrCl}_2/\text{MAO}$. A study was performed to compare this system with that of $\text{Cp}_2\text{ZrCl}_2/\text{MAO}$. The influence of different support materials for the Cp_2ZrCl_2 was also evaluated, using silica, MgCl_2 , and the zeolite sodic mordenite NaM. The copolymer produced by the $\text{Et}(\text{Ind})_2\text{ZrCl}_2/\text{MAO}$ system

showed higher molecular weight and narrower molecular weight distribution, compared with that produced by $\text{Cp}_2\text{ZrCl}_2/\text{MAO}$ system. Because of the extremely congested environment of the fluorenyl rings surrounding the transition metal, which hinders the beta hydrogen interaction, and therefore, the chain transference. Moreover, the most active catalyst was the one supported on SiO_2 , whereas the zeolite sodic mordenite support resulted in a catalyst that produced copolymer with higher molecular weight and narrower molecular weight distribution. Both homogeneous catalytic systems showed the comonomer effect, considering that a significant increase was observed in the activity with the addition of a larger comonomer in the reaction medium.

The effect of different catalyst support treatments in the 1-hexene/ethylene copolymerization with supported metallocene catalyst was investigated by Soares *et al.* [31]. The catalysts in the study were supported catalysts containing SiO_2 , commercial MAO supported on silica (SMAO) and MAO pretreated silica (MAO/silica) with Cp_2HfCl_2 , $\text{Et}(\text{Ind})_2\text{HfCl}_2$, Cp_2ZrCl_2 and $\text{Et}(\text{Ind})_2\text{ZrCl}_2$. All the investigated supported catalysts showed good activities for the ethylene polymerization (400-3000 kg polymer/mol metal.h). Non-bridged catalysts tend to produce polymers with higher molecular weight when supported on to SMAO and narrow polydispersity. The polymer produced with Cp_2HfCl_2 supported on silica has only a single low crystallinity peak. On the other hand, Cp_2HfCl_2 supported on SMAO and MAO/silica produced ethylene/1-hexene copolymers having bimodal CCDs. For the case of Cp_2ZrCl_2 and $\text{Et}(\text{Ind})_2\text{ZrCl}_2$, only unimodal CCDs were obtained. It seems that silica-MAO-metallocene and silica-metallocene site differ slightly in their ability to incorporate comonomer into the growing polymer chain, but not enough to form bimodal CCDs.

Soares *et al.* [4] studied copolymerization of ethylene and 1-hexene. It was carried out with different catalyst systems (homogeneous $\text{Et}(\text{Ind})_2\text{ZrCl}_2$, supported $\text{Et}(\text{Ind})_2\text{ZrCl}_2$ and in-situ supported $\text{Et}(\text{Ind})_2\text{ZrCl}_2$). Supported $\text{Et}(\text{Ind})_2\text{ZrCl}_2$: an $\text{Et}(\text{Ind})_2\text{ZrCl}_2$ solution was supported on SMAO. It was used for polymerization of ethylene and 1-hexene. In-situ supported $\text{Et}(\text{Ind})_2\text{ZrCl}_2$: an $\text{Et}(\text{Ind})_2\text{ZrCl}_2$ solution was directly added to SMAO in the polymerization reactor, in the absence of soluble MAO. Homogeneous $\text{Et}(\text{Ind})_2\text{ZrCl}_2$ showed higher catalytic activity than the corresponding supported and in-situ supported metallocene catalysts. The relative reactivity of 1-hexene increased in the following order: supported metallocene \approx in-situ supported metallocene <

homogeneous metallocene catalysts. The MWD and short chain branching distribution (SCBD) of the copolymer made with the in-situ supported metallocene were broader than those made with homogeneous and supported metallocene catalysts. They concluded that there are at least two different active species on the in-situ supported metallocene catalyst for the copolymerization of ethylene and 1-hexene.

Soares *et al.* [5] investigated copolymerization of ethylene and 1-hexene with different catalysts: homogeneous $\text{Et}(\text{Ind})_2\text{ZrCl}_2$, Cp_2HfCl_2 and $[(\text{C}_5\text{Me}_4)\text{SiMe}_2\text{N}(\text{tert-Bu})]\text{TiCl}_2$, the corresponding in-situ supported metallocene and combined in-situ supported metallocene catalyst (mixture of $\text{Et}(\text{Ind})_2\text{ZrCl}_2$ and Cp_2HfCl_2 and mixture of $[(\text{C}_5\text{Me}_4)\text{SiMe}_2\text{N}(\text{tert-Bu})]\text{TiCl}_2$. They studied properties of copolymers by using ^{13}C -NMR, gel permeation chromatography (GPC) and crystallization analysis fractionation (CRYSTAF) and compared with the corresponding homogeneous metallocene. The in-situ supported metallocene produced polymers having different 1-hexene fractions, SCBD and MDW. It was also demonstrated that polymers with broader MWD and SCBD can be produced by combining two different in-situ supported metallocenes.

In addition, Soares *et al.*[32] studied copolymerization of ethylene and 1-hexene with an in-situ supported metallocene catalysts. Copolymer was produced with alkylaluminum activator and effect on MWD and SCBD was examined. They found that TMA exhibited the highest activity while TEA and TIBA had significantly lower activities. Molecular weight distributions of copolymers produced by using the different activator types were unimodal and narrow, however, short chain branching distributions were very different. Each activator exhibited unique comonomer incorporation characteristics that can produce bimodal SCBD with the use of a single activator. They used individual and mixed activator system for controlling the SCBDs of the resulting copolymers while maintaining narrow MWDs.

2.2 Heterogeneous System

The new metallocene/MAO systems offer more possibilities in olefin polymerization compared to conventional Ziegler-Natta catalysts, such as narrow stereoregularity, molecular weight and chemical composition distributions (CCDs) through ligand design. However, only heterogeneous catalysts can be practically used for

the existing gas phase and slurry polymerization processes. Without using a heterogeneous system, high bulk density and narrow size distribution of polymer particles cannot be achieved. The advantages of supporting catalysts include improved morphology, less reactor fouling, lower Al/metal mole ratios required to obtain the maximum activities in some cases the elimination of the use of MAO, and improved stability of the catalyst due to much slower deactivation by bimolecular catalyst interactions. Therefore, developing heterogeneous metallocene catalysts, that still have all the advantages of homogeneous systems, became one of the main research objectives of applied metallocene catalysis.

Steinmetz *et al.* [33] examined the particle growth of polypropylene made with a supported metallocene catalyst using scanning electron microscopy (SEM). They noticed formation of a polymer layer only on the outer surface of catalyst particles during the initial induction period. As the polymerization continued, the whole particle was filled with polymer. Particle fragmentation pattern depended on the type of supported metallocene.

2.2.1. Catalyst Chemistry

The nature of the active sites affects the polymer morphology, catalyst stability and activity, and the characteristics of the polymer produced. However, structure and chemistry of the active sites in supported catalysts are not clearly understood. Catalytic activities for supported metallocene are usually much lower than that of their counterpart homogeneous system. Formation of different active species, deactivation of catalyst during supporting procedure, and mass transfer resistance may contribute to decreased catalyst activity.

Tait *et al.* [34] reported general effects of support type, treatment, supporting procedure, and type of diluents on reaction kinetics and physical properties of polymer produced. Although the activities of supported catalysts are much lower compared to homogeneous systems. The activity of catalysts increased slightly when *o*-dichlorobenzene was introduced in toluene

The catalytic activities of supported catalyst depended on the percentage of the incorporated metallocene was reported by Quijada *et al.* [35]. However, in the case of metallocenes supported on MAO pretreated silica, depending on how the surface bound MAO complex with the catalyst, the activity can be as high as that of homogeneous system. According to the experiment by Chein *et al.* [36], if a single MAO is attached to silica, it would complex with zirconocene and lowers its activity. On the other hand, if multiple MAOs are attached to the surface silanol, the supported zirconocene will not be further complexed with MAO and have activity.

2.2.2. Supporting Methods

In the case of carriers like silica or other inorganic compounds with OH group on the surface, the resulting catalyst displayed very poor activities even combined with MAO. The reaction of metallocene complexes with the Si-OH groups might cause the decomposition of active species. Such decomposition could be suppressed by fixing MAO on the silica surface and then reacting with metallocenes [37]. Therefore, silica must be pretreated before the interaction with metallocene, to reduce the OH concentration and to prepare an adequate surface for metallocene adsorption and reaction in a non-deactivating way [38]. Metallocene immobilization methods can be divided in to three main groups. The first method is the direct support of catalyst onto an inert support. The second method involves the pretreatment of the inert support with MAO or other alkylaluminum followed by metallocene supporting. The third method, the catalyst is chemically anchored to the support, which often involves in-situ catalyst synthesis. These methods produce catalysts with distinct activities, comonomer reactivity ratios, and stereospecificities.

2.2.2.1 Direct Supporting of Inert Material

Collins *et al.* [39] reported that $\text{Et}(\text{Ind})_2\text{ZrCl}_2$, when supported on partially dehydrated silica, reacted with surface hydroxyl groups during adsorption to form inactive catalyst precursors and free ligands (Fig 2.14.). Therefore, the activity is lower compared to the case of using dehydrated silica. Figure 2.15 shows the proposed structure $\text{Et}(\text{Ind})_2\text{ZrCl}_2$ supported on alumina. For the case of alumina, the activity of catalyst supported on dehydrated alumina is lower than the one supported on partially

dehydrated alumina. The high Lewis acidity of aluminum sites on dehydrated alumina facilitates the formation of Al-Cl bonds and Zr-O bonded species when the metallocene compound is adsorbed on these sites. However, the metal sites in this case remain inactive even after MAO addition.

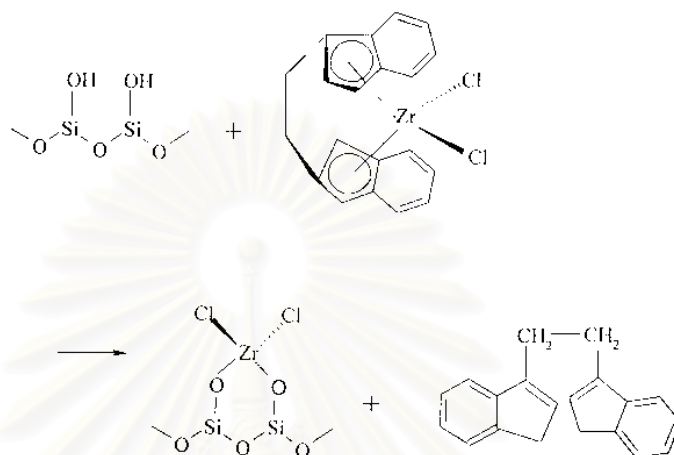


Figure 2.14 Structure of $\text{Et}(\text{Ind})_2\text{ZrCl}_2$ supported on silica [39]

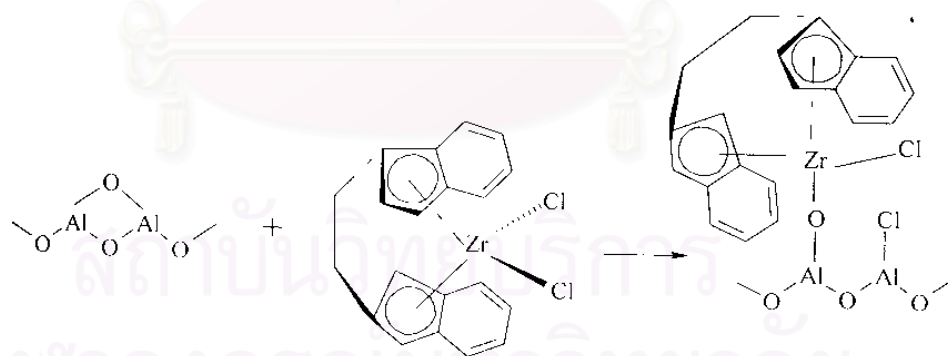


Figure 2.15 Structure of $\text{Et}(\text{Ind})_2\text{ZrCl}_2$ supported on alumina [39]

Kaminsky *et al.* [40] proposed a possible explanation for the different behavior of metallocene supported directly on to silica, homogeneous systems, or supported onto MAO-pretreated silica. It is assumed that the supporting of metallocenes on silica takes place in three stages. First, the metallocene reacts with OH groups of the silica as shown in Figure 2.16.

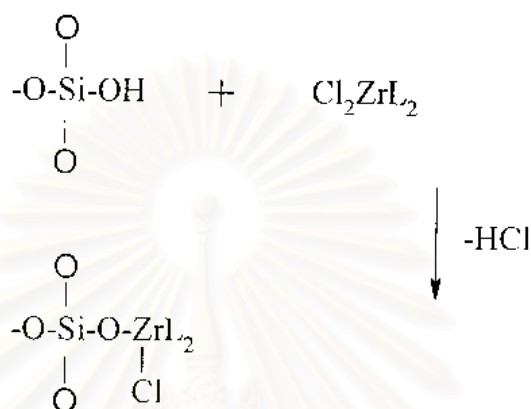


Figure 2.16 Reaction of silica and metallocene during catalyst supporting [40], where L is a ligand (Cp, Ind).

The second step is the alkylation by MAO as shown in Figure 2.17:

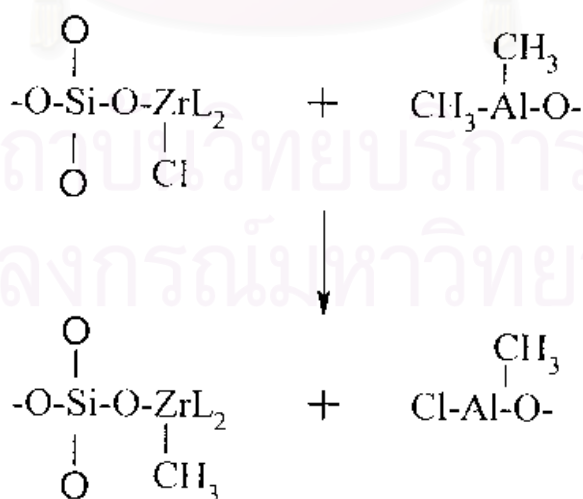


Figure 2.17 Alkylation of supported metallocene by MAO [40]

The third step is the dissociation of the $-\text{SiO}_2\text{-O-Zr-}$ bond to an ion pair to form the cation active center $(\text{SiO})^-(\text{Zr})^+$. The polydispersity of polymers produced with these supported metallocenes are reported to be relatively high ($5 \approx 8$) due to different electronic and steric interactions between the silica surface and the metal active sites. The immobilization of the zirconocene on silica inhibits bimolecular deactivation processes because the active sites are separated from each other.

As a consequence less use of MAO is required, increased molecular weights are achieved due to the reduction of β -hydrogen transfer by a second zirconocene center, and polypropylene of higher isotacticity and melting point is formed.

2.2.2.2. Supporting Catalyst on Materials Treated with Alkylaluminum

When silica is pretreated with MAO, the supporting mechanism is different. The zirconocene is complexed to MAO supported on silica, which will make the catalyst similarly to a homogeneous system. The polymers produced in this way have lower molecular weights.

Hiatky and Upton [41] reported that supporting of the aluminum-alkyl free catalysts can formed 2 complexes as shown in Figure 2.18, (a) deactivation through coordination of Lewis- basic surface oxides to the electrophilic metal center or (b) reaction of the ionic complex with residual surface hydroxyl groups.

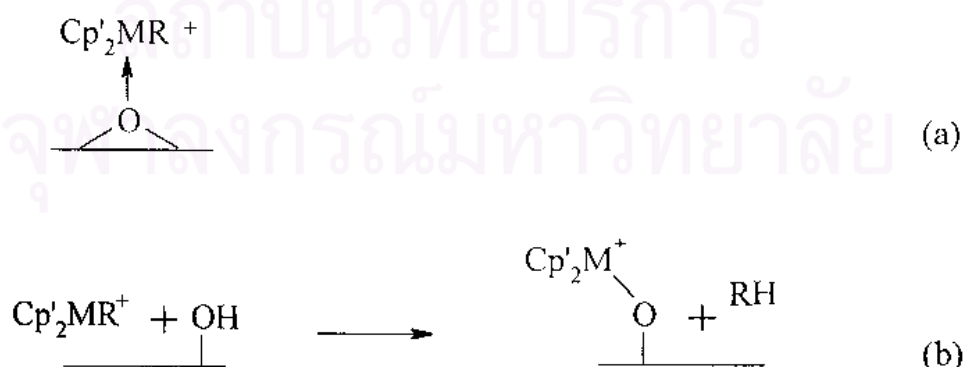


Figure 2.18. Effect of surface hydroxyl groups on ionic metallocene catalysts [41]

However, highly active supported ionic metallocene catalysts for olefin polymerization can be prepared by pretreating the support with scavenger. It is assumed that pretreatment of the support with a scavenger serves to activate the support and compatibilize it with the ionic metallocene complex.

Lee *et al.* [42] used TMA pretreated-silica as the support for metallocene catalysts. The activity of supported catalysts showed dependency to H₂O content in silica, H₂O/TMA ratio, metallocene, and cocatalyst. The supported catalyst was also able to polymerize ethylene in the absence of MAO when common alkyl aluminum was used as the cocatalyst.

The surface aluminum and metallocene loading was studied by Santos *et al.* [43]. About 7 wt% of MAO can be supported on silica when the initial amount of MAO in mixture of silica was ca. 10 wt%. Depending on silica types, saturation of MAO supported on silica can occur at lower MAO contents.

Harrison *et al.* [44] compared a variety of silica and alumina supports with different degrees of surface hydroxylation as the supports. It was shown that as the concentration of OH groups on the surface of the support increased, more MAO could be impregnated and thus catalyst with more metallocene content could be produced. The most obvious benefit of supported catalyst with more metallocene was increased activities compared to catalysts with lower concentration of surface hydroxyl groups (increased activities both in kg PE/mol Zr/hr and kg PE /g-support/h). However, at high polymerization temperatures, leaching of catalyst from the support was observed. In lower polymerization temperatures, leaching was less significant, however, the morphology and bulk density of the polymer formed were still unsuitable for use in gas-phase polymerization.

For the case of propylene polymerization, a decrease in syndiotacticity was observed by Xu *et al.* [45] when the metallocene catalyst was supported on pretreated silica.

2.2.2.3. Chemically Anchoring Catalyst on Support

Soga *et al.* [46] described a method to support zirconocenes more rigidly on SiO_2 . The supporting steps are as follows: 1) Silica was treated with SiCl_4 to substitute the OH groups with chlorine atoms. 2) The resulting silica was filtered and washed with tetrahydrofuran (THF). 3) The solid was re-suspended in THF and a lithium salt of indene, dissolved in THF, was added drop-wise. 4) The resulting solid was filtered and washed again with THF. And to re-suspended solid in THF, $\text{ZrCl}_4 \cdot 2\text{THF}$ dissolved in THF was added. The final solid part was separated by filtration, washed with THF and diethyl ether, and dried under vacuum. The supported catalyst produced in this way showed higher isospecificity than the corresponding homogenous system for propylene polymerization. MAO or ordinary alkylaluminums were used as cocatalysts. The yield was higher when MAO was used as the cocatalyst, but the molecular weight of the polypropylene was half of the molecular weight obtained when TIBA was used as the cocatalyst (3.4×10^5 g/mol and 7.2×10^5 g/mol, respectively). Figure 2.19 shows the structure of the silica supported metallocenes.

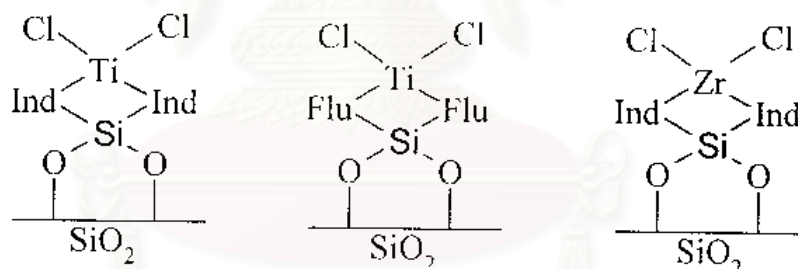


Figure 2.19. Structure of some silica supported metallocene catalysts [46]

Lee *et al.* [47] used spacer molecules in supporting metallocene catalysts onto silica to eliminate the steric hindrance near the active site caused by the silica surface (Figure 2.20).

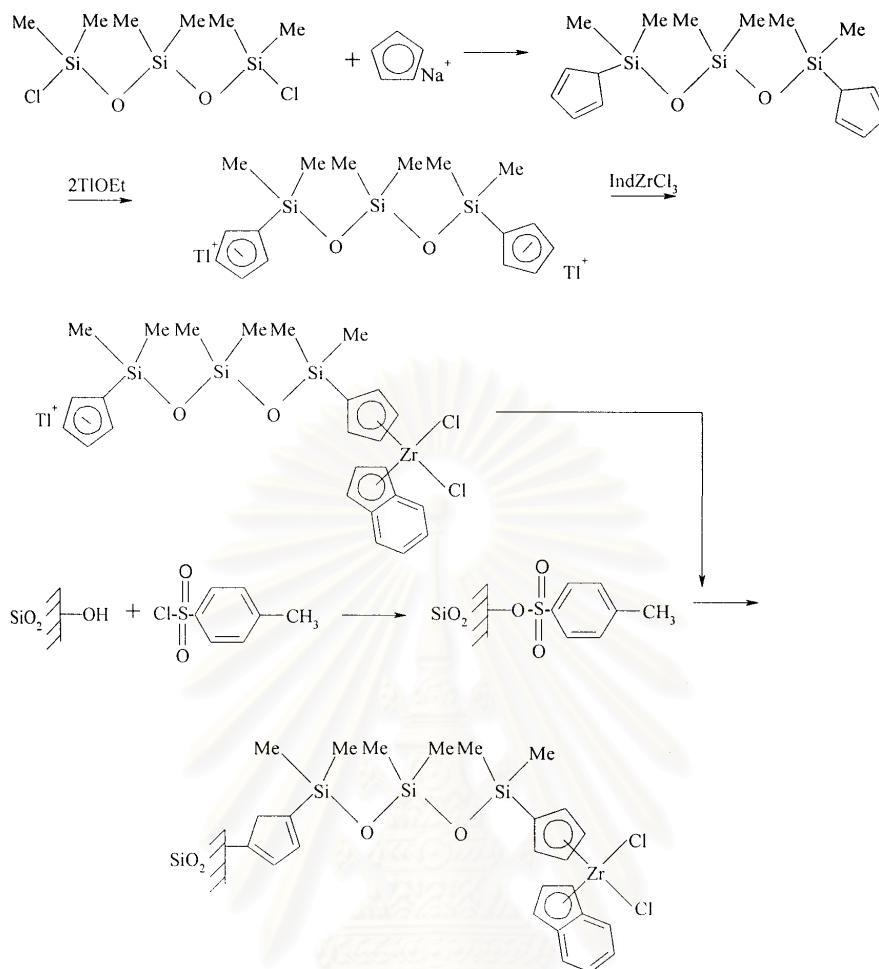


Figure 2.20. Mechanism for supporting metallocene catalysts on silica using spacer molecules [47].

By distancing the active site from the silica surface, higher catalytic activities but lower polymer molecular weights were obtained in comparison with analogous silica-supported catalysts without spacer between silica and CpIndZrCl_2 .

Iiskola *et al.* [48] treated the surface of partially dehydroxylated silica with a silane coupling agents, $\text{Cp}(\text{CH}_2)_3\text{Si}(\text{OCH}_2\text{CH}_3)_3$, and then immobilized CpZrCl_3 onto cyclopentadienyl surface formed on the silica to obtain a highly active catalyst (Figure 2.21) for ethylene polymerization in the presence of MAO. Depending on the calcination temperature and the modification methods, the catalysts show different

activities and produced polymers with different molecular weights. In general, when compared to homogeneous Cp_2ZrCl_2 systems, all the supported catalysts showed lower activities, but the polymers produced had higher molecular weights. On the other hand, when compared to homogeneous Cp_2ZrCl_2 systems, the activities of the supported catalysts were similar but molecular weights of polymer produced were lower and depended on the silica surface modification method used. The polydispersity index of the polymers ranged from 2.2 to 2.8.

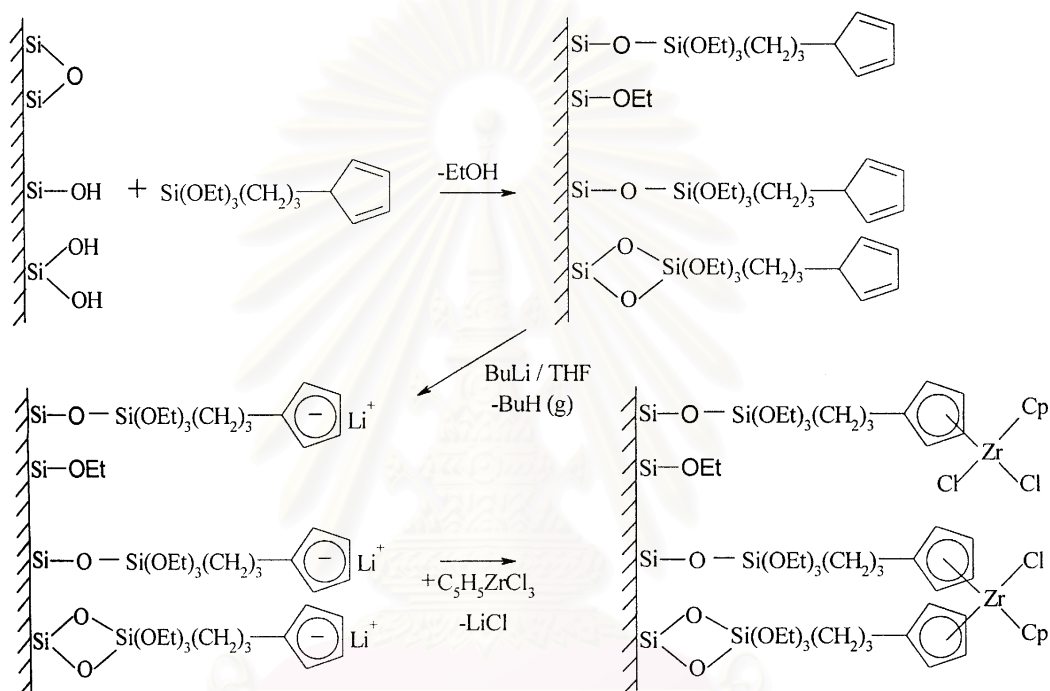


Figure 2.21. Modification of silica with $\text{Cp}(\text{CH}_2)_3\text{Si}(\text{OCH}_2\text{CH}_3)_3$ and preparation of supported metallocene catalysts [48].

2.2.2.4. Supporting on Other Supports

Lee and Yoon [49] studied ethylene and styrene homopolymerization initiated by cyclodextrin (CD) supported Cp_2ZrCl_2 or Cp^*TiCl_3 catalyst. The effect of CD pretreatment with MAO or TMA on catalyst behaviors was shown that either TMA or MAO could be used as cocatalyst for ethylene polymerization while only MAO could initiate the styrene polymerization with α -CD supported catalysts.

Marques *et al.* [50] investigated ethylene polymerization by using Y zeolite-supported Cp_2ZrCl_2 catalysts. These system produced polyethylene with higher molecular weight and as narrow a molecular weight distribution as the homogeneous precursor, however, at relatively lower activity. The main characteristic that makes a zeolite a good support for metallocene catalyst seems to be a high Si/Al value and therefore a low Al density on the surface of the zeolite. This suggests that the presence of isolated aluminium atoms favors the fixation of zirconocene.

Moreover, Michelotti *et al.* [51] studied copolymerization of ethylene with higher α -olefins, such as 4-methyl-1-pentene, 1-hexene, 1-octene and 1-dodecene. The catalytic behavior of various metallocene (Cp_2ZrCl_2 , $\text{Ind}_2\text{ZrCl}_2$, $\text{Et}(\text{Ind})_2\text{ZrCl}_2$, and $\text{Et}(\text{Ind})_2\text{HfCl}_2$) supported on methylalumoxane-pretreated HY zeolite ($\text{SiO}_2/\text{Al}_2\text{O}_3=5.7$) were compared.

Meshkova *et al.* [52] investigated ethylene polymerization in the presence of ZSM-5(H_2O)/TMA- $\text{Et}(\text{Ind})_2\text{ZrCl}_2$. They found that the synthesis of MAO directly on the zeolite support and the absence of free MAO may be one of the way of the reduction of supported zirconocene catalyst leaching. The positive temperature coefficient of polymerization rate as well as the increase of molecular weight and melting point of PE obtained with the zeolite supported zirconocene catalyst developed in this work compared to PE produced by homogeneous zirconocene system confirms this view.

Weiss *et al.* [53] investigated the clay minerals kaolin and montmorillonite as inorganic carriers for the polymerization of ethylene and propylene with Cp_2ZrCl_2 , Cp_2ZrHCl or Cp_2TiCl_2 catalyst and TMA as cocatalyst. The heterogeneous catalysts on kaolin were less active in ethylene polymerization than comparable homogeneous catalysts. But the heterogeneous catalysts on montmorillonite are often more active in ethylene or propylene polymerization than comparable homogeneous catalysts.

Looveren *et al.* [54] studied methylalumoxane (MAO)-MCM-41 as support in the co-oligomerization of ethene and propene with $[\text{C}_2\text{H}_4(\text{Ind})_2\text{Zr}(\text{CH}_3)_2]$.

They were found that the MAO-MCM-41 was catalytically more active than the corresponding silica-based MAO derivative or the homogeneous system.

2.3. Polymer Characterization

2.3.1. Size Exclusion Chromatography (SEC)

Size exclusion chromatography (SEC) is also known as the gel permeation chromatography (GPC). In this method, the polymer chains are fractionated based on their hydrodynamic volume in solution as they flow through column(s) packed with particles of varying porosity.

The MWD obtained by GPC can be modeled as a superposition of polymer chains produced at different catalyst site types. Therefore, by deconvoluting broad MWDs into narrower theoretical distributions, such as Flory's most probable distribution, information on active center types can be obtained in addition to the information on polymer chain length [55].

2.3.2. Fractionation Methods Based on Polymer Crystallinity

Fractionation based on polymer crystallinity in dilute solutions can be used to estimate the distribution of chemical composition and stereoregularity of polyolefins.

2.3.2.1. Temperature Rising Elution Fractionation (TREF)

The primary steps of preparation involved in TREF are 1) dissolution of polymer in solvent at high temperature, 2) precipitation of polymer onto an inert support under very slow cooling rate (not more than 0.1°C/hr), and 3) elution and fractionation of polymer under slow heating to re-dissolve the precipitated polymer chains. TREF can be operated in analytical or preparative modes.

An attempt to model the fractionation process on TREF based on thermodynamic model was made by Borrajo *et al.* [56]. In addition to Flory-Huggins

theory, they considered effects of melting temperature, melting enthalpy, average crystallinity, average crystallizable sequence length, and polymer-solvent interactions. The thermodynamic model divides each chain by crystallizable homopolymer blocks and non-crystallizable highly branched copolymer blocks. Therefore, statistically, every individual chain has distribution of longest to the shortest crystallizable lengths. Since molecular weights of commercial copolymers are large enough for a single chain to form crystallites of different lamella thickness, the effect of chain length is not usually considered in this kind of approach. Their model further assumes that the crystallites have similar thickness. The model predicted the dependence of previously mentioned parameters in reasonable manner when was compared with experimental results.

2.3.2.2. Crystallization Analysis Fractionation (CRYSTAF)

Polymers with different ethylene sequence lengths will crystallize at different temperature due to the differences in minimum crystallite thickness that can be in different temperatures. Unlike TREF, CRYSTAF analysis is conducted during the crystallization period by measuring polymer concentration in solution. Randall [57] used homogeneous ethylene/1-octene copolymers with narrow CCDs, made with a constrained geometry catalyst, to establish a correlation between CRYSTAF result and comonomer content in the polymer. The calibration curve obtained was linear and could be used for ethylene/1-octene copolymers for the weight of 1-octene up to about 40%.

2.3.3. Other Characterization Methods

2.3.3.1. Nuclear Magnetic Resonance (NMR)

NMR is an absolute method that does not require calibration. The locations of the resonance peaks identify type of branches or end groups. Santos *et al.* [6] used ^{13}C -NMR for studying the incorporation of the α -olefins in the polymeric chain, sequence of the type ethylene-comonomer-ethylene-comonomer and ethylene-comonomer-comonomer are found in very low concentrations. The tendency of incorporations is: 1-hexene > 1-octene > 1-decene.

2.3.3.2. Differential Scanning Calorimetry (DSC)

Melting points and melting enthalpies can be measured by DSC. Depending on comonomer presence and polymerization conditions, the melting points of copolymers can be changed significantly. In addition to measuring melting points and fusion enthalpies, attempts were made to use DSC to get information on the distribution of microstructure of polymer samples. DSC can be used to determine rough chemical composition distributions based on the peak broadness in DSC curve. To enhance this result, polymer samples can be slowly annealed at different temperature ranges before the analysis or by using more sensitive solution phase DSC [58].



สถาบันวิทยบริการ
จุฬาลงกรณ์มหาวิทยาลัย

CHAPTER III

EXPERIMENTAL

In the present study of the copolymerization of ethylene/ α -olefin with the supported metallocene catalysts, the experiments were divided into four parts:

- (i) Catalyst preparation,
- (ii) Ethylene and α -olefin copolymerization with the prepared catalyst,
- (iii) Characterization of catalyst precursor,
- (iv) Characterization of ethylene and α -olefin copolymer products.

The details of the experiments are explained as follows.

3.1 Chemicals

The chemicals used in these experiments were analytical grade, but only major materials are specified as follows:

1. rac-Ethylenebis(indenyl)zirconium dichloride ($\text{Et}(\text{Ind})_2\text{ZrCl}_2$) was supplied from Aldrich Chemical Company, Inc. and used without further purification.
2. Ethylene gas (99.96%) was devoted from National Petrochemical Co., Ltd., Thailand and used as received.
3. 1-Hexene (99+%) was purchased from Aldrich Chemical Company, Inc. and purified by distilling over sodium under argon atmosphere before use.
4. 1-Octene (98%) was purchased from Aldrich Chemical Company, Inc. and used as received.
5. 1-Decene ($\geq 97\%$) was purchased from Fluka Chemie A.G. Switzerland. and used as received.
6. Methylaluminoxane (MAO) 2.534 M in toluene was donated from Tosoh Akso, Japan and used without further purification.
7. Trimethylaluminum $[\text{Al}(\text{CH}_3)_3]$ 2.0 M in toluene was supplied from Nippon Aluminum Alkyls Ltd., Japan and used without further purification.

8. Silica gel from Fuji Silasia Chemical Ltd., (Cariact P-10, surface area 300 m²/g) was calcined at 400 °C for 6 hours under vacuum.

9. Silicon tetrachloride (SiCl₄) was obtained from Aldrich Chemical Company, Inc. and used without further purification.

10. Sodium hydrogen carbonate was purchased from Fluka Chemie A.G., Switzerland was used as received.

11. Toluene was devotes from EXXON Chemical Ltd., Thailand. This solvent was dried over dehydrated CaCl₂ and distilled over sodium/benzophenone under argon atmosphere before use.

12. Ultra high purity argon gas (99.999%) was purchased from Thai Industrial Gas Co., Ltd., and further purified by passing through columns packed with molecular sieve 3 A, BASF Catalyst R3-11G, sodium hydroxide (NaOH) and phosphorus pentaoxide (P₂O₅) to remove traces of oxygen and moisture.

3.2 Equipments

All types of equipments used in the catalyst precursor preparation and polymerization are listed below:

3.2.1 Cooling System

The cooling system was in the solvent distillation in order to condense the freshly evaporated solvent.

3.2.2 Inert Gas Supply

The inert gas (argon) was passed through columns of BASF catalyst R3-11G as oxygen scavenger, molecular sieve 3A to remove moisture. The BASF catalyst was regenerated by treatment with hydrogen at 300 °C overnight before flowing the argon gas through all the above columns. The inert gas supply system is shown in Figure 3.1.

3.2.3 Magnetic Stirrer and Heater

The magnetic stirrer and heater model RTC basis from IKA Labortechnik were used.

3.2.4 Reactor

A 100 ml stainless steel autoclave was used as the copolymerization reactor.

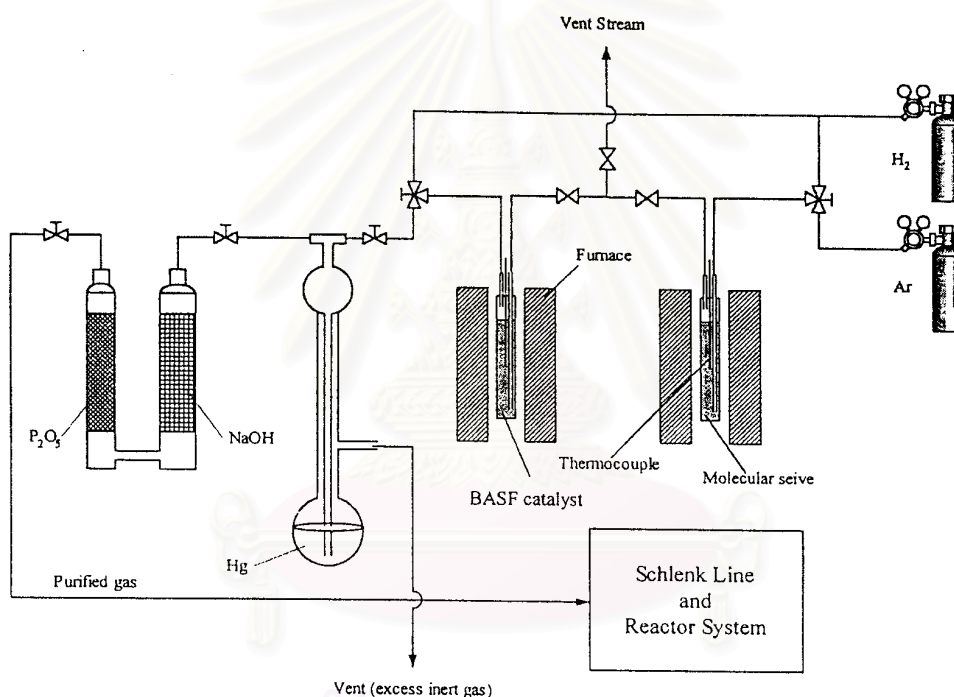


Figure 3.1 Inert gas supply system

3.2.5 Schlenk Line

Schlenk line consists of vacuum and argon lines. The vacuum line was equipped with the solvent trap and vacuum pump, respectively. The argon line was connected with the trap and the mercury bubbler that was a manometer tube and contain enough mercury to provide a seal from the atmosphere when argon line was evacuated. The Schlenk line was shown in Figure 3.2.

3.2.6 Schlenk Tube

A tube with a ground glass joint and side arm, which was three-way glass valve as shown in Figure 3.3. Sizes of Schlenk tubes were 50, 100 and 200 ml used to prepare catalyst and store materials which were sensitive to oxygen and moisture.

3.2.7 Vacuum Pump

The vacuum pump model 195 from Labconco Corporation was used. A pressure of 10^{-1} to 10^{-3} mmHg was adequate for the vacuum supply to the vacuum line in the Schlenk line.

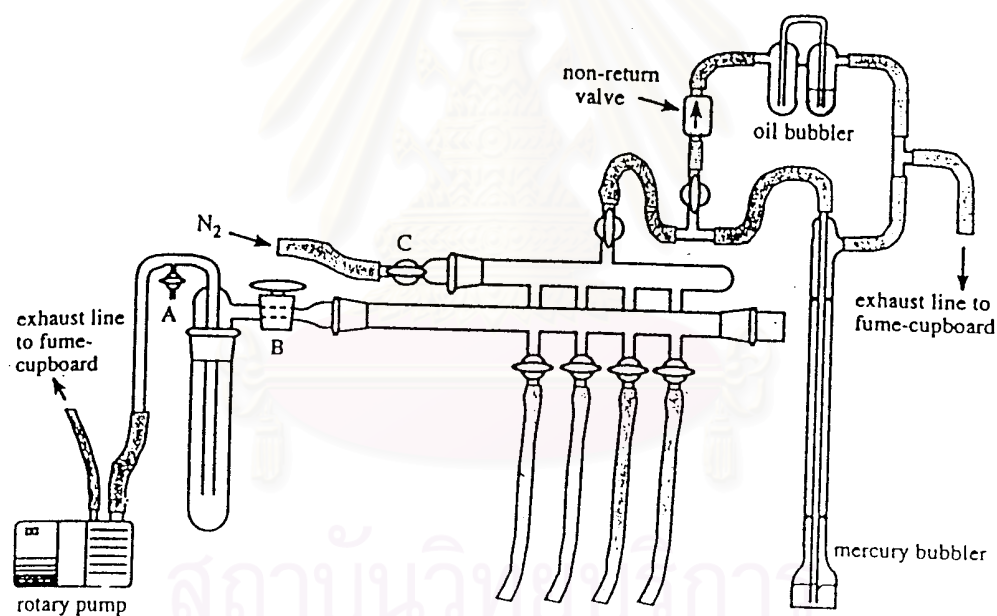


Figure 3.2 Schlenk line

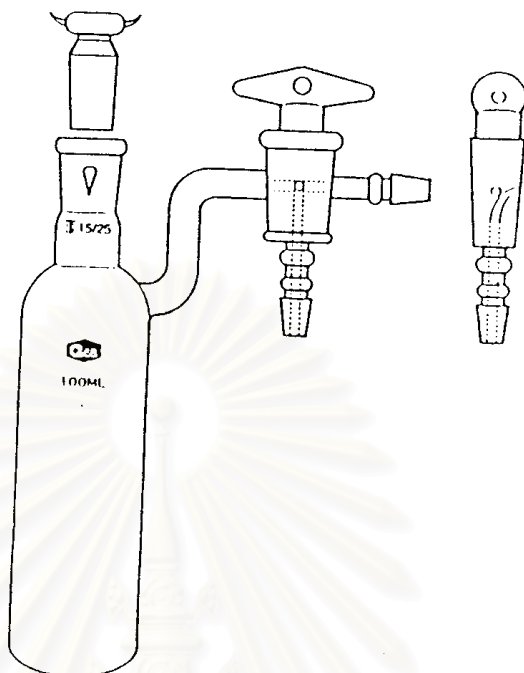


Figure 3.3 Schlenk tube

3.3 Characterizing Instruments

The instruments used for characterizing catalysts and ethylene/ α -olefin copolymer products are specified below.

3.3.1 Differential Scanning Calorimetry (DSC)

The melting temperature of ethylene/ α -olefin copolymer products was determined with a NETZSCH DSC 200 at Scientific Technological Research Equipment Center, Chulalongkorn University. The analyses were performed at the heating rate of 10 °C/min in the temperature range of 30-200 °C. The heating cycle was run twice. In the first scan, samples were heated and the cooled to room temperature. In the second, samples were reheated at the same rate, but only the results of the second scan were

reported because the first scan was influenced by the mechanical and thermal history of samples.

3.3.2 Gel Permeation Chromatography (GPC)

Molecular weight and molecular weight distribution of the produced ethylene/ α -olefin copolymer were measured at 135 °C using 1,2-dichlorobenzene as solvent by a Shodex Gel Permeation Chromatography at Thai Polyethylene Public Company Limited. The GPC instrument was equipped with a viscometric detector, differential optical refractometer and three Shodex AT type columns (AT-803/s, AT-805 and AT-807/s) with a 1×10^7 exclusion limit for polystyrene. The columns were calibrated with standard narrow molar mass distribution polystyrenes and linear low density polyethylene and polystyrene.

3.3.3 Nuclear Magnetic Resonance (NMR)

The ^{13}C -NMR spectra were recorded at 100°C using JEOL JNM-A500 operating at 125 MHz. Copolymer solutions were prepared using 1,2,4-trichlorobenzene as solvent and benzene- d_6 for internal lock.

3.3.4 Scanning Electron Microscope (SEM)

SEM observation with a JSM-5800 LV Scanning Microscope, Microspec WDX at Scientific Technological Research Equipment Center, Chulalongkorn University was employed to investigate the morphology of catalyst precursor and polymer. The polymer samples for SEM analysis were coated with gold particles by ion sputtering device to provide electrical contact to the specimen.

3.3.5 Inductively Coupled Plasma Atomic Emission Spectrometer (ICP-AES)

The amounts of Al and Zr from SiO_2/MAO and $\text{SiO}_2/\text{MAO}/\text{Et}(\text{Ind})_2\text{ZrCl}_2$ were determined with a Perkin-Elmer Plasma 1000 at Scientific Technological Research Equipment Center, Chulalongkorn University. Samples were digested using 37% HCl

and heat. After that, sample solutions were filtered and adjusted desire volume by distilled water.

3.4 Supporting Procedure

All reactions were conducted under argon atmosphere using Schlenk techniques and glove box.

3.4.1 Preparation of Catalyst Precursor SiO_2/MAO

Silica gel was calcined under vacuum at 400 °C for 6 hours. Calcined silica 1 g was reacted with the desired amount of MAO in 10 ml of toluene at room temperature for 30 minutes. The solid part was separated and washed 5 times with 20 ml of toluene, followed by drying in vacuum at room temperature to obtain the catalyst support precursor SiO_2/MAO .

3.4.2 Preparation of Catalyst Precursor $\text{SiO}_2/\text{MAO}/\text{Et}(\text{Ind})_2\text{ZrCl}_2$

The catalyst precursor SiO_2/MAO was stirred at room temperature with the desired amount of $\text{Et}(\text{Ind})_2\text{ZrCl}_2$ solution in toluene for 30 minutes. The solid part was washed 2 times with 20 ml of toluene and then dried in vacuum at room temperature.

3.5 Ethylene and α -olefins Copolymerization Procedure

The ethylene and α -olefins (1-hexene, 1-octene and 1-decene) copolymerization reaction were carried out in a 100 ml semi-batch stainless steel autoclave reactor equipped with magnetic stirrer. The autoclave and magnetic bar were dried in oven at 110 °C for 30 minutes and purged with argon 5 times in glove box before use in copolymerization of ethylene and α -olefins. Toluene (to make a total volume of 30 ml), 100 mg of catalyst precursor, 3 ml of α -olefins were introduced into the autoclave in the glove box. The amount of $\text{Et}(\text{Ind})_2\text{ZrCl}_2$ and TMA were mixed and stirred for 5 minutes at room temperature. After that, the mixture of metallocene and TMA was injected into the reactor. The reactor was frozen in liquid nitrogen to stop reaction and then the

autoclave was evacuated to remove the argon. After that, the reactor was heated up to polymerization temperature and the polymerization was started by feeding ethylene gas (total pressure 50 psi) until the consumption of ethylene 0.018 mol (6 psi was observed from pressure gauge). The small amount of ethylene was used to avoid the mass transfer effect and increase the homogeneity of polymer. If the amount of comonomer remained higher than 90% after the reaction, the obtained polymer is homogeneous. The reaction of polymerization was terminated by addition of acidic methanol. The time of reaction was recorded for purposes of calculating the activity. The precipitated polymer was washed with methanol and dried in room temperature.

The various effects on the ethylene/ α -olefins copolymerization with silica-supported metallocene catalyst and optimized condition were investigated. The effects of copolymerization on production of ethylene/ α -olefins copolymer were systematically varied as follow.

3.5.1 The Effect of Catalyst Concentration

The concentrations of $\text{Et}(\text{Ind})_2\text{ZrCl}_2$ catalyst were investigated at 1.67×10^{-5} to 8.33×10^{-5} M. The Al/Zr molar ratios, the consumption of ethylene and amount of α -olefins comonomer were fixed at 2500, 0.018 mol and 3 ml, respectively. The polymerization temperature was kept constant at 70 °C.

3.5.2 The Effect of Polymerization Temperature

The ethylene/ α -olefins copolymerization was further studied by varying the polymerization temperature from 30 to 80 °C using the best result of catalyst concentration from section 3.5.1.

3.5.3 The Effect of $\text{Al}_{(\text{MAO})}/\text{Zr}$ Mole Ratios

The $\text{Al}_{(\text{MAO})}/\text{Zr}$ molar ratios were varied from 160 to 1135. The consumption of ethylene and amount of α -olefins comonomer were fixed at 6 psi and 3

ml, respectively. The catalyst concentration and polymerization temperature using the suitable condition selected from section 3.5.1 and 3.5.2, respectively.

3.5.4 The Effect of Al_(TMA)/Zr Mole Ratios

The Al_(TMA)/Zr molar ratios were varied from 1000 to 4000. The conditions of polymerization were used from the best results of section 3.5.1 to 3.5.3.

3.5.5 The Effect of Catalyst Precursor

The ethylene polymerization and ethylene/ α -olefin copolymerization over two different catalyst precursors were studied. In this study using the catalyst precursors: SiO₂/MAO and SiO₂/MAO/Et(Ind)₂ZrCl₂. The conditions of polymerization were chosen according to the best results of section 3.5.1-3.5.4.

3.6 Characterization of Catalyst Precursor

3.6.1 Morphology

Scanning electron microscopic (SEM) technique was the effective method to investigate catalyst precursor morphologies. The term of morphology was referred to shape, texture or form of catalyst precursor.

3.6.2 The Amount of Al and Zr on Catalyst Precursors

Inductively Coupled Plasma Atomic Emission Spectrometer (ICP-AES) method was used to investigate amount of Al and Zr that were supported on surface of SiO₂/MAO and SiO₂/MAO/Et(Ind)₂ZrCl₂, respectively.

3.7 Characterization of Ethylene and α -olefins Copolymer Products

3.7.1 Chemical Structure Determination

The nuclear magnetic resonance technique was widely used for characterizing incorporated comonomer. Comparison of the position of peak in the ^{13}C -NMR spectrum of polymer sample led to identification of the sequences of the comonomer incorporation.

3.7.2 Morphology

The morphology of ethylene/ α -olefins copolymer obtained was observed with scanning electron microscopy (SEM).

3.7.3 Melting Temperature (T_m)

Differential scanning calorimetry (DSC) was an instrument designed to measure the thermal properties especially melting temperature (T_m). The melting temperature of ethylene/ α -olefins copolymers were determined from the critical point of DSC curve.

3.7.4 Average Molecular Weight and Molecular Weight Distribution

One of the most widely used methods for the routine determination of molecular weight (M_w) and molecular weight distribution (MWD) was gel permeation chromatography (GPC), which employed the principle of size exclusion chromatography (SEC) to separate samples of polydispersed polymers into fractions of narrower molecular weight distribution. Basic instrument for GPC analysis was shown in Figure 3.4.

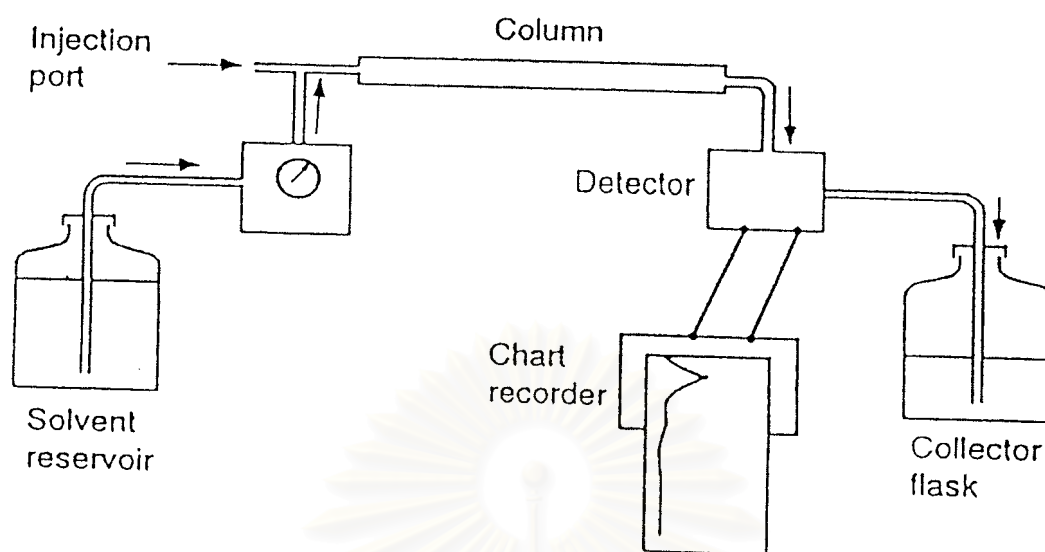


Figure 3.4 Basic Instrument for Gel Permeation Chromatography.

สถาบันวิทยบริการ
จุฬาลงกรณ์มหาวิทยาลัย

CHAPTER IV

RESULTS AND DISCUSSIONS

4.1 Ethylene/1-Octene Copolymerization using the In-Situ Supported (SiO₂/MAO) catalyst

4.1.1 The Effect of Catalyst Concentration on the Catalytic Activity

The effect of catalyst concentration was investigated with SiO₂/MAO by using Et(Ind)₂ZrCl₂ catalyst. The catalyst concentration was tested in the range of 1.67x10⁻⁵ M to 8.33x10⁻⁵ M. The polymerization were preformed in toluene at 70°C using 0.018 mol (6 psi) of ethylene consumption, 100 mg of catalyst precursor with Al_(TMA)/Zr mole ratio of 2500, Al_(MAO)/Zr mole ratio of 1135, and total solution volume of 30 ml. The results for the effect of catalyst concentration on the catalytic activity are shown in Table 4.1 and Figure 4.1.

Table 4.1 Catalytic activity of different catalyst concentrations^a

Catalyst Concentration, [Zr] x10 ⁻⁵ (M)	Yield (g)	Polymerization Time (sec)	Catalytic Activity (kgPE/molZr.h)
1.67	0.8770	160	13200
3.33	1.1854	156	18200
5.00	1.0940	122	21500
6.67	1.0691	129	19900
8.33	1.0754	137	18800

^acopolymerization conditions: Al_(MAO)/Zr = 1135, Al_(TMA)/Zr = 2500, precursor = 100 mg, 70°C, 0.018 mol of ethylene consumption, 3 ml of 1-octene, total volume = 30 ml

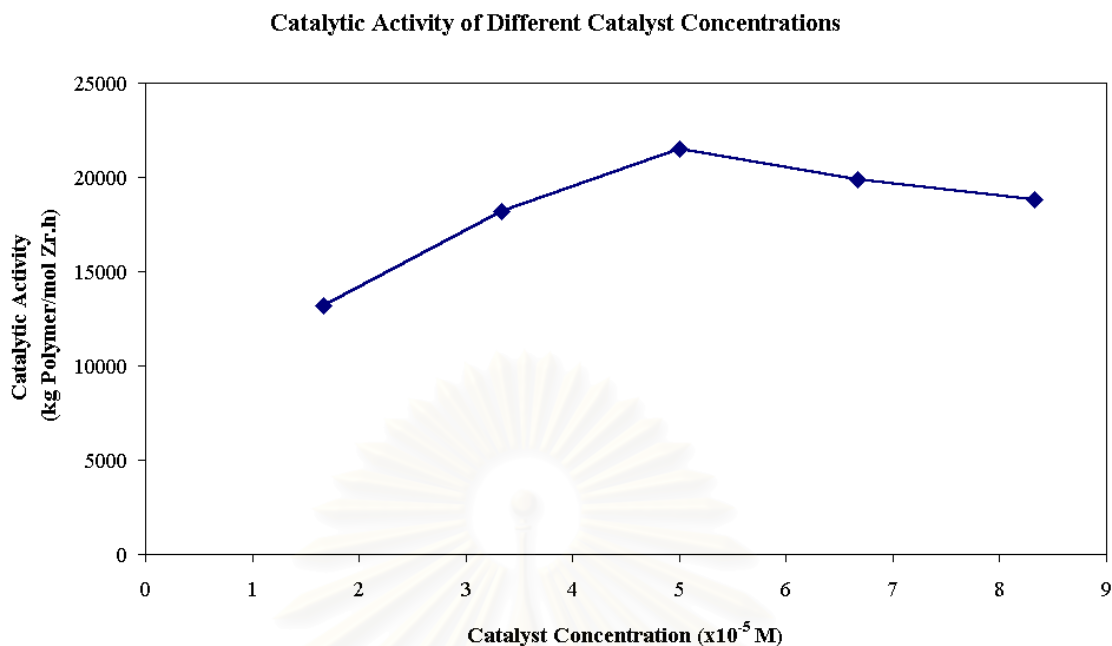


Figure 4.1 Catalytic activity of different catalyst concentrations

Table 4.1 and Figure 4.1 show that the catalytic activity increases with increasing catalyst concentration and the highest activity is reached at the catalyst concentration of 5.0×10^{-5} M. Then, the catalytic activity decreases with the increasing in catalyst concentration.

Marques and Conte [59] reported that the increase of Zr concentration added to the catalyst preparation promoted an enhancement on Zr content fixed on the support, although the bimolecular deactivation of the metallocene compound occurred during the support treatment and then inactive bimetallic species were fixed.

For the preactivation of $\text{Et}(\text{Ind})_2\text{ZrCl}_2$ and TMA, possibly $\text{Et}(\text{Ind})_2\text{ZrCl}_2$ is monoalkylated by TMA to form $\text{Et}(\text{Ind})_2\text{ZrClCH}_3$. And then it interacts with the MAO fixed on the modified silica surface. The surface MAO removes a Cl^- ion from $\text{Et}(\text{Ind})_2\text{ZrClCH}_3$ and produces the cationic Zirconocene methyl species floats over the solid surface, much like in solution. Both ionic species are postulated to be trapped and stabilized as multicoordinated "crown" aluminoxane complexes. These complex would be quite stable against dissociation [60].

From this consideration, it may be described that the increasing catalytic activity with the increase of catalyst concentration is ascribed to the building up of active species ($\text{Et}(\text{Ind})_2\text{ZrClCH}_3$). When catalyst concentration above 5.0×10^{-5} M, some part of catalysts formed $\text{Et}(\text{Ind})_2\text{Zr}(\text{CH}_2)_2(\text{Ind})_2\text{Et}$ which is inactive species.

Kaminsky and Strubel [61] suggested that beside complexation, methylation and activation, alpha-hydrogen transfer between MAO and metallocene occurs as a side reaction. This side reaction is responsible for the production of methane. Consideration of the metallocene and MAO takes place causing the formation of Zr-CH₂-Al or Zr-CH₂-Zr structures. Metallocene compounds with a Zr-CH₂-Zr structure are known to be inactive and a specific cause for the deactivation of metallocene catalyst. It is possible to prevent deactivation reactions of metallocene by supporting them on silica, thus blocking the alpha-hydrogen transfer. This effect can also be observed in the long stability of the metallocene in TMA solutions, in which the activity does not decrease within twenty hours.

4.1.2 The Effect of Polymerization Temperature on Catalytic Activity

The influence of the polymerization temperature (T_p) was investigated with different polymerization temperatures in the range of 30 to 80 °C. The other parameters such as $\text{Al}_{(\text{TMA})}/\text{Zr}$ mole ratio, $\text{Al}_{(\text{MAO})}/\text{Zr}$ mole ratio, Zr concentration, catalyst precursor and ethylene consumption were fixed at 2500, 1135, 5.0×10^{-5} M, 100 mg and 0.018 mol, respectively. Table 4.2 and Figure 4.2 illustrate the results for the influence of temperature on catalytic activity.

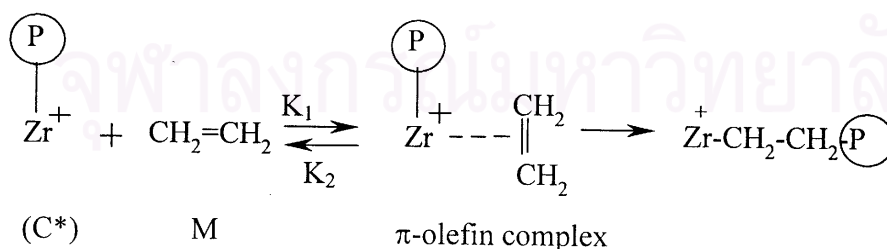
Table 4.2 Catalytic activity of different polymerization temperatures^b

Polymerization Temperature (°C)	Yield (g)	Time (sec)	Catalytic Activity (kgPE/mol Zr.h)
30	0.2026	363	1300
40	0.4656	275	4100
50	1.2862	247	12500
60	0.9893	156	15200
70	1.0940	122	21500
80	1.0663	132	19400

^bcopolymerization conditions: $[Zr] = 5 \times 10^{-5}$ M, $Al_{(MAO)}/Zr = 1135$, precursor = 100 mg, $Al_{(TMA)}/Zr = 2500$, 0.018 mol of ethylene consumption, 3 ml of 1-octene, total volume = 30 ml

From the above results, the dependence of catalyst activity on polymerization temperature is shown in Figure 4.2. The catalyst system showed polymerization activity over the whole temperature range investigated. It can be explained by a widely accepted mechanism of propagation in Ziegler-Natta catalyst which involves the initial formation of a π -complex of an olefin with the catalyst metal, followed by chain migratory insertion [62].

The same mechanism was used to explain the above results. The propagation process in zirconocene system for olefin polymerization can be written as,



When C^* = active site

M = monomer

\textcircled{P} = polymer chain

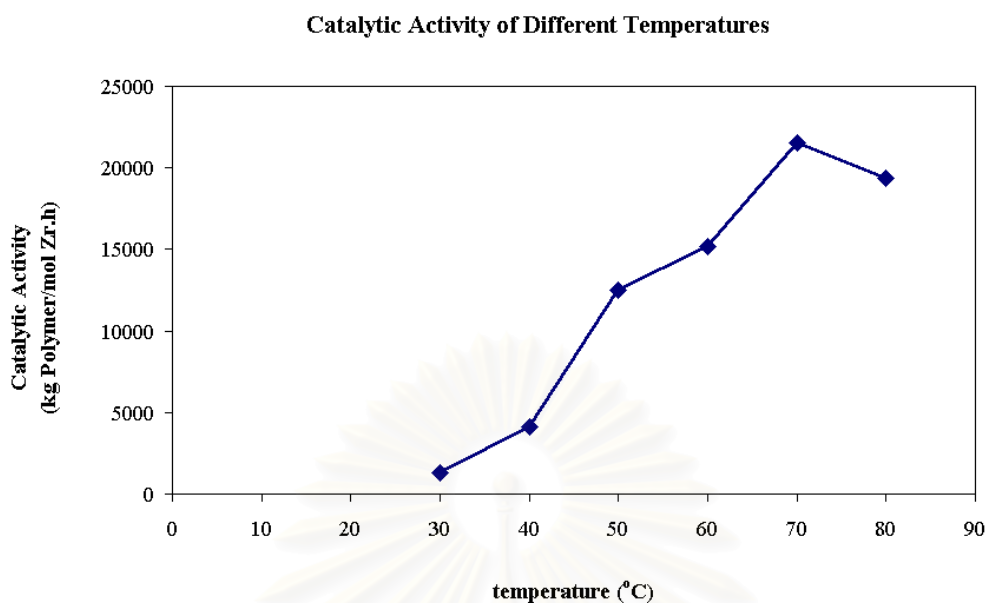


Figure 4.2 Catalytic activity of different polymerization temperature

In the low temperature range, the π -olefin complex is more stable which is associated to the process of activated insertion. This affects to the increase of activity with the increasing of polymerization temperature. On the other hand, the decreasing activity with further rising polymerization temperature probably involves the readily dissociation of the complex causing the low propagation rate [63].

Chien et al. [64] have speculated on the possible mechanism for deactivation. One possibility is a slow dissociation of stable active species to form inactive forms. A second possible deactivation mechanism is by β -hydride elimination to give metallocene hydride, which has very low propensity for monomer insertion.

Shan, Soares and Penlidis [25] were studies ethylene/1-octene copolymerization with in-situ supported *rac*-[dimethylsilylbis(methylbenzoindeyl)] zirconium dichloride catalyst. This is generally observed as an increase in the catalyst activity and a decrease in the molecular weight as the temperature increase. However, most metallocene catalyses deactivate at temperature greater than 80-100 °C. This deactivation reduces the number of active sites and the catalytic activity.

Figure 4.2 shows how the activity varies with the temperature. For the temperature range studied, with increasing temperature, the catalyst activity increased. This is not always the case because the rate of catalyst deactivation also increase with temperature. It has been reported that the catalyst activity can reach a maximum between 30 and 80 °C, depending on the polymerization time and polymerization condition. It might be possible that at high temperatures the extraction of the metallocene or MAO from the catalyst support occurred, leading to homogeneous polymerization. It was observed that the morphology of the resulting polymer became poorer as the polymerization temperature increased, and this supports the hypothesis of metallocene or MAO leaching from the silica particle [25].

4.2 Ethylene/ α -Olefin Copolymerizations using In-Situ Supported (SiO₂/MAO) Catalyst

4.2.1 The Effect of Al_(MAO)/Zr Mole Ratio on Catalytic Activity

The effect of Al_(MAO)/Zr was investigated with SiO₂/MAO-Et(Ind)₂ZrCl₂+TMA catalyst. Methylaluminoxane (MAO) was used as cocatalyst which the molar ratio of Al_(TMA)/Zr was varied in the range of 160 to 1135. The copolymerizations were performed in toluene solvent at 70°C using ethylene consumption of 0.018 mol (pressure in reactor 50 psi), 3 ml of comonomer, 100 mg of catalyst precursor and zirconium concentration 5.0x10⁻⁵ M with total solution volume of 30 ml. The results of the influence of Al_(MAO)/Zr mole ratio on the catalytic activity are shown in Table 4.3 and Figure 4.3. And the results of the influence of Al_(MAO)/Zr mole ratio on the polymerization time are shown in Figure 4.4.

Table 4.3 Catalytic activity at different Al_(MAO)/Zr mole ratios using in-situ supported catalyst^c.

Copolymerization	Al _(MAO) /Zr Mole Ratio	Yield (g)	Time (sec)	Activity (kgPE/molZr.h)
Ethylene/1-hexene	160	0.4902	225	5200
	320	0.7246	212	8200
	635	0.8967	167	12900
	890	0.9377	136	16500
	1135	1.0699	117	21900
Ethylene/1-octene	160	0.6420	183	8400
	320	0.8644	163	12700
	635	1.1149	158	16900
	890	1.0550	134	18900
	1135	1.0940	122	21500
Ethylene/1-decene	160	0.6360	247	6200
	320	0.7449	247	7200
	635	0.8512	233	8800
	890	0.8892	179	11900
	1135	1.1182	135	19900

^ccopolymerization conditions: [Zr] = 5×10^{-5} M, Al_(TMA)/Zr = 2500, precursor = 100 mg, 70°C, 0.018 mol of ethylene consumption, 3 ml of comonomer, total volume = 30 ml

สถาบันวิทยบริการ
จุฬาลงกรณ์มหาวิทยาลัย

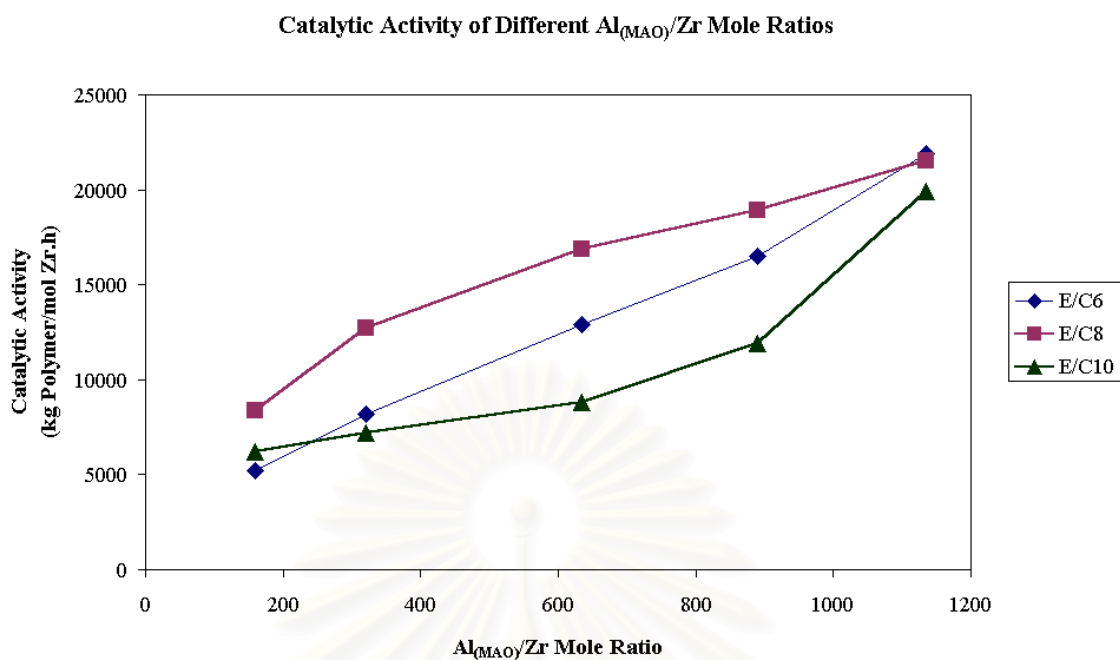


Figure 4.3 Catalytic activity of different $Al_{(MAO)}/Zr$ mole ratios using in-situ supported catalyst

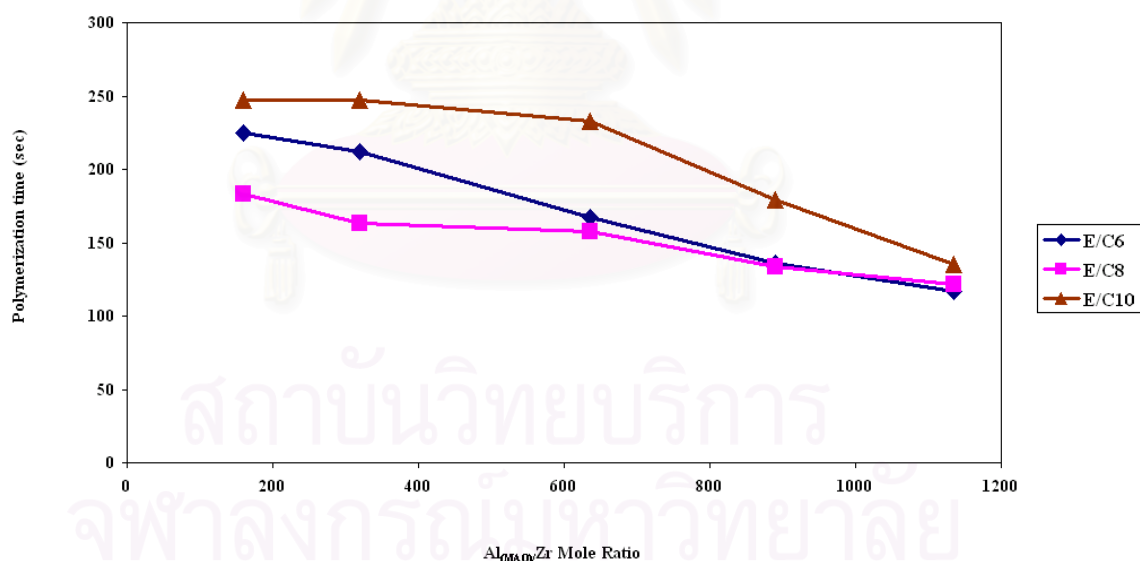


Figure 4.4 Polymerization time of different $Al_{(MAO)}/Zr$ mole ratios using in-situ supported catalyst

In copolymerization of ethylene with three different comonomers, the catalytic activity continuously increase with the increase of the $Al_{(MAO)}/Zr$ ratio. In contrast the polymerization time decrease with the increase of the $Al_{(MAO)}/Zr$ ratio.

4.2.2 The Effect of Al_(TMA)/Zr Mole Ratios on Catalytic Activity

The effect of Al_(TMA)/Zr was investigated with SiO₂/MAO-Et(Ind)₂ZrCl₂+TMA catalyst. Trimethylaluminum (TMA) was used as cocatalyst which the molar ratio of Al_(TMA)/Zr was varied in the range of 1000 to 4000. The copolymerizations were performed in toluene solvent at 70°C using ethylene consumption of 0.018 mol (pressure within reactor 50 psi), 3 ml of α -olefin, 100 mg of catalyst precursor and zirconium concentration 5.0×10^{-5} M with total solution volume of 30 ml. The results of the influence of Al_(TMA)/Zr mole ratio on the catalytic activity are shown in Table 4.4 and Figure 4.5 and the influence of Al_(TMA)/Zr mole ratio on the polymerization time are shown in Figure 4.6.

Table 4.4 Catalytic activity at different Al_(TMA)/Zr mole ratios using in-situ supported catalyst^d

Copolymerization	Al _(TMA) /Zr Mole Ratio	Yield (g)	Time (sec)	Activity (kgPE/molZr.h)
Ethylene/1-hexene	1000	1.0806	247	10500
	2000	1.0530	216	11700
	2500	1.0699	117	21900
	3000	1.0373	147	16900
	4000	1.0641	213	12000
Ethylene/1-octene	1000	1.0230	215	11400
	2000	1.0493	125	20100
	2500	1.0940	122	21500
	3000	1.0017	118	20400
	4000	1.0984	132	20000
Ethylene/1-decene	1000	1.0878	178	17600
	2000	1.1154	149	18000
	2500	1.1182	135	19900
	3000	1.0188	166	14700
	4000	1.0215	170	14400

^d copolymerization conditions: [Zr] = 5×10^{-5} M, Al_(MAO)/Zr = 1135, precursor = 100 mg, 70°C, 0.018 mol of ethylene consumption, 3 ml of comonomer, total volume = 30 ml

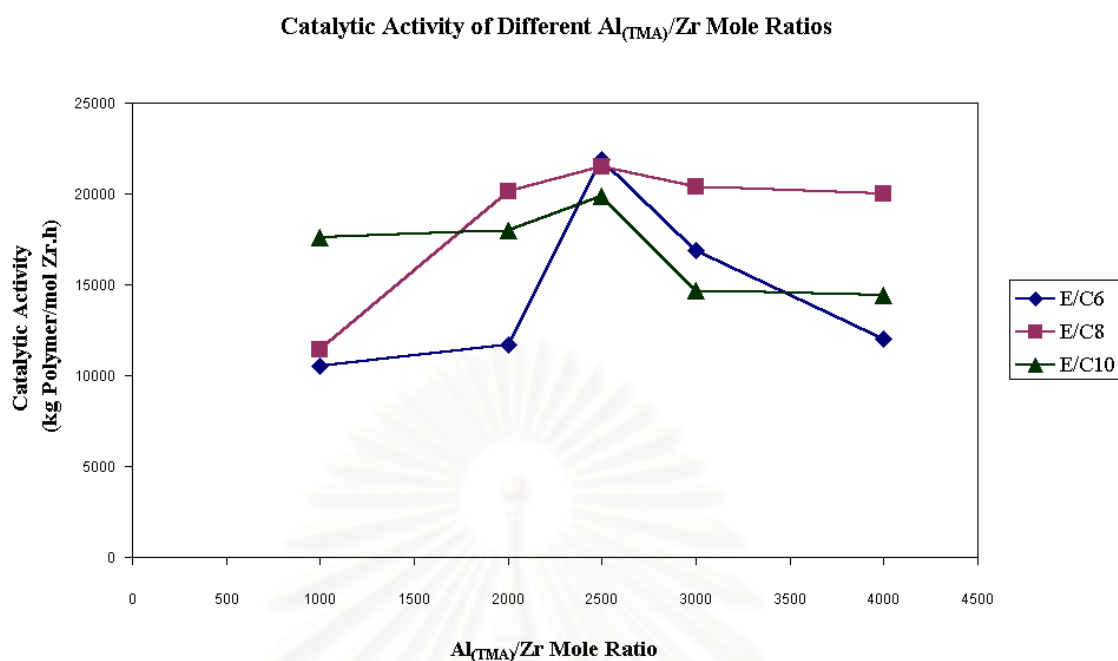


Figure 4.5 Catalytic activity of different $Al_{(TMA)}/Zr$ mole ratios using in-situ supported catalyst

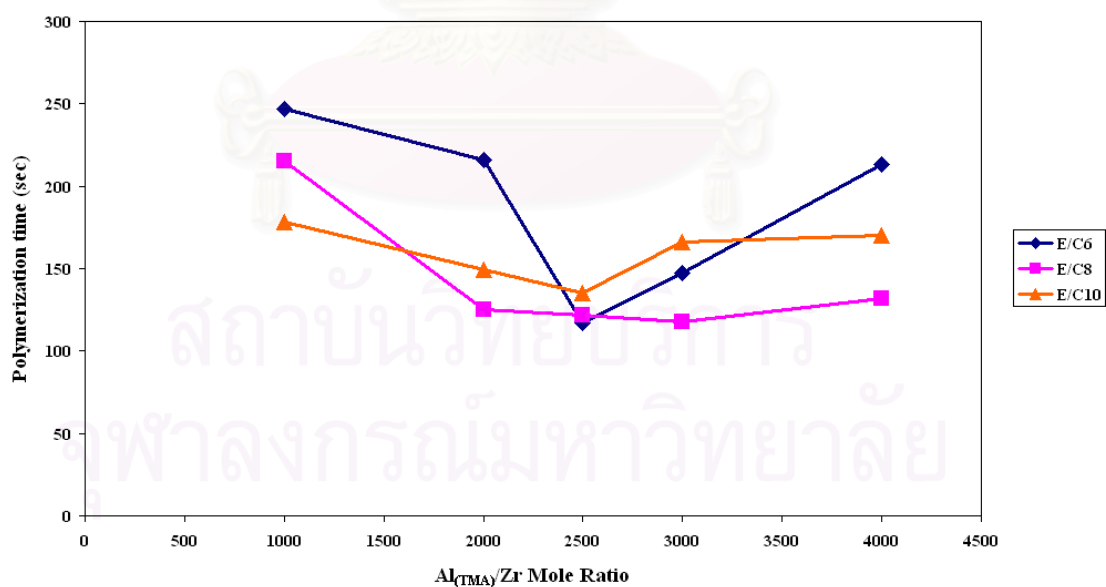


Figure 4.6 Polymerization time of different $Al_{(TMA)}/Zr$ mole ratios using in-situ supported catalyst

The catalytic activity of copolymerization in different comonomers, increased with increasing $\text{Al}_{(\text{TMA})}/\text{Zr}$ ratio up to 2500 where after the inverse effect was observed. The results of polymerization time were contrasted with the catalytic activity in each comonomer.

Lastly, the polymerization rate passes through a maximum as the ratio of aluminum to transition metal increase. The exact location of this maximum value depends on the catalyst type and whether the polymerization is homogeneous or heterogeneous. Heterogeneous polymerization tend to be less sensitive to changes in the aluminum/transition metal ratio. Chain transfer to aluminum is also favored at high aluminum concentrations. This increase in chain transfer would presumably produce a lower molecular weight polymer. However, some researchers have observed decreases, and some others have observed no changes in the molecular weight with increasing aluminum concentration [25].

The catalyst activity decreases with the addition of an activator. Although activators are required to activate the catalyst, it is possible that a large excess of an activator may block the catalytic sites. For a similar system, it was observed that with an increasing ratio of trimethylaluminum to the silica MAO support, a decrease in activity occurred at ratios up to 2500. This decrease was attributed to the bimolecular deactivation caused by the complexation of homogeneous metallocene and trimethyl aluminum.

Ethylene/ α -olefin copolymers produced with in-situ supported catalysts can sometimes have very broad and bimodal SCBDs. It was shown in previous study that different alkylaluminum activators could generate active sites with quite different reactivity ratios. However, previous work with poly(ethylene-co-1-hexene) made with in situ supported $\text{Et}(\text{Ind})_2\text{ZrCl}_2$ indicates that this effect has a chemical nature. In that investigation, it was noticed that changing the type of activator (trimethylaluminum, triethylaluminum or triisobutylaluminum) led to polymers with unimodal or bimodal SCBDs. Because it is unlikely that the type of activator will have marked influence on mass-transfer resistances, one is led to conclude that the observed bimodal SCBDs are, at least in part, due to the presence of different site types on the in situ supported catalyst [25].

4.3 Ethylene/ α -olefins Copolymerization using Supported ($\text{SiO}_2/\text{MAO}/\text{Et}(\text{Ind})_2\text{ZrCl}_2$) Catalyst

4.3.1 The Effect of $\text{Al}_{(\text{MAO})}/\text{Zr}$ Mole Ratios on Catalytic Activity

The effect of $\text{Al}_{(\text{MAO})}/\text{Zr}$ was investigated with $\text{SiO}_2/\text{MAO}/\text{Et}(\text{Ind})_2\text{ZrCl}_2+\text{TMA}$ catalyst. Methylaluminoxane (MAO) was used as cocatalyst which the molar ratio of $\text{Al}_{(\text{MAO})}/\text{Zr}$ was varied in the range of 160 to 1135. The copolymerizations were performed in toluene solvent at 70°C using ethylene consumption of 0.018 mol (pressure in reactor 50 psi), 3 ml of α -olefin, 100 mg of catalyst precursor and zirconium concentration 5.0×10^{-5} M with total solution volume of 30 ml. The results of the influence of $\text{Al}_{(\text{MAO})}/\text{Zr}$ mole ratio on the catalytic activity and polymerization time are shown in Table 4.5, Figure 4.7 and Figure 4.8.

Table 4.5 Catalytic activity of different $\text{Al}_{(\text{MAO})}/\text{Zr}$ mole ratios using Supported Catalyst^c

Copolymerization	$\text{Al}_{(\text{MAO})}/\text{Zr}$ Mole Ratio	Yield (g)	Time (sec.)	Activity (kgPE/molZr.h)
Ethylene/1-hexene	160	0.9159	609	3600
	320	0.9456	512	4400
	635	1.0029	241	10000
	890	1.1133	163	16400
	1135	1.1884	159	17900
Ethylene/1-octene	160	0.7649	434	4200
	320	0.6579	320	4900
	635	1.0032	188	12800
	890	1.0532	179	14100
	1135	1.2872	177	17500
Ethylene/1-decene	160	0.8772	504	4200
	320	0.8516	476	4300
	635	0.9162	298	7400
	890	1.0881	216	12100
	1135	0.9231	180	12300

^ccopolymerization conditions: $[\text{Zr}] = 5 \times 10^{-5}$ M, $\text{Al}_{(\text{TMA})}/\text{Zr} = 2500$, precursor = 100 mg, 70°C , 0.018 mol of ethylene consumption, 3 ml of comonomer, total volume = 30 ml

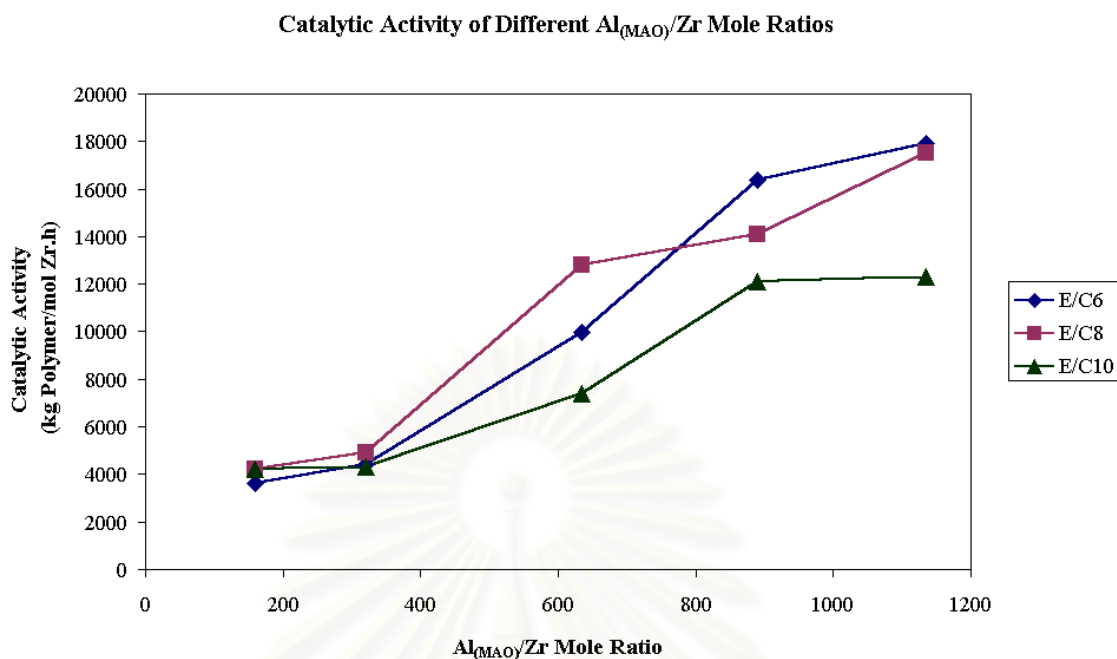


Figure 4.7 Catalytic activity of different $Al_{(MAO)}/Zr$ mole ratios using supported catalyst

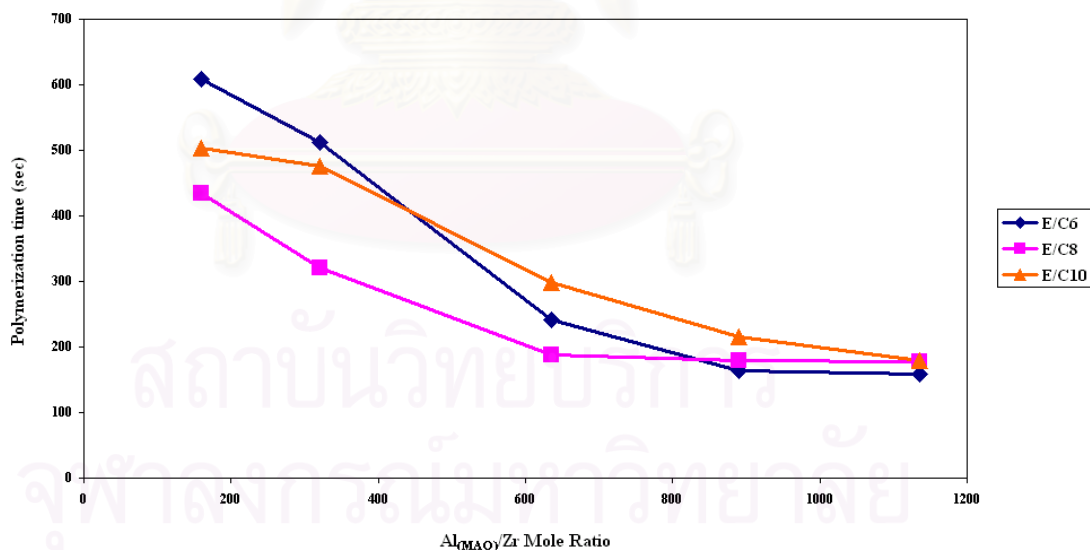


Figure 4.8 Polymerization time of different $Al_{(MAO)}/Zr$ mole ratios on supported catalyst

Similar to the in-situ supported catalyst system, catalytic activity of copolymerization increased but polymerization time of copolymerization decreased with the increase of $Al_{(MAO)}/Zr$.

4.3.2 The Effect of Al_(TMA)/Zr Mole Ratios on Catalytic Activity

The effect of Al_(TMA)/Zr was investigated with SiO₂/MAO/Et(Ind)₂ZrCl₂+TMA catalyst. Trimethylaluminum (TMA) was used as cocatalyst which the molar ratio of Al_(TMA)/Zr was varied in the range of 1000 to 4000. The copolymerizations were performed in toluene solvent at 70°C using ethylene consumption of 0.018 mol (pressure within reactor 50 psi), 3 ml of α -olefin, 100 mg of catalyst precursor and zirconium concentration 5.0×10^{-5} M with total solution volume of 30 ml. The results of the influence of Al_(TMA)/Zr mole ratio on the catalytic activity and polymerization time are shown in Table 4.6, Figure 4.9 and Figure 4.10.

Table 4.6 Catalytic Activity at Different Al_(TMA)/Zr Mole Ratios using Supported Catalyst^d

Copolymerization	Al _(TMA) /Zr Mole Ratio	Yield (g)	Time (sec)	Activity (kgPE/molZr.h)
Ethylene/1-hexene	1000	1.0230	225	10900
	2000	1.0428	218	11500
	2500	1.1884	159	17900
	3000	1.0828	206	12600
	4000	0.8402	279	7200
Ethylene/1-octene	1000	0.8671	237	8800
	2000	0.9465	204	11100
	2500	1.2872	177	17500
	3000	0.9112	202	10800
	4000	1.0967	264	10000
Ethylene/1-decene	1000	0.8924	228	9400
	2000	0.9389	231	9800
	2500	0.9231	180	12300
	3000	0.9688	210	11100
	4000	0.9954	231	10300

^d copolymerization conditions: [Zr] = 5×10^{-5} M, Al_(MAO)/Zr = 1135, precursor = 100 mg, 70°C, 0.018 mol of ethylene consumption, 3 ml of comonomer, total volume = 30 ml

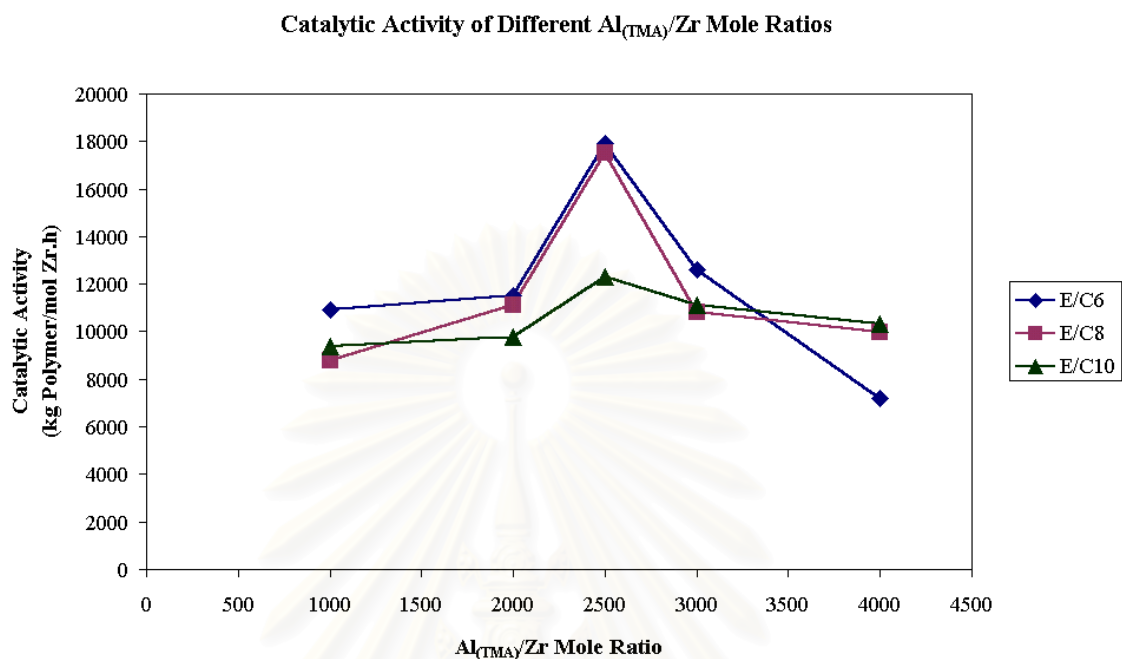


Figure 4.9 Catalytic Activity of different $Al_{(TMA)}/Zr$ Mole Ratios using supported catalyst

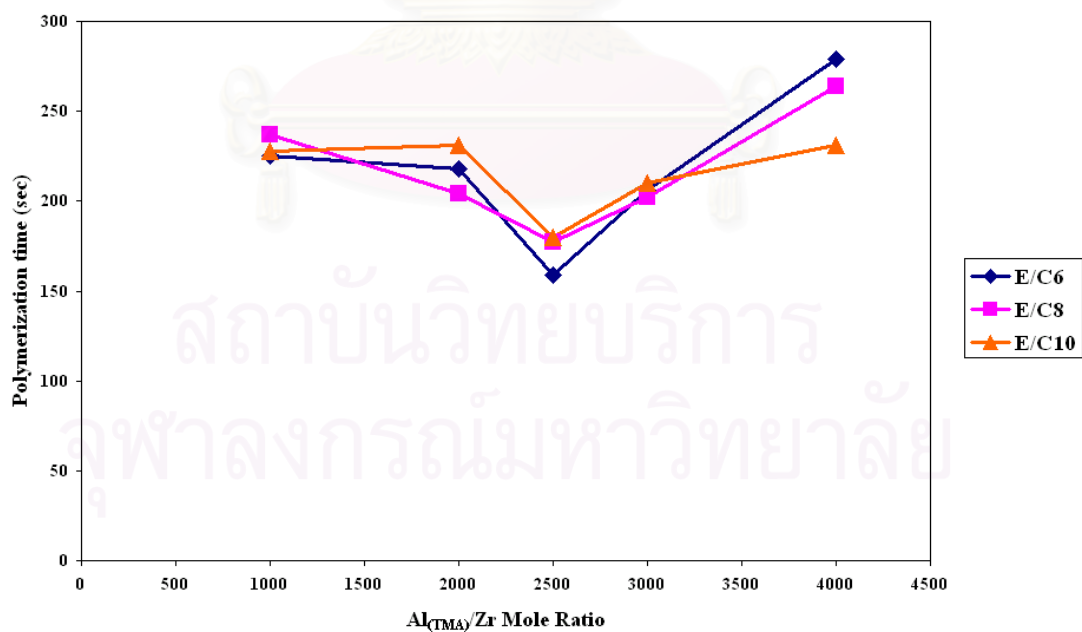


Figure 4.10 Polymerization time of different $Al_{(TMA)}/Zr$ Mole Ratios using supported catalyst

The catalytic activity increased with increasing $\text{Al}_{(\text{TMA})}/\text{Zr}$ ratio and reached the highest at the $\text{Al}_{(\text{TMA})}/\text{Zr}$ ratio of 2500 after that the activity decreased with the increasing $\text{Al}_{(\text{TMA})}/\text{Zr}$ ratio. The pattern of graph in polymerization time are contrast with the catalytic activity.

Kaminsky and Strubel [61] suggested that beside complexation, methylation and activation, alpha-hydrogen transfer between MAO and metallocene occurs as a side reaction. This side reaction is responsible for the production of methane. Consideration of the metallocene and MAO takes place causing the formation of $\text{Zr-CH}_2\text{-Al}$ or $\text{Zr-CH}_2\text{-Zr}$ structures. Metallocene compounds with a $\text{Zr-CH}_2\text{-Zr}$ structure are known to be inactive and a specific cause for the deactivation of metallocene catalyst. It is possible to prevent deactivation reactions of metallocene by supporting them on silica, thus blocking the alpha-hydrogen transfer. This effect can also be observed in the long stability of the metallocene in TMA solutions, in which the activity does not decrease within twenty hours.

4.4 Ethylene/ α -Olefin Copolymerization and Ethylene Homopolymerization using different catalyst precursors

4.4.1 The Effect of Different Catalyst Precursor on Catalytic Activity

Ethylene/ α -olefin copolymerizations with three types of catalyst precursors were performed keeping other parameters the same at polymerization temperature 70°C , $\text{Al}_{(\text{TMA})}/\text{Zr}$ mole ratio at 2500, catalyst concentration 5.0×10^{-5} M, ethylene consumption 0.018 mol, 3 ml of α -olefin and 100 mg of catalyst precursor. The results for the effect of different catalysts on the catalytic activity are shown in the Table 4.7 and Figure 4.11.

Table 4.7 Catalytic activity of different catalyst precursor^{e,f}

Precursor	Copolymerization or polymerization	Time (sec)	Yield (g)	Activity (kgPE/molZr.h)
SiO ₂ /MAO	Ethylene/1-hexene	117	1.0699	21900
	Ethylene/1-octene	122	1.0940	21500
	Ethylene/1-decene	135	1.1182	19900
	Ethylene	137	0.6396	11200
SiO ₂ /MAO/Et(Ind) ₂ ZrCl ₂	Ethylene/1-hexene	159	1.1884	17900
	Ethylene/1-octene	177	1.2872	17500
	Ethylene/1-decene	180	0.9231	12300
	Ethylene	191	0.7233	9100

^ecopolymerization conditions: [Zr] = 5×10^{-5} M, Al_(MAO)/Zr = 1135, Al_(TMA)/Zr = 2500, precursor = 100 mg, 70°C, 0.018 mol of ethylene consumption, 3 ml of comonomer, total volume = 30 ml

^fpolymerization conditions: [Zr] = 5×10^{-5} M, Al_(MAO)/Zr = 1135, Al_(TMA)/Zr = 2500, precursor = 100 mg, 70°C, 0.018 mol of ethylene consumption, total volume = 30 ml

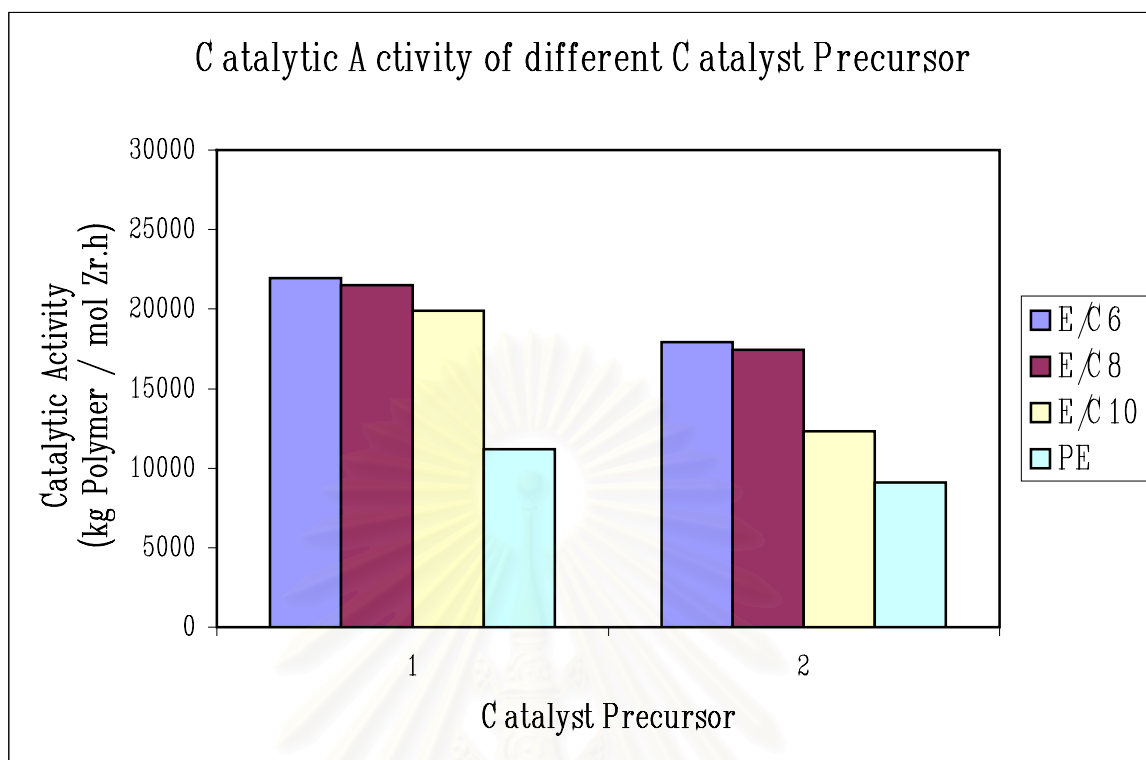


Figure 4.11 Catalytic activity of different catalyst precursor

Catalyst precursor 1 = SiO_2/MAO

Catalyst precursor 2 = $\text{SiO}_2/\text{MAO}/\text{Et}(\text{Ind})_2\text{ZrCl}_2$

From figure 4.11 the catalytic activity increased following this order : ethylene/1-hexene > ethylene/1-octene > ethylene/1-decene copolymerization > ethylene polymerization. And it was clear that the catalytic activity obtained from in-situ supported ($\text{SiO}_2/\text{MAO}-\text{Et}(\text{Ind})_2\text{ZrCl}_2+\text{TMA}$) catalyst showed a tendency higher activity than preformed supported ($\text{SiO}_2/\text{MAO}/\text{Et}(\text{Ind})_2\text{ZrCl}_2+\text{TMA}$) catalyst.

As the previous results from table 4.3 to 4.7, the ethylene/ α -olefin (1-hexene, 1-octene, 1-decene) copolymerization was carried out with various amount of TMA and MAO. With increased the amounts of MAO used in the catalyst precursor, the activity increased with increasing amount of MAO. Soga *et al.*[65] found that the use of SiO_2 pretreated with MAO caused a marked increase in the activity of supported catalysts, most of the MAO being consumed to scavenge surface silanols. In part of varying TMA, the activity was found increase further with increase of TMA up to a $\text{Al}_{(\text{TMA})}/\text{Zr}$ mole ratio as high as 2500. As the $\text{Al}_{(\text{TMA})}/\text{Zr}$ mole ratio was increased further, the activity was

found to decrease. TMA is scavenger which may help in reducing the amount of impurity in the system thereby leading to an increase in activity. TMA is also able to inhibit certain functions of MAO. Several explanations for this are possible. Since TMA is stronger alkylation and reducing agent than MAO, TMA could cause the reduction of the zirconocene compound resulting in an inactive species. It may compete with MAO as a complexing ligand leading to a catalyst of lower polymerization activity. Moreover, addition of TMA can lower the degree of oligomerization of MAO and its overall effectiveness. Therefore, addition of TMA has both advantages and disadvantages to activity [65].

In metallocene catalyst systems, MAO has many possible functions, such as scavenging of impurities, alkylation, ionization and reduction of the transition element, stabilization of cationic metallocene alkyl and/or the counter ion. One important role of MAO is apparently to prevent the formation of a $ZrCH_2CH_2Zr$ species (bimolecular process). This is the reason why a very large amount of MAO is needed to realize the maximum catalytic of the ansa-metallocene complexes in solution polymerization. One method to solve this problem is to immobilize the complex on support. Chu *et al.*[3] compared homogenous, supported and in-situ supported $Et(Ind)_2ZrCl_2$ on SiO_2 for ethylene and 1-hexene copolymerization. They found that the in-situ supported system showed higher activity than the supported system, corresponding to the results from Table 4.7 and Figure 4.11.

4.5 Characterization of Catalyst Precursor

4.5.1 Morphology

The morphology of catalyst precursors was observed by scanning electron microscopy technique as shown in Figures 4.12-4.14.



Figure 4.12 Scanning electron microscope image of silica

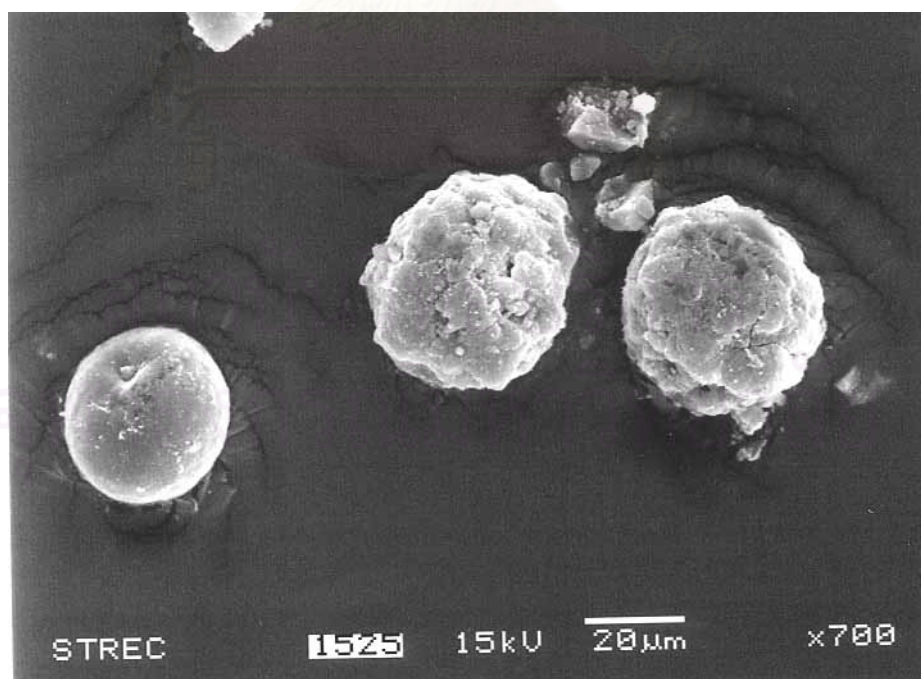


Figure 4.13 Scanning electron microscope image of silica/MAO



Figure 4.14 Scanning electron microscope image of silica/MAO/Et(Ind)₂ZrCl₂

From Figure 4.12-4.14, it was shown that the morphology of catalyst precursors are almost sphere and some parts of catalyst are fragmented.

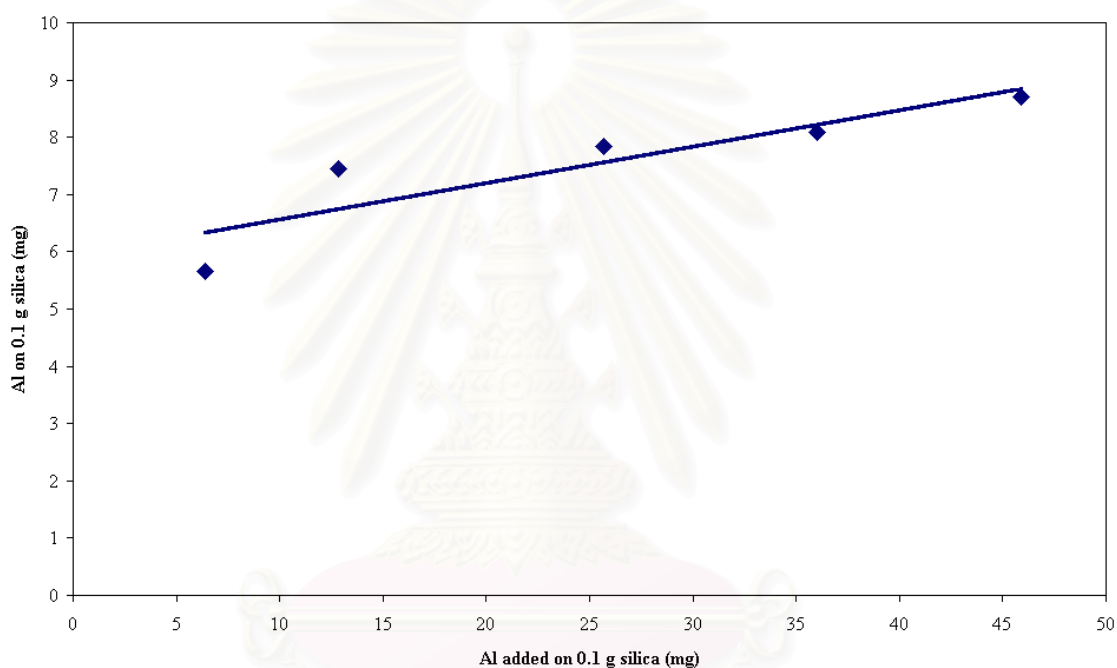
4.5.2 The Amount of Aluminium and Zirconium on Catalyst Precursor

4.5.2.1 Inductively Coupled Plasma Atomic Emission Spectrometer (ICP-AES)

The amount of Al impregnated on the silica that added various amount of MAO were measured by ICP-AES. The results of aluminium that supported on silica were shown in Table 4.8 and Figure 4.15. In the other, zirconium that supported on silica were shown in Table 4.9.

Table 4.8 The amount of aluminium on SiO₂ supported MAO

Precursor	Al added (mg)	Al supported (mg)
SiO ₂ /MAO	6.4	5.66
	12.87	7.45
	25.68	7.85
	36.01	8.09
	45.90	8.71

**Figure 4.15** Amount of Al impregnated on the silica measured by ICP at various Al added**Table 4.9** The amount of zirconium on SiO₂ supported MAO and Et(Ind)₂ZrCl₂

Precursor	Al on SiO ₂ (μmol)	Zr on SiO ₂ (μmol)
SiO ₂ /MAO/Et(Ind) ₂ ZrCl ₂	209.63	0.39
	275.93	0.31
	290.73	0.24
	299.67	0.23
	322.42	0.25

From the results in Table 4.8–4.9 and Figure 4.15 , considering the correlation between the amount of MAO added to silica in the impregnation step and the aluminum content of SiO₂/MAO precursor obtained, Al on silica relating increased with Al weight added.

Then the SiO₂ that supported with different amount of MAO was further treated with the Et(Ind)₂ZrCl₂, Zr content on the support was investigated that almost all the loaded Zr were immobilized on the support. This results reported by Chao *et. al.* [66]. The results in this study contrast with previous work, the content of zirconium that supported on silica decreased with increased the content of aluminium that added may caused from the filtration step which all of zirconium didn't through pass the filter paper.

The most important factor for the preparation of the heterogeneous catalysts to obtain high activity is not the Zr content fixed on the catalyst surface but how much of the Zr is effectively active [59].

4.6 Characterization of Ethylene and α -olefins Copolymer

4.6.1 Chemical Structure Determination

4.6.1.1 Nuclear Magnetic Resonance (NMR)

The copolymers of ethylene/ α -olefin using Et(Ind)₂ZrCl₂ as the catalyst with SiO₂/MAO catalyst precursor were determined by ¹³C-NMR as shown in Figures 4.13-4.18 Resonance attributions in the ¹³C-NMR spectra of the copolymers were taken from the literature [67]. The ¹³C-NMR identification of ethylene/ α -olefin copolymer is assigned to the sequence of the comonomer incorporation as summarized in Table 4.10, 4.11 and 4.12. The triad distributions were evaluated from the spectra following Randall's methodology.

Table 4.10 The ^{13}C -NMR identification of ethylene/1-hexene copolymer

Position (Figure4.13)	Assignment of Triad distribution	Chemical Shift
A	EHE	38.246
B	EHEE	34.564
C	EHE	34.224
D	HEEE	31.142
E	(EEE) _n	30.688
F	EHE	29.798
G	EHEE	27.639
H	EHE	24.057
I	EHE	14.948

E refer to ethylene monomer

H refer to 1-hexene monomer

Table 4.11 The ^{13}C -NMR identification of ethylene/1-octene copolymer

position (Figur4.15)	Assignment of Triad Distribution	Chemical Shift
A	EOE	38.144
B	OEE	34.491
C	EOE	32.369
D	OEEE	30.181
E	(EEE) _n	27.368
F	EOEE	27.286
G	EOE	23.091
H	EOE	14.306

E refer to ethylene monomer

O refer to 1-octene monomer

Table 4.12 The ^{13}C -NMR identification of ethylene/1-decene copolymer

Position (Figure4.17)	Assignment of Triad Distribution	Chemical Shift
A	EDE	38.287
B	DEE	34.564
C	EDE	32.798
D	DEEE	31.135
E	(EEE) _n	30.689
F	EDE	30.325
G	EDEE	27.631
H	EDE	23.572
I	EDE	14.880

E refer to ethylene monomer

D refer to 1-decene monomer

สถาบันวิทยบริการ
จุฬาลงกรณ์มหาวิทยาลัย

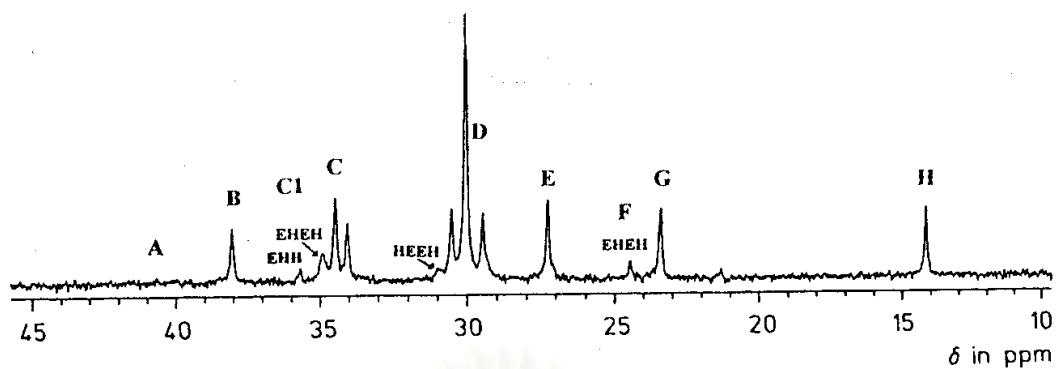


Figure 4.16 ^{13}C -NMR spectrum of ethylene/1-hexene copolymer from ref.[67]

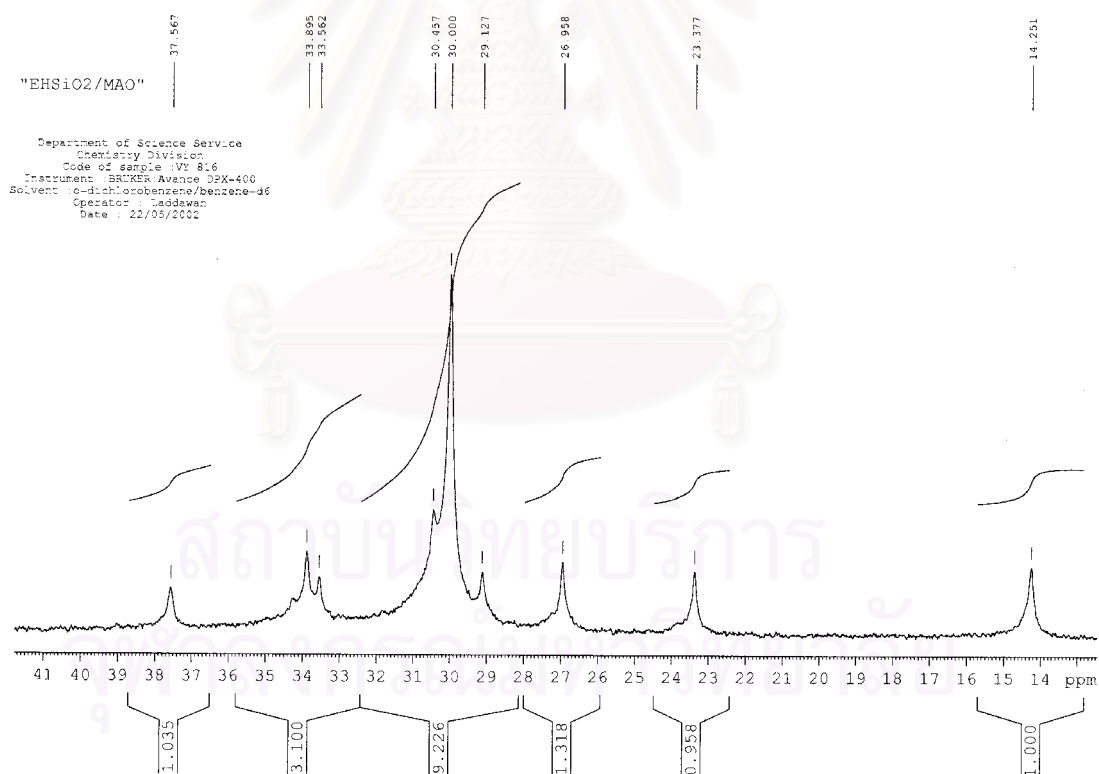


Figure 4.17 ^{13}C -NMR spectrum of ethylene/1-hexene copolymer produced with $\text{SiO}_2/\text{MAO-Et}(\text{Ind})_2\text{ZrCl}_2+\text{TMA}$

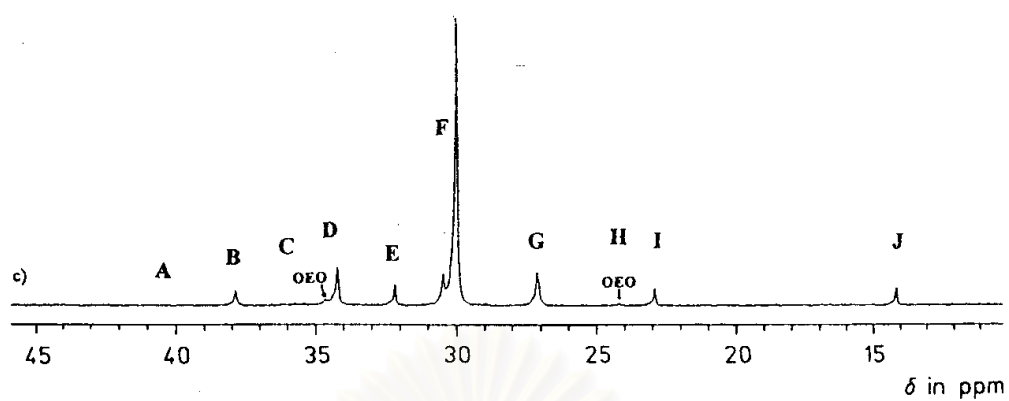


Figure 4.18 ^{13}C -NMR spectrum of ethylene/1-octene copolymer copolymer from ref [67]

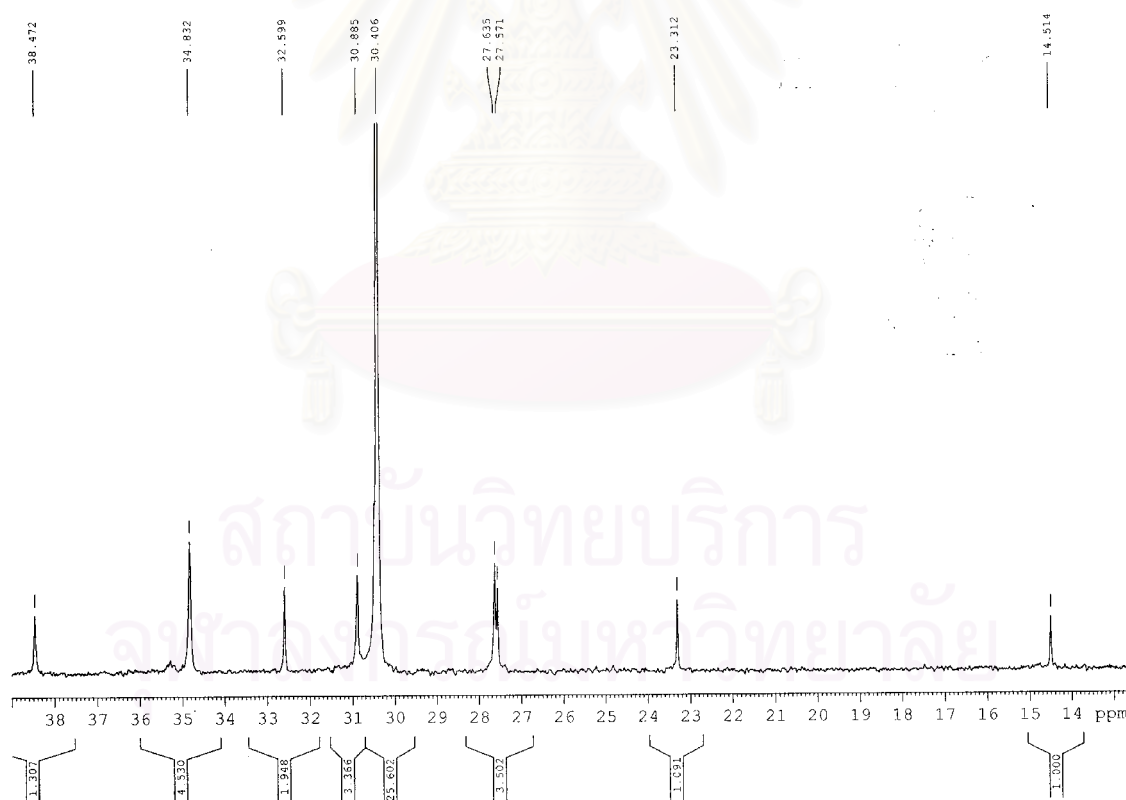


Figure 4.19 ^{13}C -NMR spectrum of ethylene/1-octene copolymer produced with $\text{SiO}_2/\text{MAO-Et}(\text{Ind})_2\text{ZrCl}_2+\text{TMA}$

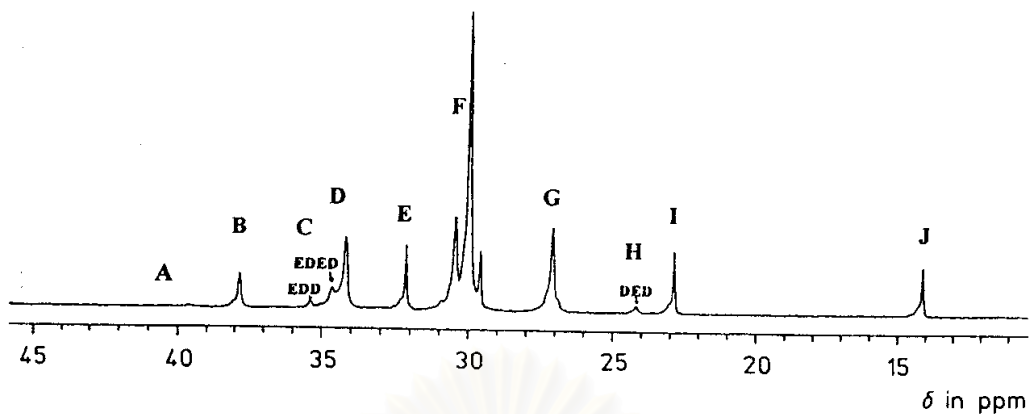


Figure 4.20 ^{13}C -NMR spectrum of ethylene/1-decene copolymer produced from ref [67]

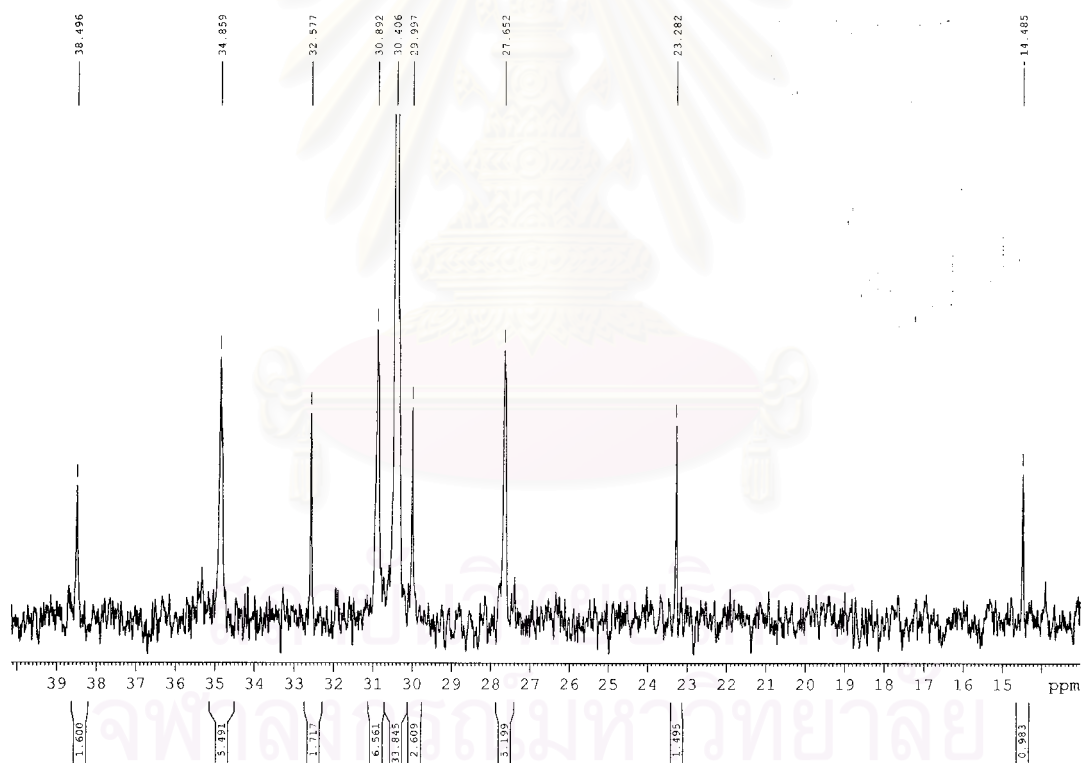


Figure 4.21 ^{13}C -NMR spectrum of ethylene/1-decene copolymer produced with $\text{SiO}_2/\text{MAO-Et}(\text{Ind})_2\text{ZrCl}_2+\text{TMA}$

Table 4.13 Triad distribution of ethylene / α -olefins copolymer prepared with SiO₂/MAO-Et(Ind)₂ZrCl₂+TMA

Copolymer	EEE	CEE+EEC	CEC	ECE	CCE+ECC	CCC
Ethylene/1-hexene	0.62	0.21	-	0.17	-	-
Ethylene/1-octene	0.82	0.10	-	0.08	-	-
Ethylene/1-decene	0.75	0.17	-	0.08	-	-

E refers to ethylene and **C** refers to corresponding comonomers: 1-hexene, 1-octene, or 1-decene.

¹³C NMR spectroscopy was used to determine comonomer incorporation and polymer microstructure. Chemical shift were referred internally to the major backbone methylene resonance and calculated according to the method of Randall [67]. The result obtained for the triad sequence distribution of copolymer shown in Table 4.13. The result suggested that the copolymer had a random distribution of comonomer insertion with very low amount of comonomer triad in the polymer chain.

4.6.2 Morphology

The morphologies of ethylene/ α -olefins (1-hexene, 1-octene and 1-decene) copolymers polyethylene obtained with different catalyst precursors were observed by scanning electron microscopy technique as shown in Figures 4.22-4.29.

สถาบันวิทยบริการ
จุฬาลงกรณ์มหาวิทยาลัย

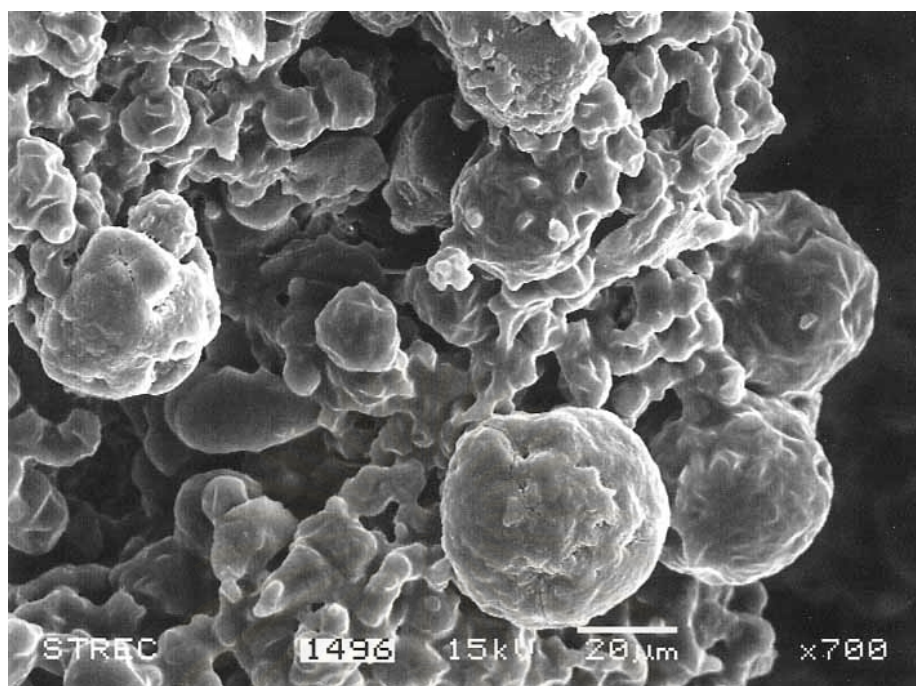


Figure 4.22 Scanning electron microscope image of ethylene/1-hexene copolymer produced with $\text{SiO}_2/\text{MAO-Et}(\text{Ind})_2\text{ZrCl}_2+\text{TMA}$

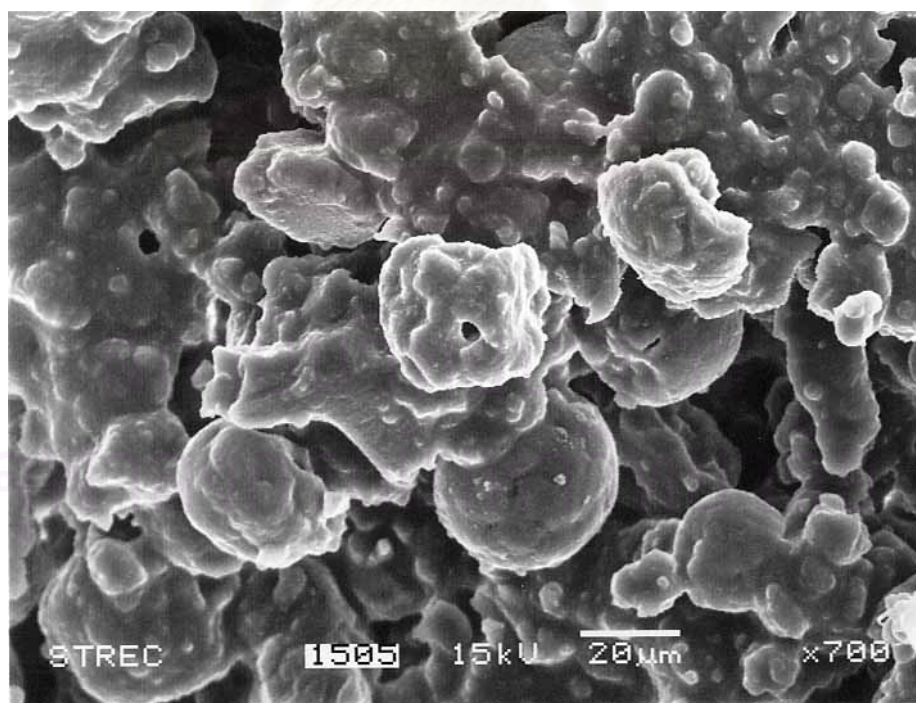


Figure 4.23 Scanning electron microscope image of ethylene/1-hexene copolymer produced with $\text{SiO}_2/\text{MAO/Et}(\text{Ind})_2\text{ZrCl}_2+\text{TMA}$

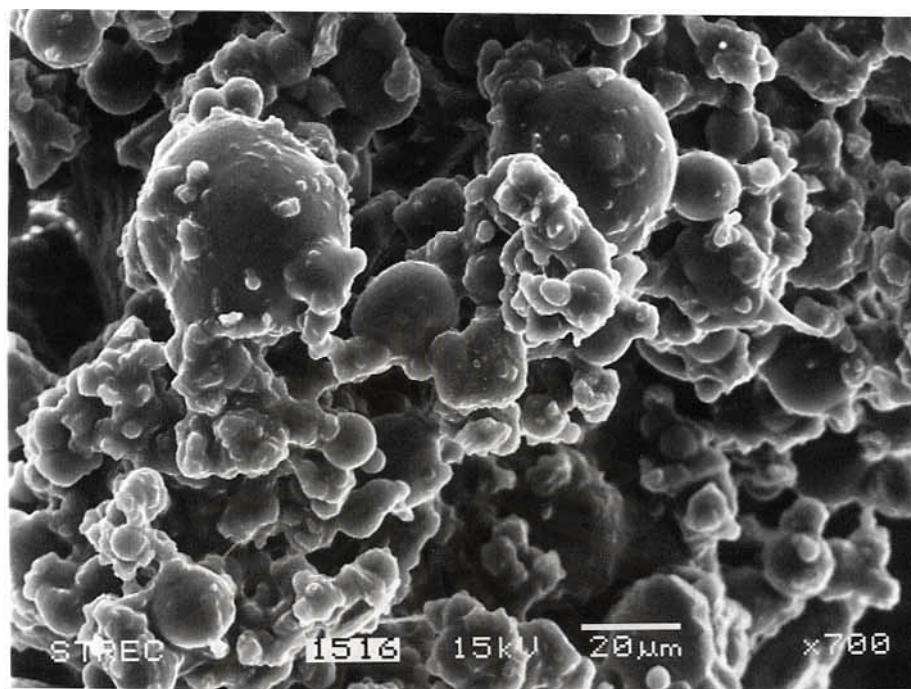


Figure 4.24 Scanning electron microscope image of ethylene/1-octene copolymer produced with $\text{SiO}_2/\text{MAO-Et}(\text{Ind})_2\text{ZrCl}_2+\text{TMA}$

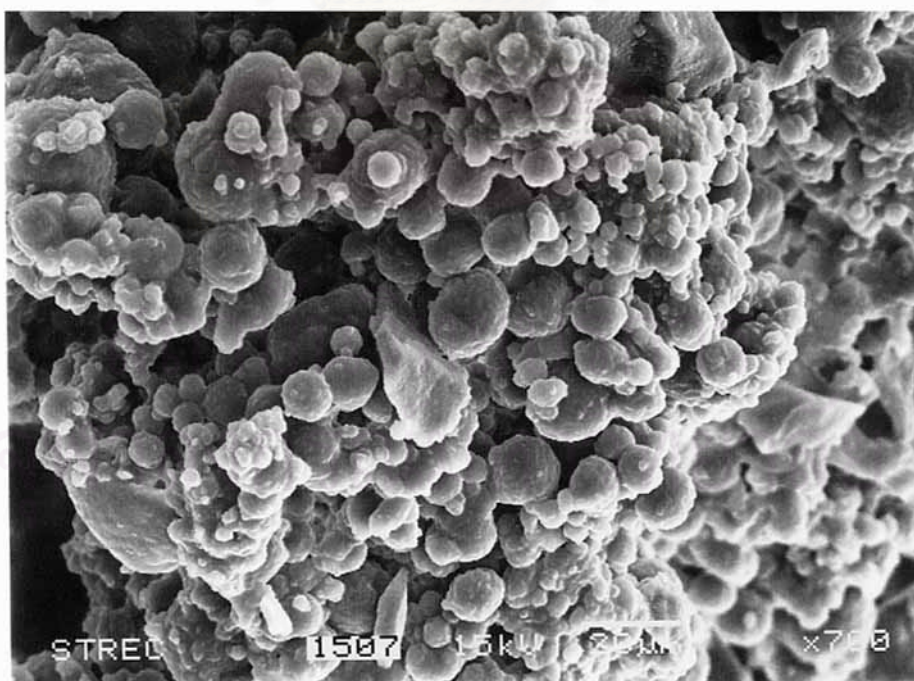


Figure 4.25 Scanning electron microscope image of ethylene/1-octene copolymer produced with $\text{SiO}_2/\text{MAO}/\text{Et}(\text{Ind})_2\text{ZrCl}_2+\text{TMA}$

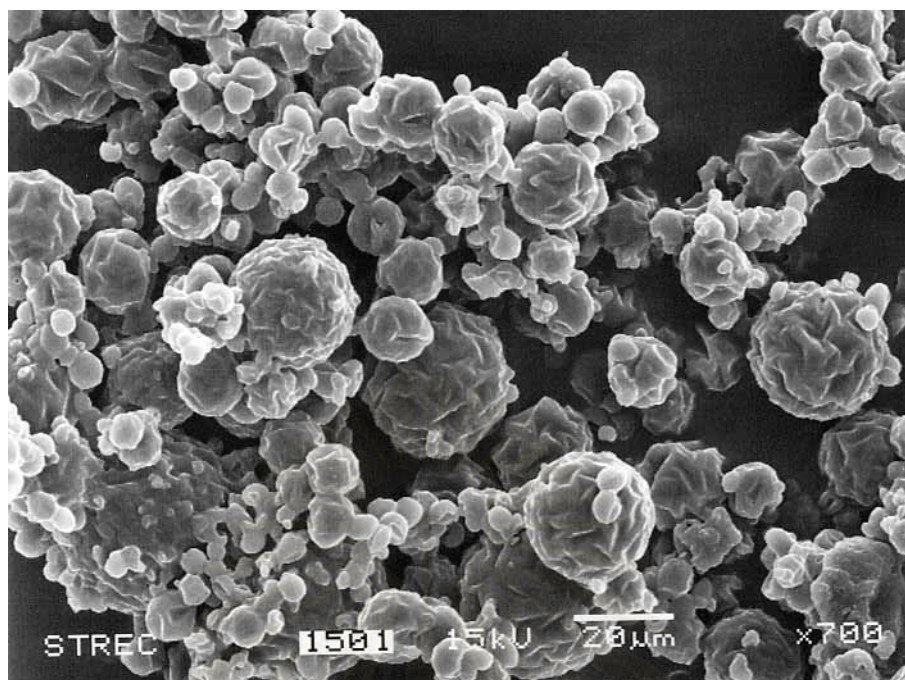


Figure 4.26 Scanning electron microscope image of ethylene/1-decene copolymer produced with $\text{SiO}_2/\text{MAO-Et}(\text{Ind})_2\text{ZrCl}_2+\text{TMA}$

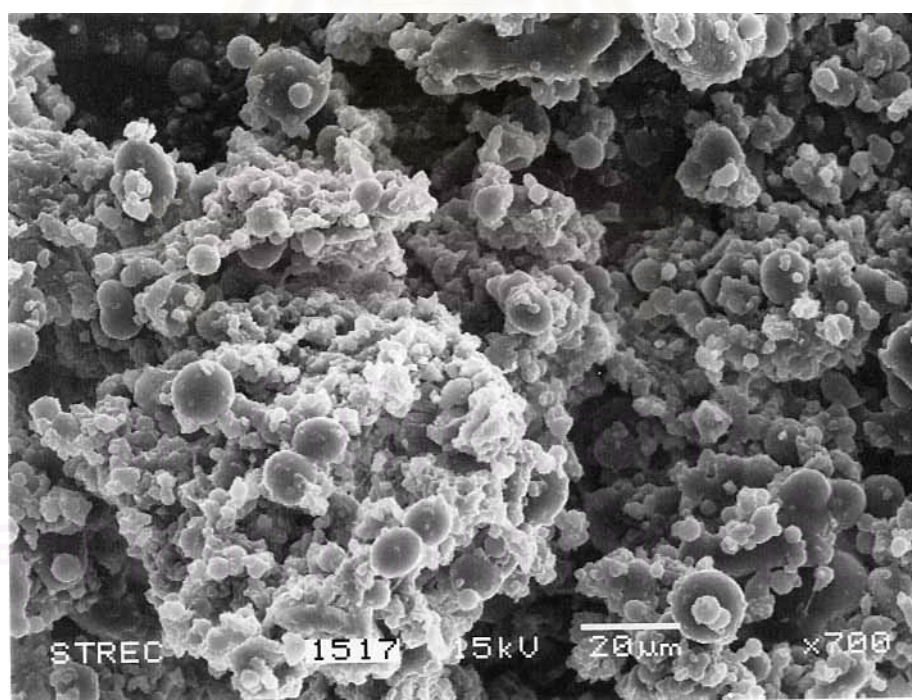


Figure 4.27 Scanning electron microscope image of ethylene/1-decene copolymer produced with $\text{SiO}_2/\text{MAO}/\text{Et}(\text{Ind})_2\text{ZrCl}_2+\text{TMA}$

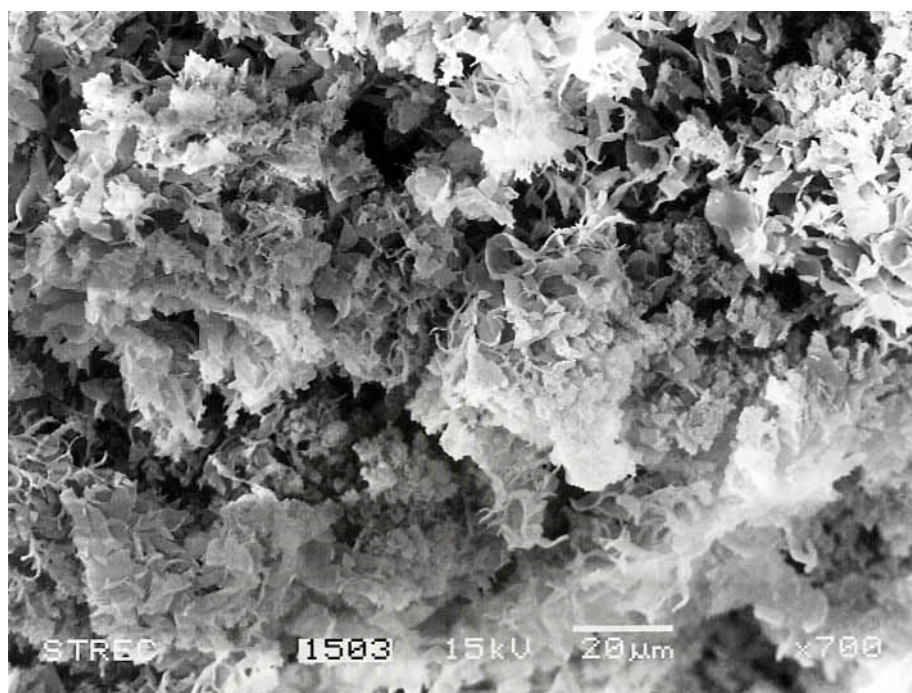


Figure 4.28 Scanning electron microscope image of polyethylene produced with $\text{SiO}_2/\text{MAO-Et}(\text{Ind})_2\text{ZrCl}_2+\text{TMA}$

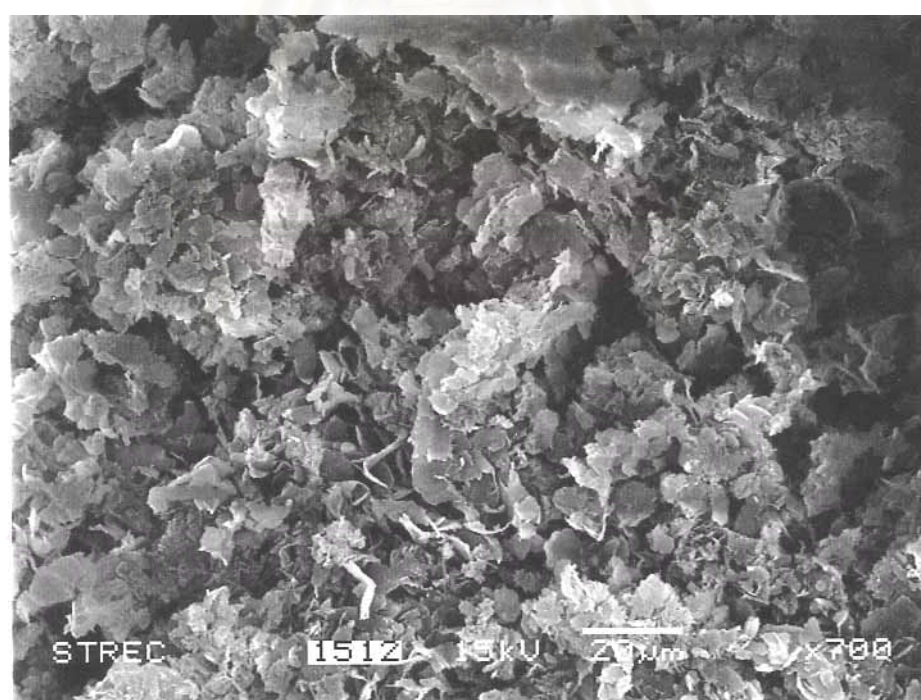


Figure 4.29 Scanning electron microscope image of polyethylene produced with $\text{SiO}_2/\text{MAO}/\text{Et}(\text{Ind})_2\text{ZrCl}_2+\text{TMA}$

From Figures 4.22-4.27 the morphology of ethylene/ α -olefin copolymer produced with different catalyst precursor is shown. The morphology of obtained polymers are similar to that of catalyst precursor. Molecule of ethylene/ α -olefin formed into pellet and expanded continuously around catalyst precursor. But in Figure 4.28-4.29, the morphology of both polymers are different from catalyst precursor.

4.6.3 Melting Temperature (T_m)

The melting temperatures of ethylene/ α -olefin copolymer produced with the supported metallocene catalysts were evaluated by differential scanning calorimeter. The results of various comonomer, such as 1-hexene, 1-octene, 1-decene that copolymerization with ethylene are demonstrated in Tables 4.14 in both supported system. The DSC curves of the copolymers are also shown in Appendix B.

Table 4.14 Melting temperature of ethylene/ α -olefin copolymer and polyethylene with various catalyst precursors.

Precursor	Copolymerization or polymerization	Activity (kgPE/molZr.h)	$T_m(^{\circ}\text{C})$
SiO ₂ /MAO	Ethylene/1-hexene	21900	n.d
	Ethylene/1-octene	21500	n.d.
	Ethylene/1-decene	19900	n.d.
	Ethylene	11200	131
SiO ₂ /MAO/Et(Ind ₂ ZrCl ₂)	Ethylene/1-hexene	17900	n.d.
	Ethylene/1-octene	17500	n.d.
	Ethylene/1-decene	12300	97
	Ethylene	9100	132

n.d. = not determine (no peak appear)

Arnold *et al* [68] has investigated the copolymerization of ethylene with α -olefins by metallocene catalysis. A small amount of comonomer incorporation of 1-butene, 1-hexene or 1-octene leads to linear low density polyethylene (LLDPE), a product of great

industrial interest. One effect of the comonomer incorporation is a decrease in crystallinity. As a result, polymers with a lower melting point and density, and an increased flexibility and processibility are obtained.

Then, the results from Table 4.14 shown that most of copolymers of ethylene/ α -olefins in both supported system were not determined for the melting point except copolymer of ethylene/1-decene in supported system had lower melting point than homopolyethylene.

4.6.4 Average Molecular Weight and Molecular Weight Distribution

The molecular weight and molecular weight distribution of copolymer produced at different catalyst precursors were presented in Tables 4.15 and GPC curves were also shown in Appendix C.

Table 4.15 Mw and MWD of the obtained ethylene/ α -olefin copolymer using various catalyst precursor

Precursor	Copolymerization or polymerization	Mw	Mn	Mw/ Mn
SiO ₂ /MAO-Et(Ind) ₂ ZrCl ₂ +TMA	Ethylene/1-hexene	27930	11701	2.4
	Ethylene/1-octene	23042	10292	2.2
	Ethylene/1-decene	25179	10467	2.4
	Ethylene	55833	18649	3.0
SiO ₂ /MAO/Et(In d ₂ ZrCl ₂ +TMA	Ethylene/1-hexene	27450	11999	2.3
	Ethylene/1-octene	32727	13289	2.5
	Ethylene/1-decene	46949	14567	3.2
	Ethylene	65599	23637	2.8

From Table 4.15, the Mw and Mn of ethylene/ α -olefins copolymer are lower than homopolyethylene which the ratios of Mn/Mn are in the interval of 2.24-3.22. This might be resulted from chain transfer to monomer [25].

Cerrada *et. al.* [69] reported that metallocene catalysts present single-site characteristics (and very high activities) and thus all the sites produce nearly the same chain architecture, leading to polymers with narrow molecular weight distributions, and, in the case of copolymer with α -olefins, the side branches are randomly distributed along the polymer backbone. If the comonomer content in linear low density polyethylene (LLDPE) is high enough, around 4 mol% depending upon the used catalyst system, a material behaving as a plastomer can be achieved. The plastomer term refers to a polymeric material that exhibits the dual characteristic of plastic and elastomeric behavior. Plastomers are ethylene/ α -olefin copolymers with lower density than typical LLDPE for use in a variety of films and polymer modification applications.

From Shan, Soares, and Penlidis [25], ethylene is copolymerized with α -olefins to produce polymers with lower densities. It is commonly observed that the addition of a comonomer generally increases the polymerization rate significantly. This comonomer effect is sometimes linked to the reduction of diffusion limitations by producing a lower crystallinity polymer or to the activation of catalytic sites by the comonomer. The polymer molecular weight often decreases with comonomer addition, possibly because of a transfer to comonomer reactions. An increase in activity was observed with an increased addition of 1-octene. This increase is presumably due to the comonomer effect that is often associated with polymerization rate enhancement. The origin and nature of this effect are still debated and it is believed that it might be both physical and chemical in nature. Physically, the presence of 1-octene enhances the diffusion of ethylene to the active sites because a polymer with low crystallinity is formed. The presence of 1-octene may also activate and increase the number of catalytic sites that were not formerly present in the absence of 1-octene. Recently, Ystenes [1] proposed an insertion mechanism that involves a monomer unit triggering the insertion of an already complexed monomer. This mechanism accounts for the formation of different catalytic sites and different propagation rates in the presence of a comonomer. Other researchers have reported that the molecular weight increases and sometimes decreases with the addition of 1-octene, but generally the molecular weight decreases because of increased transfer to 1-octene. PDI decreases as the amount of 1-octene increases. The SCBD can vary greatly, and MWD can still remain narrow [25].

Chu *et al.* [3] carried out ethylene polymerization with an in-situ supported metallocene catalyst. In the absence of trimethyl aluminum (TMA), in-situ supported $\text{Et}(\text{Ind})_2\text{ZrCl}_2$ was not active, while $\text{Et}(\text{Ind})_2\text{ZrCl}_2$ was active. The addition of TMA during polymerization activated the catalyst.

Soga *et al.* [70] reported that TMA can act as a cocatalyst in ethylene polymerization without MAO present when in-situ supported Cp_2ZrCl_2 with $\text{Cl}_2\text{Si}(\text{CH}_3)_2$ modified silica was used.

Chien and He [71] suggested that TMA is a scavenger, which may help in reducing the amount of impurities in the system thereby leading to an increase in activity. TMA is also able to inhibit certain functions of MAO. Since TMA is a stronger alkylating and reducing agent than MAO, TMA could cause the reduction of the zirconocene compound resulting in an inactive species. It may also compete with MAO as a complexing ligand leading to a catalyst of lower polymerization activity. Moreover, addition of TMA can lower the degree of oligomerization of MAO and its overall effectiveness. Therefore, addition of TMA has both advantages and disadvantages to activity. Molecular weight slightly decreased when more TMA was added. This might result from increasing the chance of the chain transfer to alkylaluminum reaction leading to termination of the growing chain. However, chain transfer to TMA might not be the major chain transfer reaction in this system since only little change in Mw resulted even when a high excess of TMA was added. MWD broadening likely resulted from the interactions between the metallocene and the support, which leads to the formation of active sites differing in electronic and steric character. Ethylene incorporation in copolymers was found to be close to the ratio of the ethylene to propylene feed ratio. No significant effect to TMA on ethylene incorporation was observed, All the copolymers produced were amorphous with no melting temperature.

Liu, Stovneng and Rytter [72] studied ethylene polymerization with the catalytic system $\text{L}_2\text{ZrCl}_2/\text{MAO}/\text{TMA}$ (where $\text{L}=\text{Cp}$, Me_5Cp , or Me_4Cp). The polymerization activity was reduced with the addition of TMA for $\text{L}=\text{Cp}$ but was almost unaffected for the methyl-substituted catalysts. Increasing the TMA concentration resulted in a lower molecular weight of the polymer, with the largest effect for $\text{L}=\text{Me}_5\text{Cp}$. A gel permeation chromatography analysis of the polymers revealed a high molecular

weight shoulder and a nearly bimodal distribution for $L=Me_5Cp$ at high TMA concentration. The origin of this effect more likely stemmed from competition between chain transfer to aluminum and β -hydrogen transfer reactions at two different sites, one TMA sensitive and one TMA insensitive. Complexation of Me_3Al to Zr was much stronger for $L=Cp$ than for $L=Me_5Cp$. However, the overall chain transfer barrier was much higher for $L=Cp$. These results agree both with the reduced activity for $L=Cp$ and the strongly reduced molecular weight for $L=Me_5Cp$ observed with the addition of TMA. With the addition of TMA, polymer chains produced at a TMA sensitive site are to an increasing extent the result of chain transfer to TMA, whereas chains produced at a TMA insensitive sites mainly terminate via other mechanisms, such as β -hydrogen transfer to Zr or a co-ordinated monomer. For $L=Cp$, there is both experimental and theoretical evidence that the dominating termination mechanism is β -hydrogen transfer to a coordinate monomer. For $L=Me_5Cp$, β -hydrogen transfer to Zr is equally important because of a more hindered monomer coordination, and moreover, a relatively more stable zirconocene hydride with such sterically crowded ligands. The β -agostic conformation is the natural precursor also for chain transfer to Al in TMA. The influence of the TMA concentration on the molecular weight and, therefore, on the rate of chain transfer is found to be much stronger with Me_5Cp ligands with the addition of TMA.

Brondao, Correa, Boaventura and Vianna [73] studied the heterogenization of biscyclopentadienyl-zirconium dichloride (Cp_2ZrCl_2) on silica surface and the use of the heterogenized catalyst for ethylene polymerization. The supported catalysts when activated with a co-catalyst composed of equal parts of TMA and MAO had activity about twice as that using of the pure MAO as co-catalyst; oppositely, TMA at any concentration had always a deleterious effect on the homogeneous metallocene activity. The support used was silica previously calcined and chemically treated with trimethylaluminum (TMA); this step apparently prevented the formation of inactive surface species. The main feature of the heterogenized metallocene catalyst is the loss of polymerization activity as compared with the homogeneous catalyst; similar trend has been observed in most works in this area. This activity loss may be attributed to surface silanol groups, present on the solid support, that were not modified by the TMA treatment; the homogeneous zirconocene species anchored on these residual silanol groups via the formation of μ -oxo bridges, resulting in surface species not active for ethylene

polymerization. For the homogeneous metallocene catalyst, the presence of TMA in the polymerization reactor, at any concentration, showed a deleterious effect on the catalyst activity; TMA alone did not activate either the homogeneous or heterogeneous metallocenes, producing no polymer.

Haag *et al.* [74] studied the effect of MAO in ethylene/propylene copolymerization using SiO₂/MAO supported Et(Ind)₂ZrCl₂ with an external addition of MAO. The copolymer produced gave plural CCD. The copolymer produced at higher Al_(MAO)/Zr was found to have higher ethylene content, higher melting temperature and higher molecular weight.

Chao *et al.* [66] suggested that MAO has many possible function in metallocene catalyst systems, such as scavenging of impurities, alkylation, ionization and/or reduction of the transition element, stabilization of cationic metallocene alkyl and/or the counter ion, and perhaps others. One important role of MAO is apparently to prevent the formation of a ZrCH₂CH₂Zr species (bimolecular processes). This is one of the reasons why a very large amount of MAO is needed to realize the maximum catalytic activity of the ansa-metallocene complexes in solution polymerization. With increased amounts of MAO used in the catalyst precursor, catalytic activity was continuously increased with increase of MAO while no significant effect on molecular weight was observed. The increase in activity did not linearly depend on amount of MAO used but the activity increased more when using a high level of MAO.

Charpentier, Zhu, Hamielec and Brook [97] studied polymerization of ethylene using bis(cyclopentadienyl)zirconium dichloride (Cp₂ZrCl₂). The structure and type of aluminoxane co-catalyst were found not to influence the molecular weight distribution (MWD) of Polyethylene (PE) although to influence the activity of the Cp₂ZrCl₂ catalyst. Increasing aluminium/zirconium (Al/Zr) molar ratio, by increasing the MAO concentration, led to increasing catalyst activity up to a maximum activity at an Al/Zr molar ratio was found not to influence the PE MWD. The MAO co-catalyst is believed to alkylate the metallocene catalyst and functions as a Lewis acid, promoting the formation of an active cationic form of metallocene catalyst. It has been found by ¹H and ¹³C NMR studies with Cp₂Ti(CH₃)(X) complexes where X is CH₃ or Cl, that (1) MAO was a better alkylating agent than TMA; and (2) MAO had a greater capacity for

producing and stabilizing cation-like complexes than TMA. This study, and several others for similar systems, found that the following equilibrium takes place : $\text{Cp}_2\text{TiMe}^+[-\text{Al}(\text{Me})\text{O}]_n^- \rightleftharpoons \text{Cp}_2\text{TiMe}^+\text{S}[-\text{Al}(\text{Me})\text{O}]_n^-$, where S is a solvent molecule and that the active catalytic species ($\text{Cp}_2\text{TiMe}^+[-\text{Al}(\text{Me})\text{O}]_n^-$) is a cation-like species. The equilibrium is believed to be shifted to the right for higher Al/Group IV metal molar ratios, thus increasing the concentration of the active cationic catalyst and hence increasing the activity of the catalyst. Of course, a maximum activity will be produced at a certain co-catalyst/catalyst ratio depending on various conditions. The polymerization of ethylene using $\text{Cp}_2\text{ZrCl}_2/\text{MAO}$ that the PE MW decrease when the concentration of aluminoxane increases. For the same system, when using an additional alkylaluminium, the PE MWs were found to increase with increasing concentration of TMA or TEA through a maximum at a TMA/MAO or TEA/MAO ratio of about 0.5 with decreasing PE MWs at higher ratios. Due to the high levels of MAO necessary for polymerization (Al/Zr ratios upwards of 1000:1 were most reproducible) MAO is believed to act as a scavenger, mopping up active-site impurities in the diluent like O_2 and H_2O . As metallocene polymerization is essentially cationic in nature, this form of polymerization is extremely sensitive to impurities which would react with the active site and kill polymerization. In order to have a significant active-site/impurity ratio, a sufficient amount of MAO must be present in order to mop up impurities in the diluent for a reproducible polymerization. It is clear that the role of MAO or TMA/MAO mixture is that of a cocatalyst in the activation of the catalyst. MAO may also act as a scavenger in the removal of impurities from the polymerization mixture and may, as an oligomer or polymeric form have a role in the prevention of the precipitation of polymer chains. Clearly, if the coordination of MAO co-catalyst was competitive with coordination of ethylene to the active form of the zirconocene complex, changes in the MAO structure and MAO concentration would affect the catalyst termination to propagation ratio and one would observe changes in the PE MWD, which were not observed. Aluminoxane structure and any added stabilizers were found to have no effect on the catalytically active zirconocene site type. The type of aluminoxane influenced the activity of the catalyst with generally, $\text{MAO} \geq \text{MMAO} \geq \text{IBAO}$ for polymerization activity. By increasing the MAO concentration (increasing Al/Zr mole ratio), the polymerization activity was found to increase up to a maximum at an Al/Zr ratio of 2400, after which further increase of Al/Zr molar ratio decreased the catalytic activity. The studied polyethylene MWs and PDIs were found not to vary with MAO type or concentration. Use of TMA, along with

MAO, gives lower activity than MAO by itself for a given Al/Zr molar ratio, but has no effect on MWs or PDIs of the formed PE.

D. Bianchini *et al.* [76] studied the effect of Al content on MAO-modified silicas that was evaluated on catalyst activity, on polymer properties and on residual metal content in the resulting polyethylene. MAO has many functions in the polymerization such as to remove impurities (scavenger), to alkylate the metal center, to abstract methyl of alkylated complex, to produce and to stabilize active species. MAO plays a steric role during the surface reaction, preventing non-consumed OH groups to react further. Silica surface is covered with silanol group (Si-OH) and adsorbed H₂O molecules. When silica is submitted to thermal treatment, H₂O molecules are removed and silanol groups density is decreased by intermolecular reaction. After treatment at higher temperatures (450 °C) the silica surface presents mainly isolated and, to a lesser extent, geminal hydroxyl groups and surface siloxane bridges. Zirconocene reacts with the silica surface through the silanol groups. Isolated hydroxyl groups generate active species, while geminal hydroxyl groups bidentate species, which are inactive for polymerization. The immobilization of zirconocene on MAO-modified silicas with different Al content seems to generate different active species for polymerization reaction. Molecular weight for polymers obtained in the Al/Zr = 500 is higher than that using Al/Zr = 2000. These results might suggest that MAO can act as a chain transfer agent. Homogeneous system has lower molecular weight than those obtained with heterogeneous systems. This fact could be attributed to the blocking of one of the sides of the active site by the support, hindering the deactivation step. In other words, the β -elimination transfer reaction between two metallocene centers are hindered, resulting in a larger growth of the polymer chain, and therefore in a higher molecular weight. The zirconocene species generated with MAO-modified silicas, containing Al content below and above the saturation level, produce different polymeric species.

Moroz *et al.* [77] studied ethylene polymerization by using supported catalysts that prepared by interaction of Cp₂ZrX₂ (X = Cl or CH₃) with silica modified by (CH₃)₃SiCl (TMCS) or trialkylaluminium compounds AlR₃ (R = C₂H₅ (TEA) and i-C₄H₉ (TIBA)). The addition of the co-catalyst (MAO or TIBA) led to a further increase in the activity of the supported catalysts. Aluminium alkyls are known to react with accessible

OH groups of silica at room temperature to form surface $\equiv \text{Si-O-AlR}_2$ groups and to evolve alkane RH. Dimethyl zirconocene may be supposed to interact with surface silanol groups of SiO_2 to form 'μ-oxo-like' complexes $\equiv \text{Si-OH} + \text{Cp}_2\text{Zr}(\text{CH}_3)_2$

—————▶ $\equiv \text{Si-O-Zr}(\text{CH}_3)_2\text{Cp}_2 + \text{CH}_4$. The dissolved $\text{Cp}_2\text{Zr}(\text{CH}_3)_2$ shows no polymerization activity in the absence of MAO or AlR_3 . The catalyst prepared by supporting $\text{Cp}_2\text{Zr}(\text{CH}_3)_2$ onto silylated SiO_2 exhibited the highest activity. The absence of MAO the zirconocene is bonded to the surface of silylated silica during a polymerization run, whereas the addition of MAO to the polymerization medium caused the desorption of some or all of the metallocene compound from the support and thus the heterogeneous catalytic system acts as a homogeneous one. The fact that $\text{Cp}_2\text{Zr}(\text{CH}_3)_2$, when adsorbed on silylated silica, shows a sufficiently high activity in ethylene polymerization, even without any co-catalyst specially added. The Al^{3+} ions, occurring at the surface of silylated silica as impurities, behave as relatively strong Lewis acids. Presumably, after the removal of Bronsted acid OH groups by silylation, the surface Al^{3+} cations become the main sites which interact with the supported zirconocenes and activate them.

CHAPTER V

CONCLUSIONS & RECOMMENDATIONS

5.1 CONCLUSIONS

The ethylene/alpha-olefin (1-hexene, 1-octene, 1-decene) copolymerizations using two different supported catalyst systems of SiO₂ support modified with MAO (in-situ supported catalyst system) and SiO₂ support modified with MAO and Et(Ind)₂ZrCl₂ (preformed supported catalyst system) were studied. A number of conclusions may be summarized as follows:

1. Both of in-situ supported (SiO₂/MAO-Et(Ind)₂ZrCl₂+TMA) system and preformed supported (SiO₂/MAO/Et(Ind)₂ZrCl₂+TMA) system, the effect of amount of MAO indicated that the catalytic activity for ethylene/alpha-olefin (1-hexene, 1-octene, 1-decene) copolymerizations continuously increased with increasing the amount of MAO. While the effect of TMA found that the catalytic activity for ethylene/ α -olefin copolymerizations increased with increasing Al_(TMA)/Zr mole ratio up to optimum range (2500), further an increase in Al_(TMA)/Zr mole ratio resulted in a decrease in the activity.
2. When all factors were fixed (comonomer, Al_(MAO)/Zr mole ratio and Al_(TMA)/Zr mole ratio), the in-situ supported catalyst system showed higher catalytic activity than the preformed supported catalyst system at catalyst concentration of 5.00x10⁻⁵ M and polymerization temperature of 70 °C.
3. For the in-situ supported catalyst system, the pattern of relationship between the catalytic activity for ethylene/alpha-olefin copolymerization and the amount of TMA for using 1-octene as comonomer was significantly different from that for using either 1-hexene or 1-decene as comonomer. However, the pattern of relationship between the catalytic activity and the amount of MAO for all comonomers was rather similar. On the other hand, the preformed supported catalyst system indicated the similarity of the pattern of relationship between the catalyst activity and the amount of TMA or MAO for all comonomers.

5.2. RECOMMENDATIONS

1. The effect of trimethylaluminum (TMA) on the activity of ethylene/ α -olefin copolymerizations should be studied by using the same comonomer concentration in feed.
2. The effect of other alkylaluminums on polymer properties should be studied.



สถาบันวิทยบริการ
จุฬาลงกรณ์มหาวิทยาลัย

REFERENCES

1. Huang, J. and Rempel, G. L. Prog. Polym. Sci. 20 (1995): 459-526.
2. Scheirs, J. and Kaminsky, W. Metallocene-based Polyolefins.; vol.1, Wiley: WestSussex, 2000.
3. Chu, K. J.; Soares, J. B. P. and Penlidis, A. J. Polym. Sci.: Part A: Polym. Chem. 38 (2000): 462-468.
4. Chu, K. J.; Shan, C. L. P.; Soares, J. B. P. and Penlidis, A. Macromol. Chem. Phys. 200 (1999): 2372-2376.
5. Chu, K. J.; Soares, J. B. P. and Penlidis, A. Macromol. Chem. Phys. 201 (2000): 340-348.
6. Quijada, R.; Galland, G. B. and Mauler, R. S. Macromol. Chem. Phys. 197 (1996): 3091-3098.
7. Pratchayawutthirat, W. Copolymerization of ethylene/1-hexene on the supported zirconocene catalyst, 2001.
8. Kashiwa, N. and Imuta, J. Catalysis Surveys from Japan 1 (1997): 125-142.
9. Sinclair, K. B. and Wilson, R. B. Chemistry & Industry 7 (1994): 857-862.
10. Gupta, V. K.; Satish, S. and Bhardwaj, I. S. J. M. S.-Rev. Macromol. Chem. Phys. C34(3) (1994): 439-514.
11. Naga, N. and Imanishi, Y. Macromol. Chem. Phys. 203 (2002): 159-165.
12. Lauher, J. W. and Hoffmann, R. J. Am. Chem. Soc. 98 (1976): 1729.
13. Castonguay, L. A. and Rappe, A. K. J. Am. Chem. Soc. 114 (1992): 5832-5842.
14. Yang, X.; Stern, C. L. and Marks, T. J. J. Am. Chem. Soc. 113 (1991): 3623-3625.
15. Chien, J. C. W. and Wang, B. P. J. Polym. Sci.: Part A: Polym. Chem. 26 (1988): 3089-3102.
16. Pedeutour, J. N.; Radhakrishnan, K.; Cramail, H. and Deffieux, A. J. Mol. Cat. A: Chem. 185 (2002): 119-125.
17. Pedeutour, J. N.; Cramail, H. and Deffieux, A. J. Mol. Cat. A: Chem. 176 (2001): 87-94.
18. Cam, D. and Giannini, U. Makromol. Chem. 193 (1992): 1049-1055.

19. Soga, K.; Kim, H. J. and Shiono, T. Makromol. Chem., Rapid Commun. 14 (1993): 765-770.
20. Katayama, H.; Shiraishi, H.; Hino, T.; Ogane, T. and Imai, A. Macromol. Symp. 97 (1995): 109-118.
21. Przybyla, C.; Tesche, B. and Fink, G. Macromol. Rapid Commun. 20 (1999): 328-332.
22. Harkki, O.; Lehmus, P.; Leino, R.; Luttikhedde, H. J. G.; Nasman, J. H. and Seppala, J. V. Macromol. Chem. Phys. 200 (1999): 1561-1565.
23. Cheruvu, S. US Pat 5608019 (1997).
24. Albano, C.; Sanchez, G. and Ismayel, A. Polym. Bull. 41 (1998): 91-98.
25. Shan, C. L. P.; Soares, J. B. P. and Penlidis, A. J. Polym. Sci.: Part A: Polym. Chem. 40 (2002): 4426-4451.
26. Pietikainen, P. and Seppala, J.V. Macromolecules 27 (1994): 1325-1328.
27. Soga, K. and Kaminaka, M. Makromol. Chem., Rapid Commun. 13 (1992): 221-224.
28. Nowlin, T. E.; Kissin, Y. V. and Wagner, K. P. J. Polym. Sci.: Part A: Polym. Chem. 26 (1988): 755-764.
29. Soga, K.; Uozumi, T.; Arai, T. and Nakamura, S. Macromol. Rapid Commun. 16 (1995): 379-385.
30. de Fatima V. Marques, M.; Conte, A.; de Resende, F. C. and Chaves, E. G. J. App. Polym. Sci. 82 (2001): 724-730.
31. Kim, J. D. and Soares, J. B. P. Macromol. Rapid Commun. 20 (1999): 347-350.
32. Shan, C. L. P.; Chu, K. J.; Soares, J. and Penlidis, A. Macromol. Chem. Phys. 201 (2000): 2195-2202.
33. Steinmetz, B.; Tesche, B.; Przybyla, C.; Zechlin, J. and Fink, G. Acta Polymer 48 (1997): 392-399.
34. Tait, P. J. T. and Monterio, M. G. K. Mecton'96, Houston, TX, USA June (1996).
35. Quijada, R.; Rojas, R.; Alzamora, L.; Retuert, J. and Rabagliati, F. M. Catalysis letters 46 (1997): 107-112.
36. Chen, Y. X.; Rausch, M. D. and Chein, J. C. W. J. Polym. Sci.: Part A: Polym. Chem. 33 (1995): 2093-2108.

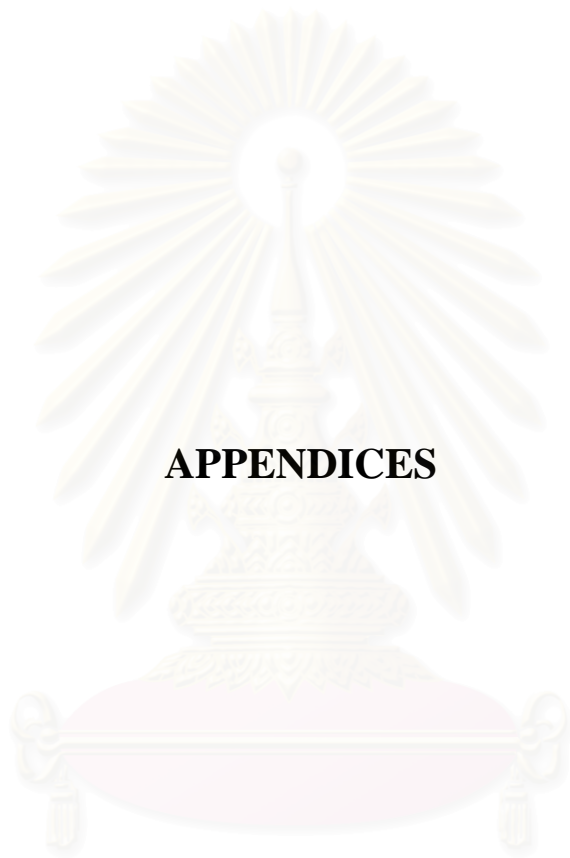
37. Ban, H.; Arai, T.; Ahn, C. H.; Uozumi, T. and Soga, T. Recent Development in Heterogeneous Metallocene Catalyst
38. Ferreira, M. L.; Belelli, P. G.; Juan, A. and Damiani, D. E. Macromol. Chem. Phys. 201 (2000): 1334-1344.
39. Collins, S.; Kelly, W. M. and Holden, D.A. Macromolecules 25 (1992): 1780-1785.
40. Kaminsky, W.; Renner, F. and Winkelbach, H. Mecton'94, Houston, TX, USA, May (1994).
41. Hlatky, G. G. and Upton, D. J. Macromolecules 29 (1996): 8019-8020.
42. Lee, D.; Shin, S. and Lee, D. Macromol. Symp. 97 (1995): 195-203.
43. dos Santos, J. H. Z.; Dorneles, S.; Stedile, F.; Dupont, J.; Forte, M. M. C. and Baumovl, I. J. R. Macromol. Chem. Phys. 198 (1997): 3529-3537.
44. Harrison, D.; Coulter, I. M.; Wang, S.; Nistala, S.; Kuntz, B. A.; Pigeon, M.; Tian, J. and Collins, S. J. Mol. Cat. A: Chem. 128 (1998): 65-77.
45. Xu, J.; Deng, Y.; Feng, L.; Cui, C. and Chen, W. Polym. J. 30 (1998): 824-827.
46. Soga, K.; Kim, H. J. and Shiono, T. Macromol. Rapid. Commun. 15 (1994): 139-144.
47. Lee, D.; Yoon, K. and Noh, S. Macromol. Rapid, commun. 18 (1997): 427-431.
48. Iiskola, E. I.; Timonen, S.; Pakkanen, T. T.; Harkki, O.; Lehmus, P. and Seppala, J. V. Macromolecules. 30 (1997): 2853-2859.
49. Lee, D. and Yoon, K. Macromol. Symp. 97 (1995): 185-193.
50. de Fatima V. Marques, M.; Henriques, C. A.; Monteiro, J. L. F.; Menezes, S. M. C. and Coutinho, F. M. B. Polym. Bull. 39 (1997): 567-571.
51. Michelotti, M.; Altomare, A.; Ciardelli, F. and Roland, E. J. Mol. Cat. A: Chem. 129 (1998): 241-248.
52. Meshkova, I. N.; Ushakova, T. M.; Ladygina, T. A.; Kovalena, N. Y. and Novokshonova, L. A. Polym. Bull. 44 (2000): 461-468.
53. Weiss, K.; Wirth-Pfeifer, C.; Hofmann, M.; Botzenhardt, S.; Lang, H.; Bruning, K. and Meichel, E. J. Mol. Cat. A: Chem. 182-183 (2002): 143-149.
54. Looveren, L. K. V.; Geysen, D. F.; Vercruyssen, K. A.; Wouters, B. H.; Grobet, P. J. and Jacobs, P. A. Angew. Chem. Int. Ed. 37 (1998): 517-520.

55. Soares, J. B. P. and Hamielec, A. E. Polymer 36 (1995b): 1639-1654.
56. Borrajo, J.; Cordon, C.; Carella, J. M.; Toso, S. and Goizueta, G. J. Polym. Sci.: Part B: Polym. Phys. 33 (1995): 1627-1632.
57. Randall, J. C. JMS-Rev. Macromol. Chem. Phys. C29 (1989): 201-317.
58. Mara, J. J. and Menard, K. P. Acta Polymer 45 (1994): 378-380.
59. de Fatima V. Marques, M. and Conte, A. J. App. Polym. Sci. 86 (2002): 2054-2061.
60. Ribeiro, M. R.; Deffieux, A. and Portela, M. F. Ind. Eng. Chem. Res. 36 (1997): 1224-1237.
61. Kaminsky, W. and Strubel, C. J. Mol. Cat. A: Chem. 128 (1998): 191-200.
62. Cossee, P. J. Catal. 3 (1964): 80.
63. dos Santos, J. H. Z.; da Rosa, M. B.; Krug, C.; Stedile, F. C.; Haag, M. C.; Dopont, J. and de Camargo Forte, M. J. Polym. Sci.: Part A: Polym. Chem. 37 (1999): 1987-1996.
64. Chu, K. J.; Soares, J. B. P. and Penlidis, A. J. Polym. Sci.: Part A: Polym. Chem. 38 (2000): 1803-1810.
65. Soga, K. and Kaminaka, M. Macromol. Chem. 194 (1993): 1745-1755.
66. Chao, C.; Praserttham, P.; Khorbunsongserm, S. and Rempel, G. L. J. Macromol. Sci.: Part A-Pure and App. Chem. 40 (2003): 181-192.
67. Galland, G. B.; Quijada, R.; Mauler, R. S. and de Menezes, S. C. Macromol. Rapid Commun. 17 (1996): 607-613.
68. Arnold, M.; Bornemann, S.; Koller, F.; Menke, T. J. and Kressler, J. Macromol. Chem. Phys. 199 (1998): 2647-2653.
69. Cerrada, M. L.; Benavente, R. and Perez, E. Macromol. Chem. Phys. 202 (2001): 2686-2695.
70. Soga, K.; Shiono, T. and Kim, H. J. Makromol. Chem. 194 (1993): 3499-3504.
71. Chien, J. C. W. and He, D. J. Polym.Sci.: Part A: Polym. Chem. 29 (1991): 1595-1601.
72. Liu, J.; Stovng, J. A. and Rytter, E. J. Polym. Sci.: Part A: Polym. Chem. 39 (2001): 3566-3577.
73. Brandao, S. T.; Correa, M. L. S.; Boaventura, J. S. and Vianna, S. C. Studies in Surface Science and Catalysis 130 (2000): 3849-3854.

74. Haag, M. C.; Krug, C.; Dupont, J.; de Galland, G. B.; dos Santos, J. H. Z.; Uozumi, T.; Sano, T. and Soga, K. J. Mol. Cat. A: Chem. 169 (2001): 275-287.
75. Charpentier, P. A.; Zhu, S.; Hamielec, A. E. and Brook, M. A. Polymer 39 (1998): 6501-6511.
76. Bianchini, D.; Bichinho, K. M. and dos Santos, J. H. Z. Polymer 43 (2002): 2937-2943.
77. Moroz, B. L.; Semikolenova, N. V.; Nosov, A. V.; Zakharov, V. A.; Nagy, S. and O'Reilly, N. J. J. Mol. Cat A: Chem. 130 (1998): 121-129.

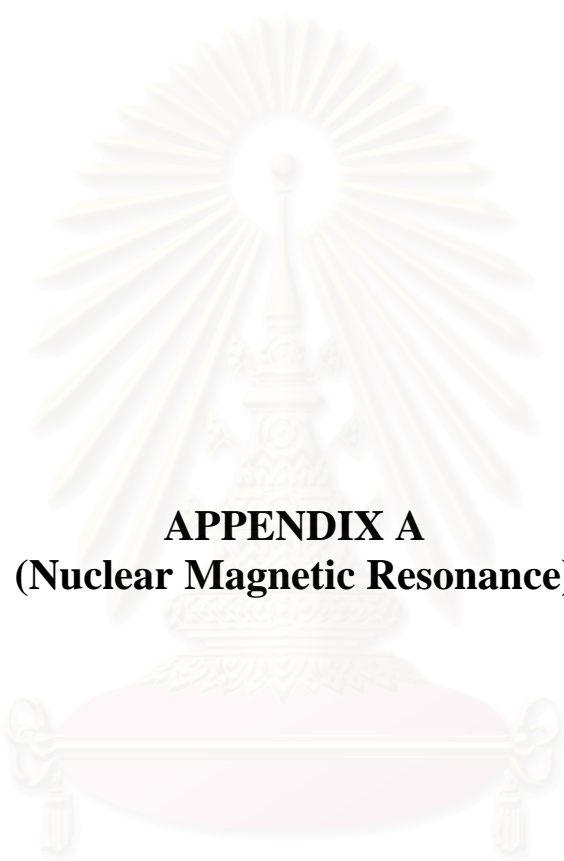


สถาบันวิทยบริการ
จุฬาลงกรณ์มหาวิทยาลัย



APPENDICES

สถาบันวิทยบริการ
จุฬาลงกรณ์มหาวิทยาลัย



APPENDIX A
(Nuclear Magnetic Resonance)

สถาบันวิทยบริการ
จุฬาลงกรณ์มหาวิทยาลัย

Department of Science Service
 Chemistry Division
 Code of sample :VY 816
 Instrument :BRUKER:Avance DPK-400
 Solvent :o-dichlorobenzene/benzene-d6
 Operator : Laddawan
 Date : 22/05/2002

Current Data Parameters
 NAME EHSiO2-MAO
 EXPNO 1
 PROCNO 1

F2 - Acquisition Parameters

Date 500000
 Time 15.33
 INSTRUM dpx400
 PROBHD 5 mm QNP 1H
 PULPROG zgpg30
 TD 131072
 SOLVENT ~~o-dichlorobenzene~~ o-dichlorobenzene
 NS 6000
 DS 0
 SWH 25125.629 Hz
 FIDRES 0.191693 Hz
 AQ 2.6083827 sec
 RG 4096
 DW 19.900 usec
 DE 7.14 usec
 TE 300.2 K
 d11 0.0300000 sec
 PL12 19.00 dB
 CPDPRG2 waltz16
 PCPD2 106.00 usec
 SFO2 400.1317746 MHz
 NUC2 1H
 PL2 120.00 dB
 D1 3.00000000 sec
 P1 6.80 usec
 DE 7.14 usec
 SFO1 100.6227903 MHz
 NUC1 13C
 PL1 -6.00 dB

F2 - Processing parameters

SI 65536
 SF 100.6127774 MHz
 WDW EM
 SSB 0
 LB 2.00 Hz
 GB 0
 PC 1.00

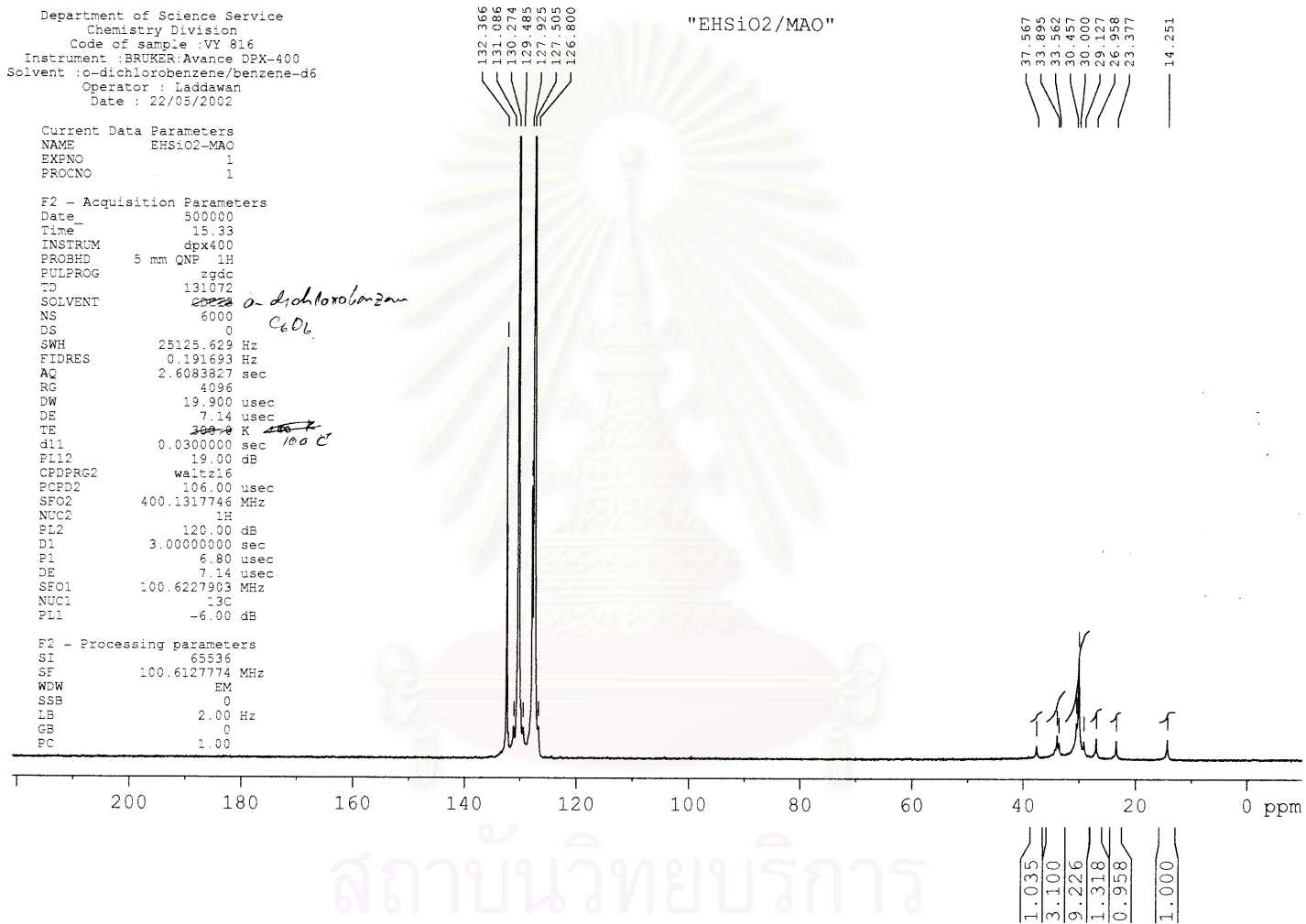


Figure A-1. ^{13}C -NMR spectrum of ethylene/1-hexene copolymer produce with $\text{SiO}_2/\text{MAO-Et}[\text{Ind}]_2\text{ZrCl}_2+\text{TMA}$

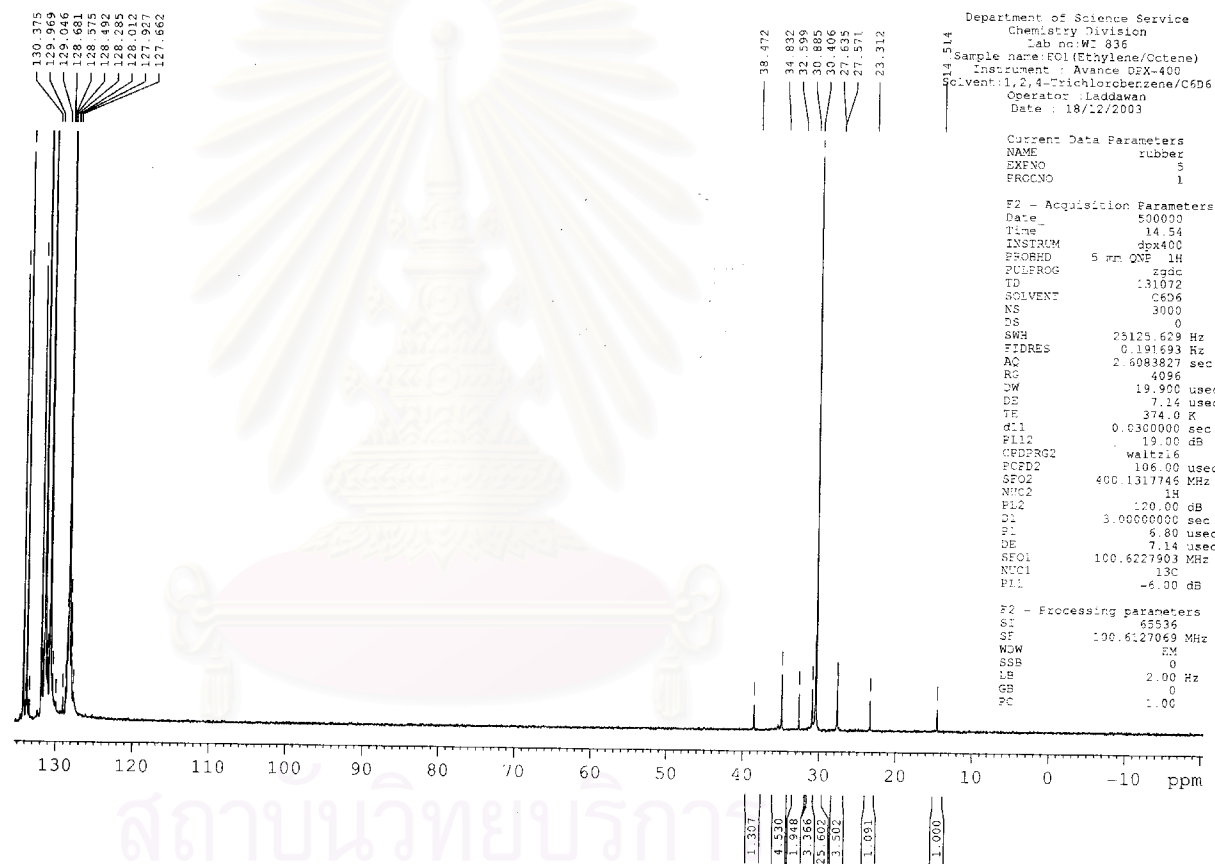


Figure A-2. ^{13}C -NMR spectrum of ethylene/1-octene copolymer produce with $\text{SiO}_2/\text{MAO-Et}_2[\text{Ind}]\text{ZrCl}_2+\text{TMA}$

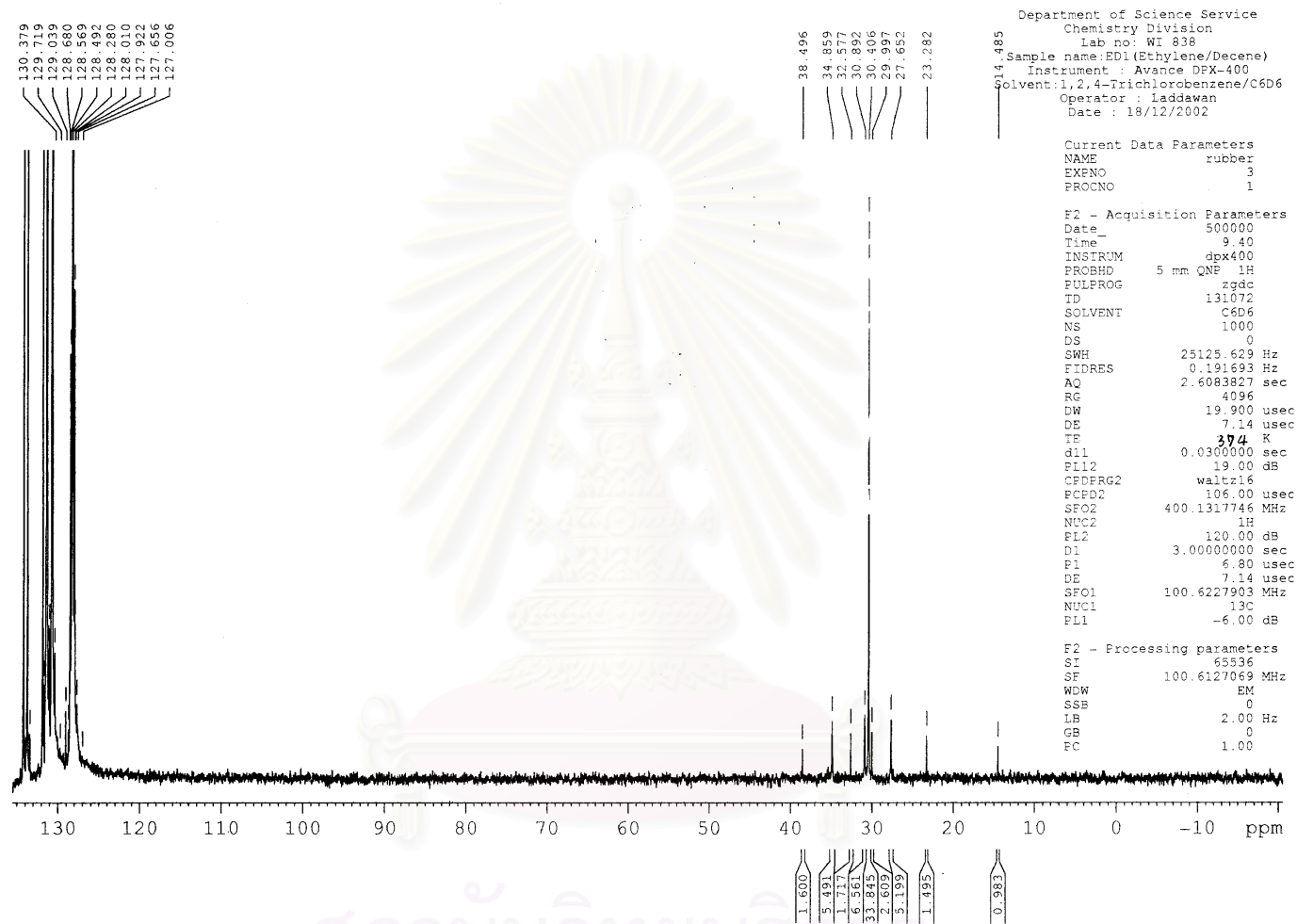


Figure A-3. ¹³C-NMR spectrum of ethylene/1-decene copolymer produce with SiO₂/MAO-Et₂[Ind]ZrCl₂+TMA



APPENDIX B
(Differential Scanning Calorimeter)

สถาบันวิทยบริการ
จุฬาลงกรณ์มหาวิทยาลัย

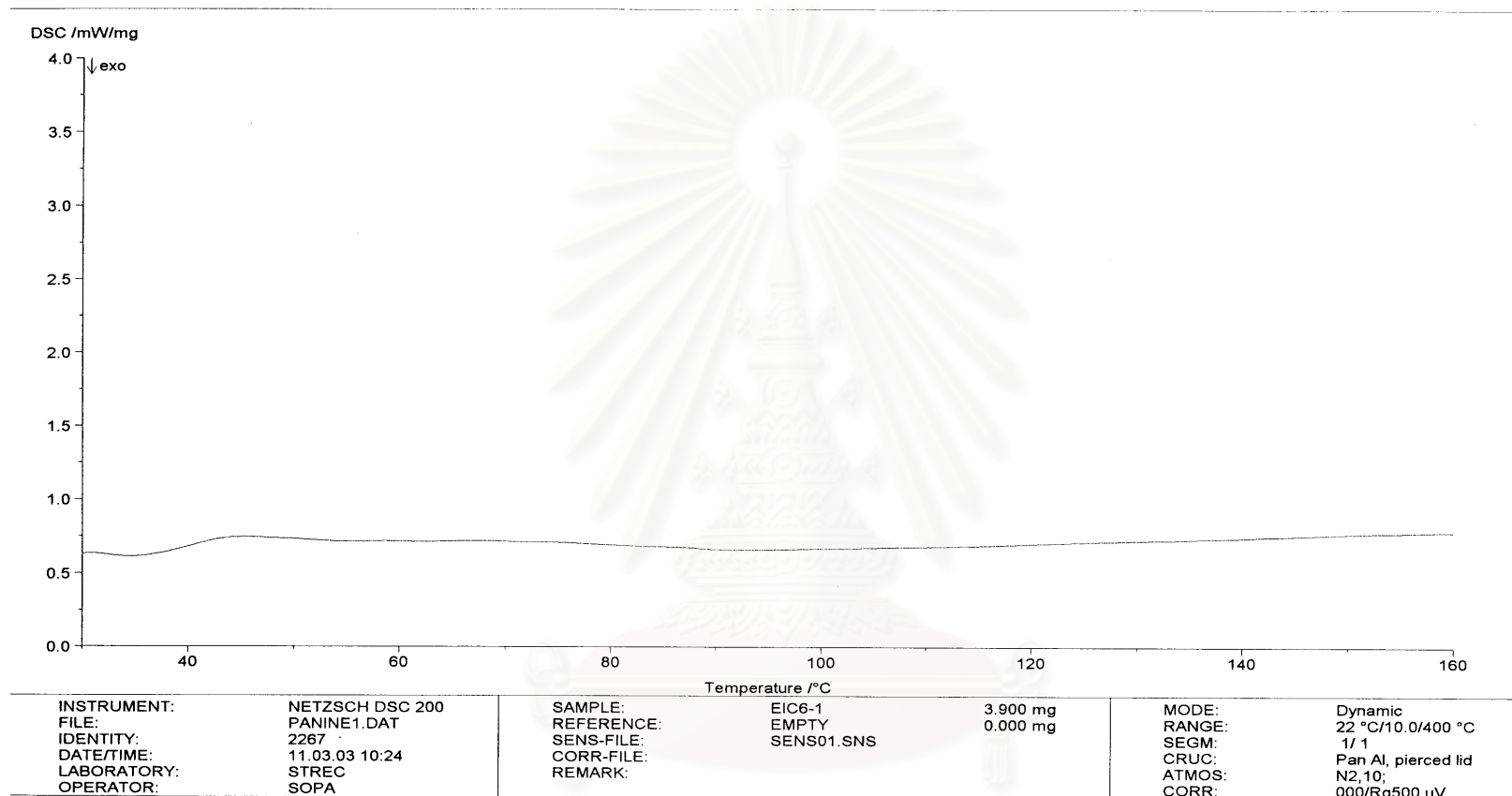


Figure B-1. DSC curve of ethylene/1-hexene copolymer produce with $\text{SiO}_2/\text{MAO-Et}[\text{Ind}]_2\text{ZrCl}_2+\text{TMA}$

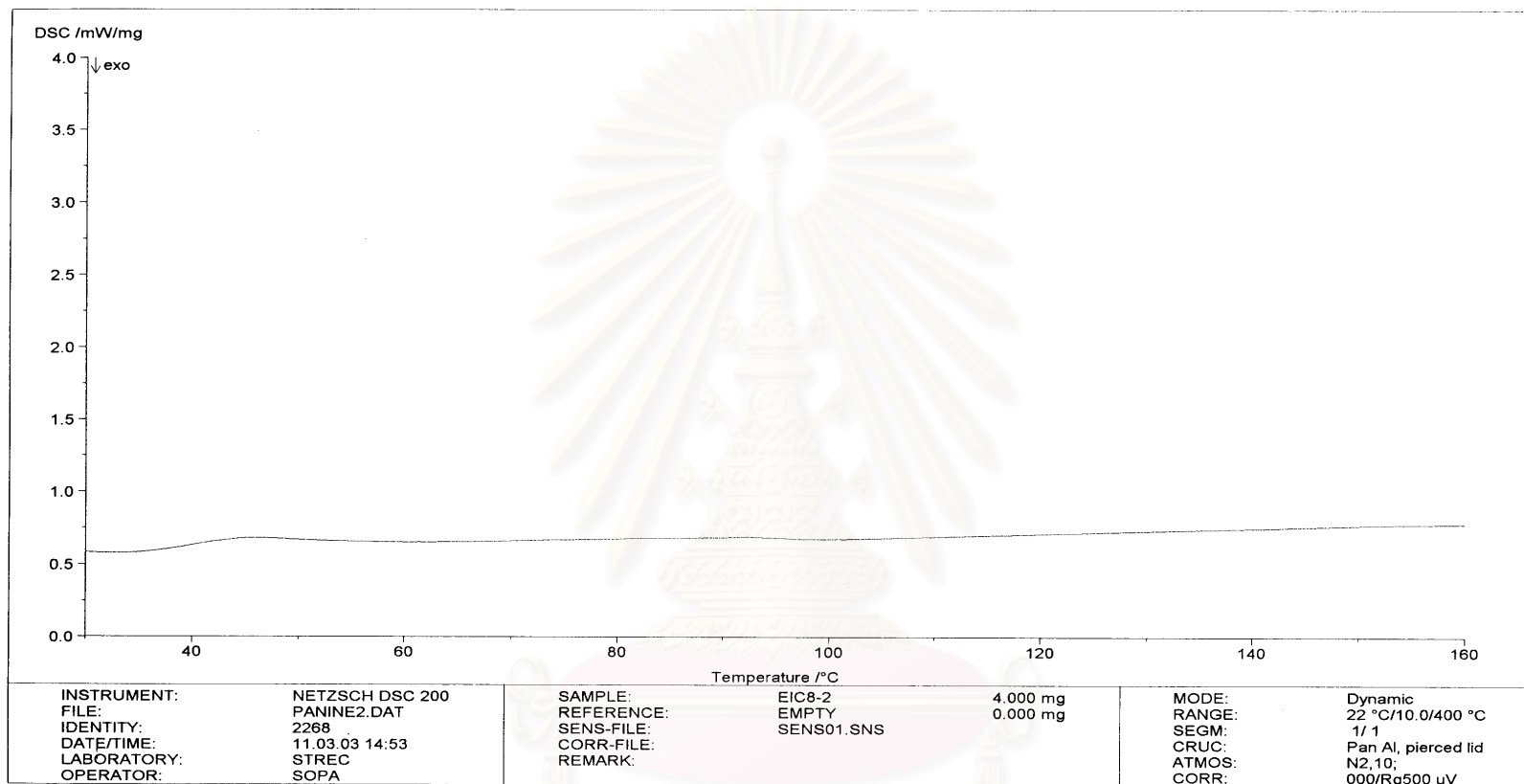


Figure B-2. DSC curve of ethylene/1-octene copolymer produce with $\text{SiO}_2/\text{MAO-Et}[\text{Ind}]_2\text{ZrCl}_2+\text{TMA}$

จุฬาลงกรณ์มหาวิทยาลัย

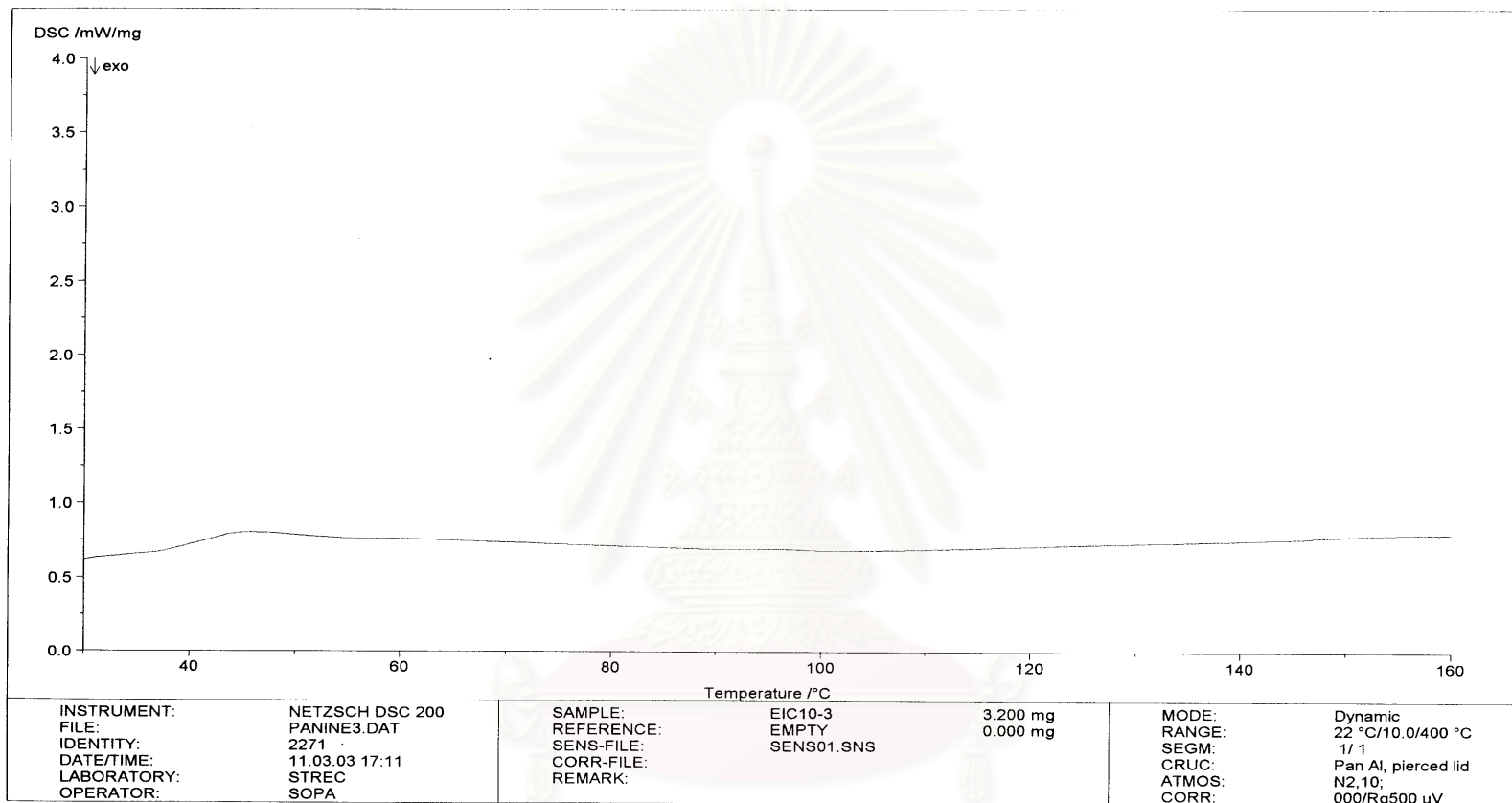


Figure B-3. DSC curve of ethylene/1-decene copolymer produce with $\text{SiO}_2//\text{MAO-Et}[\text{Ind}]_2\text{ZrCl}_2+\text{TMA}$

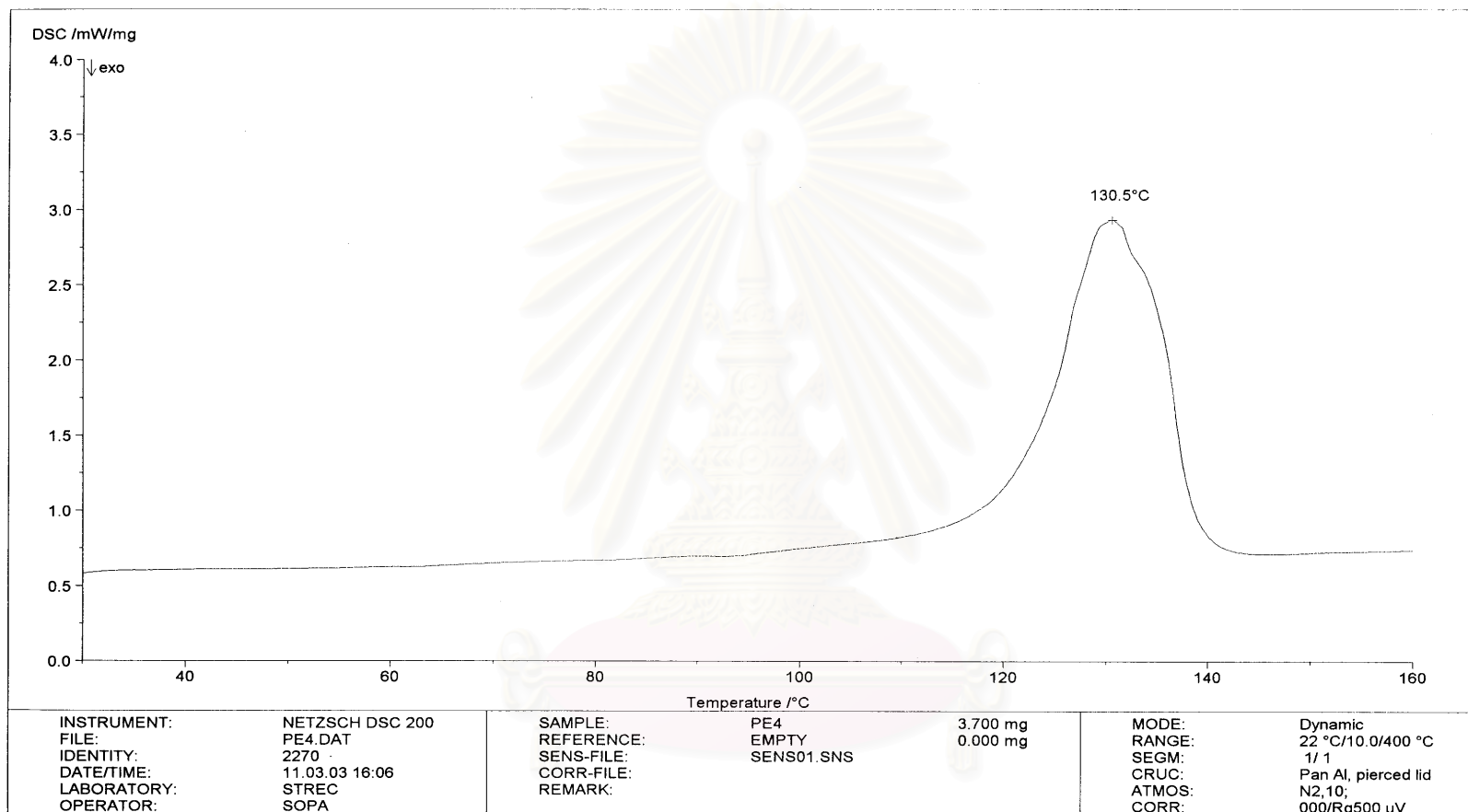


Figure B-4. DSC curve of polyethylene produce with $\text{SiO}_2/\text{MAO-Et}[\text{Ind}]_2\text{ZrCl}_2+\text{TMA}$

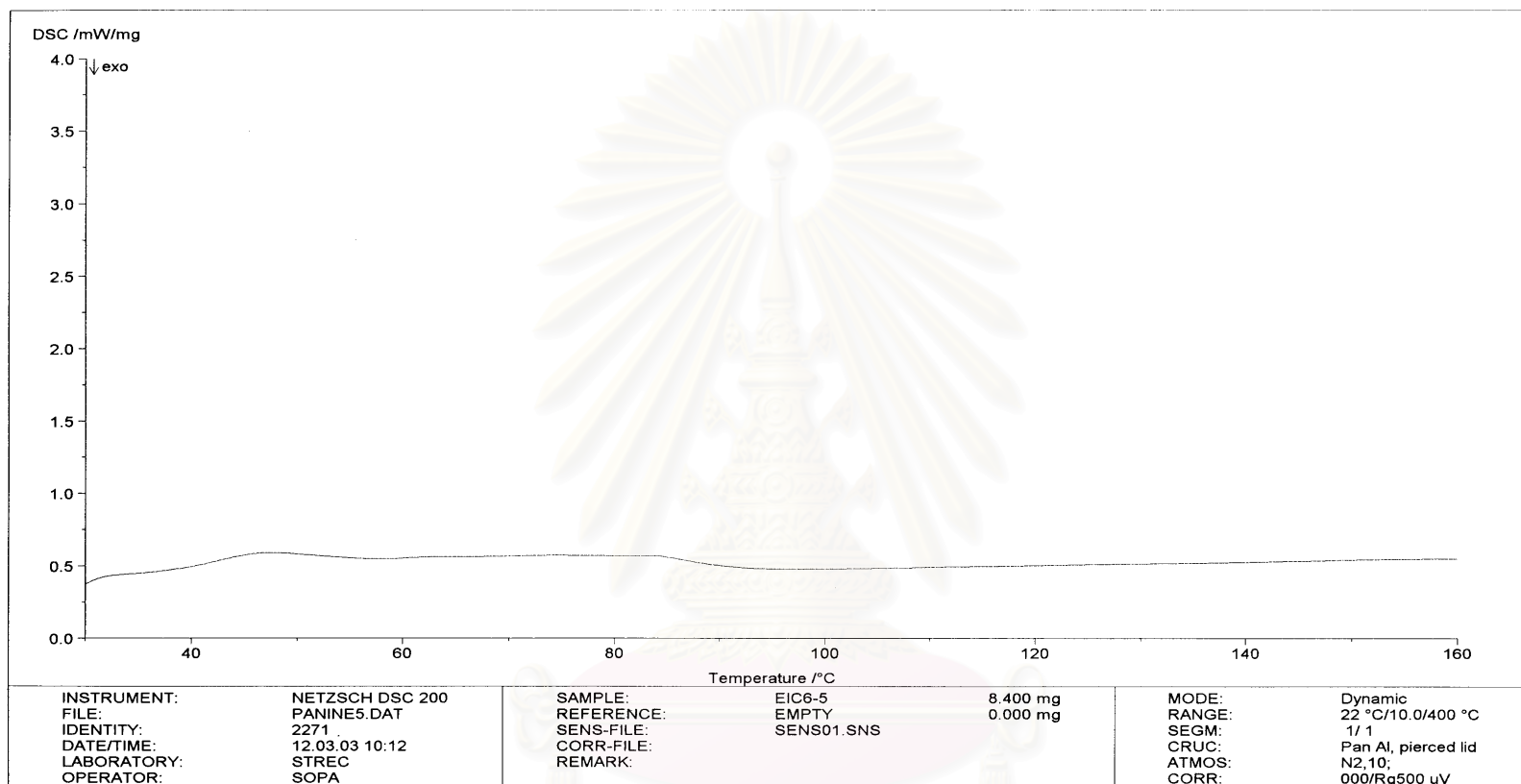


Figure B-5. DSC curve of ethylene/1-hexene copolymer produce with $\text{SiO}_2/\text{MAO}/\text{Et}[\text{Ind}]_2\text{ZrCl}_2+\text{TMA}$

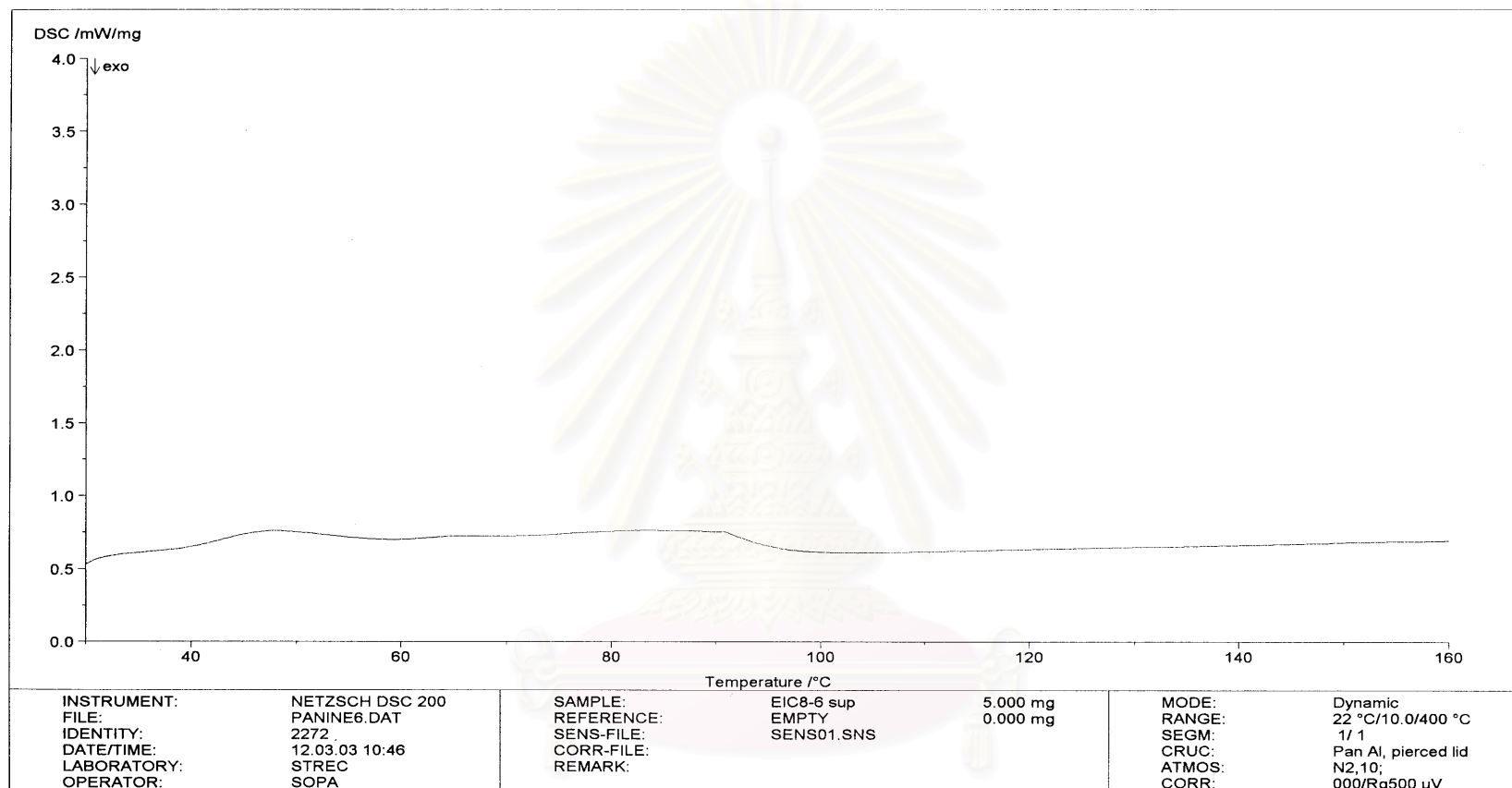


Figure B-6. DSC curve of ethylene/1-octene copolymer produce with $\text{SiO}_2/\text{MAO}/\text{Et}[\text{Ind}]_2\text{ZrCl}_2+\text{TMA}$

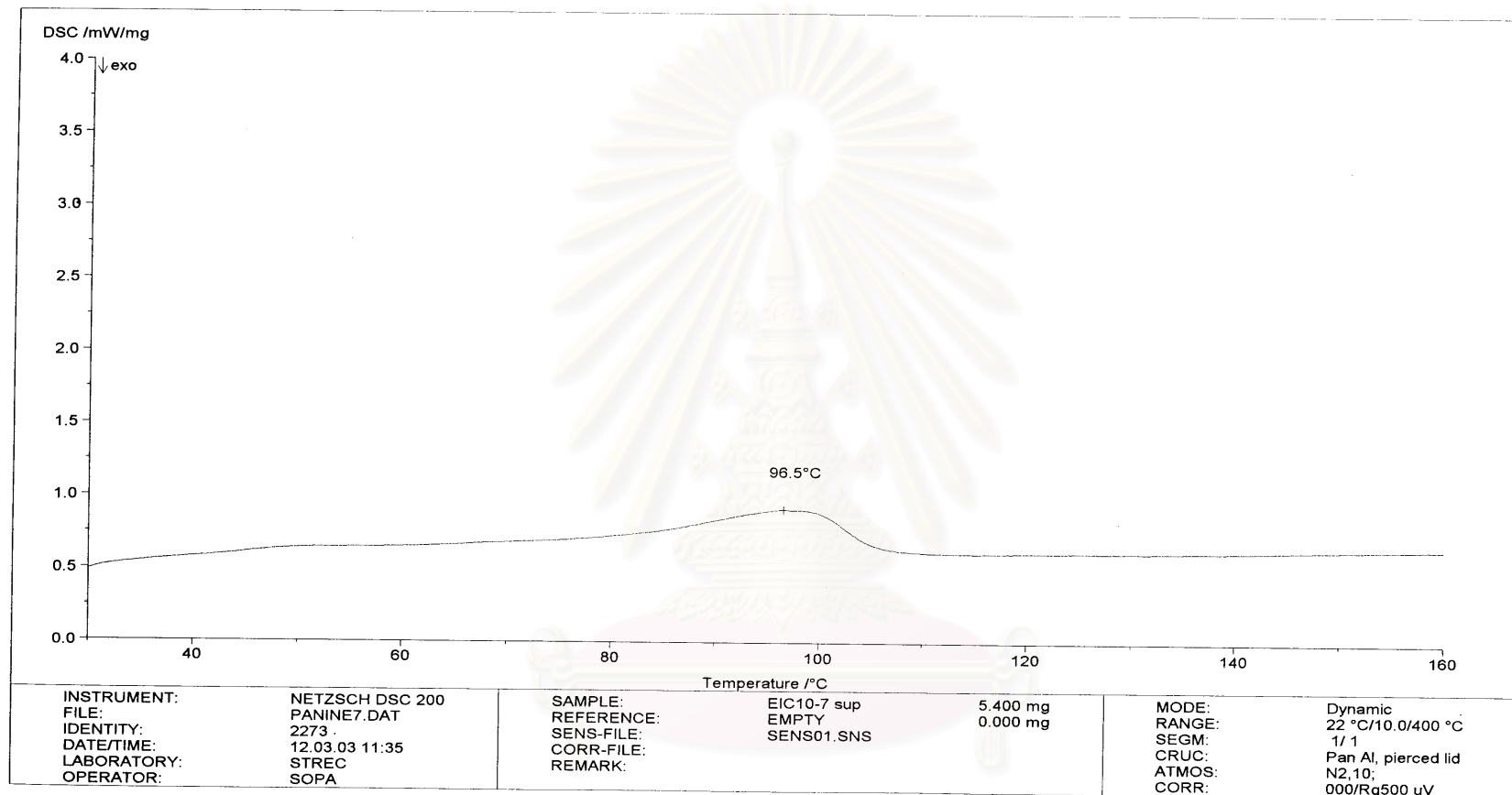


Figure B-7. DSC curve of ethylene/1-decene copolymer produce with SiO₂/MAO/Et[Ind]₂ZrCl₂+TMA

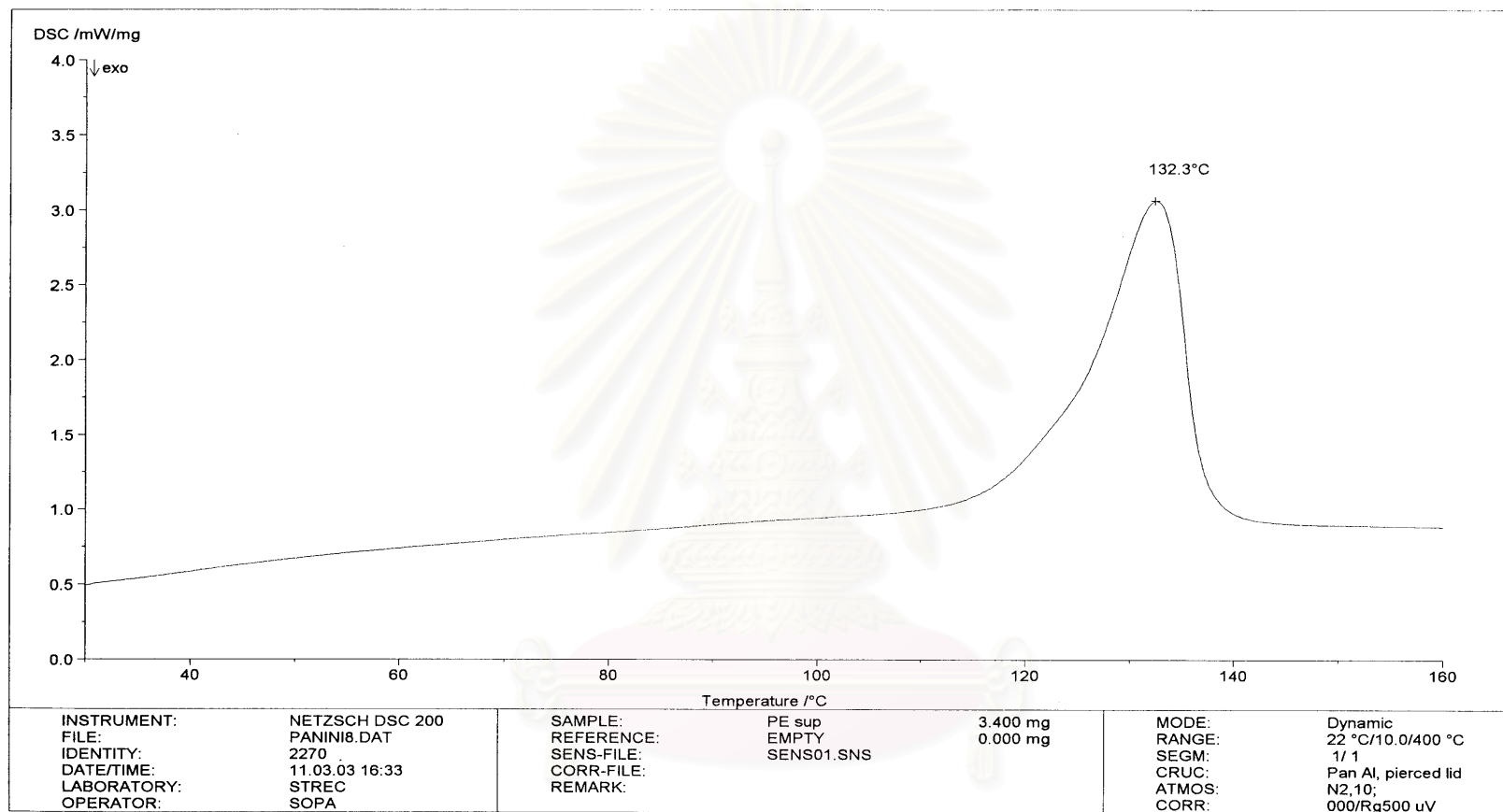


Figure B-8. DSC curve of polyethylene produce with SiO₂/MAO/Et[Ind₂ZrCl₂+TMA

สถาบันวิทยบริการ
จุฬาลงกรณ์มหาวิทยาลัย



APPENDIX C
(Gel Permeation Chromatography)

สถาบันวิทยบริการ
จุฬาลงกรณ์มหาวิทยาลัย

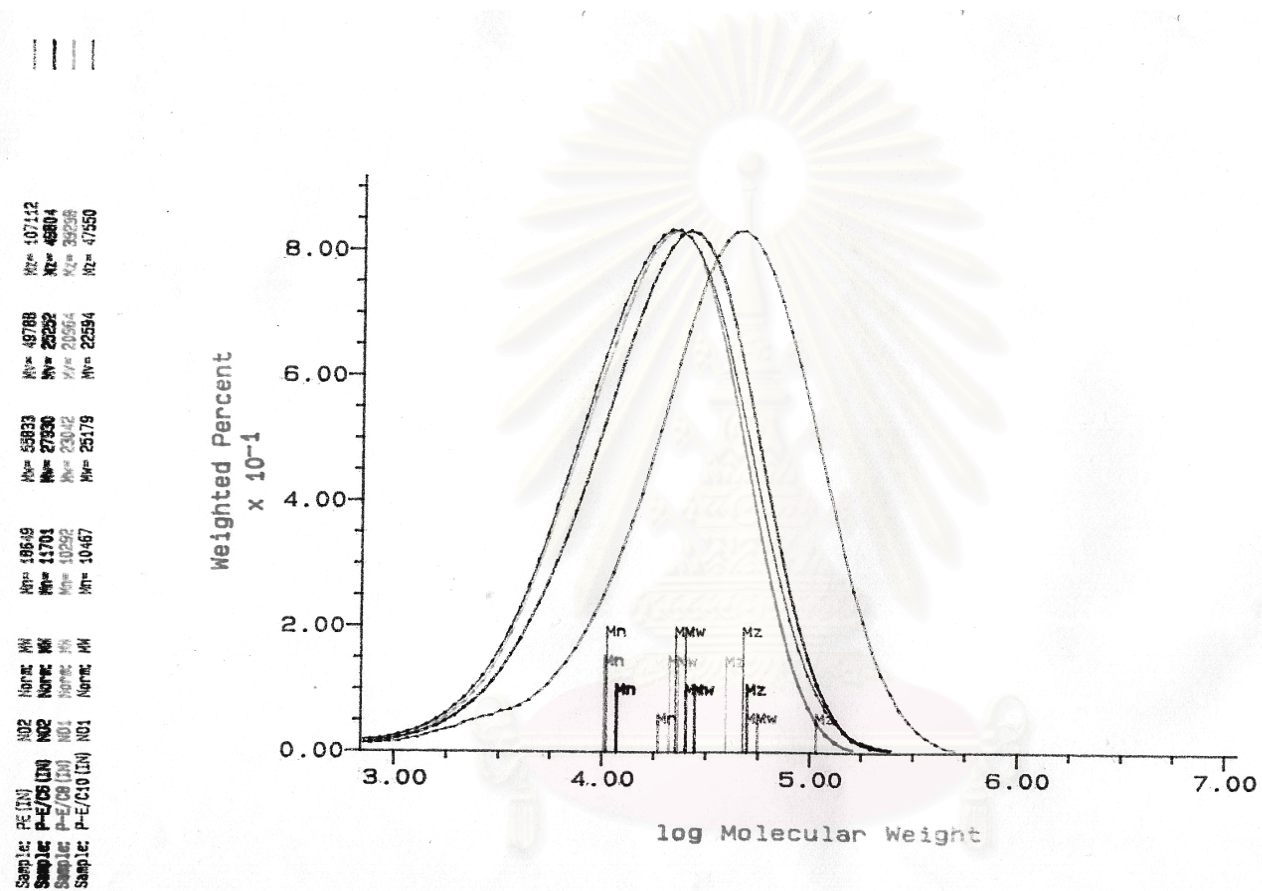


Figure C-1. GPC curve of ethylene/ α -olefin copolymerization produced with $\text{SiO}_2/\text{MAO-Et}[\text{Ind}]_2\text{ZrCl}_2+\text{TMA}$

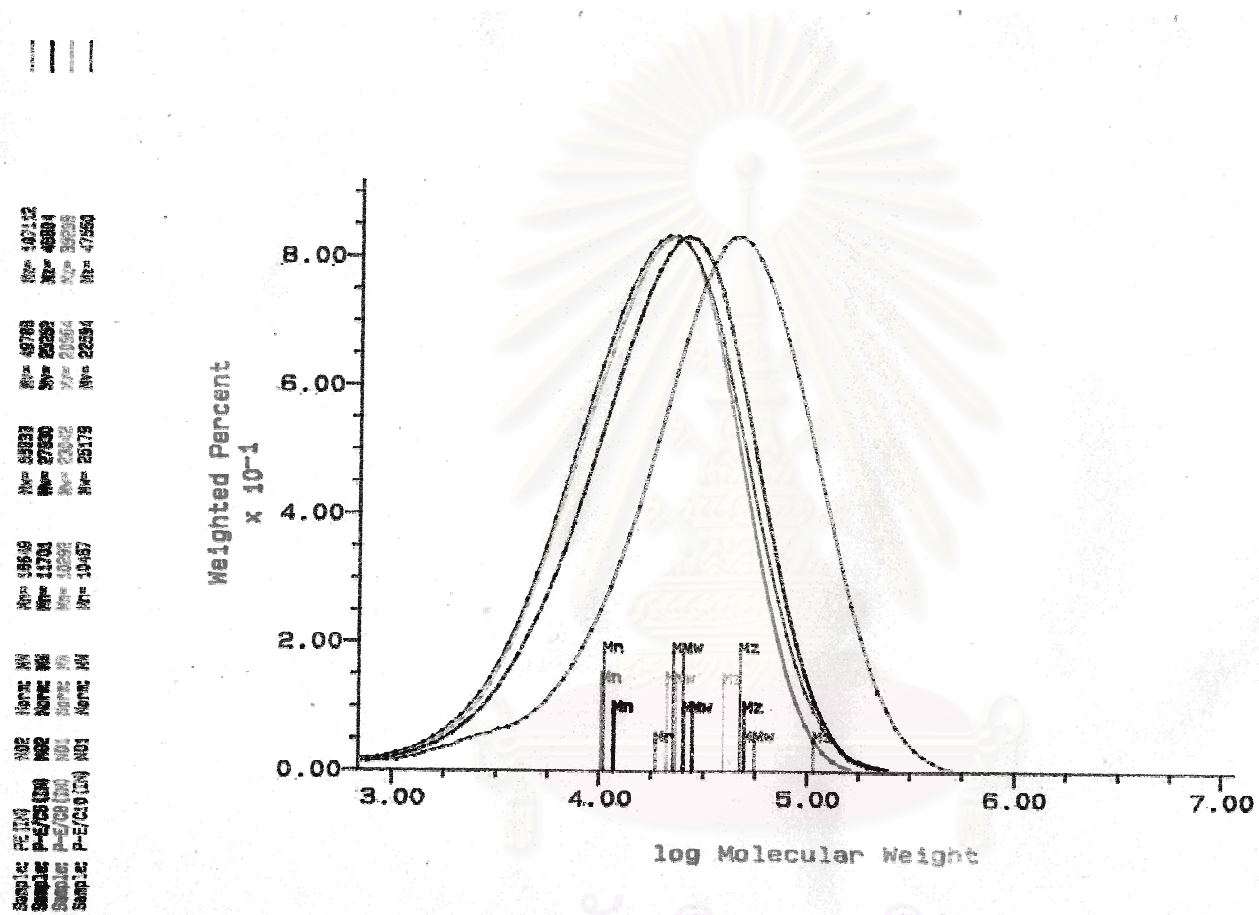


Figure C-2 GPC curve of ethylene/ α -olefin copolymerization produced with $\text{SiO}_2/\text{MAO}/\text{Et}[\text{Ind}]_2\text{ZrCl}_2+\text{TMA}$

สถาบันวิทยบริการ
จุฬาลงกรณ์มหาวิทยาลัย

VITA

Miss. Paninee Kaewkrajang was born on October 19, 1977 in Bangkok, Thailand. She received the Bachelor's Degree of Science from the Department of Chemical, Faculty of Science, King Mongkut's Institute of Technology Thonburi (KMUTT) in October 1999, She continued her Master's study at Chulalongkorn University in June, 2000.



สถาบันวิทยบริการ
จุฬาลงกรณ์มหาวิทยาลัย